



Swansea University
Prifysgol Abertawe



Cronfa - Swansea University Open Access Repository

This is an author produced version of a paper published in:

Desalination

Cronfa URL for this paper:

<http://cronfa.swan.ac.uk/Record/cronfa51081>

Paper:

Anis, S., Hashaikeh, R. & Hilal, N. (2019). Functional materials in desalination: A review. *Desalination*, 468, 114077
<http://dx.doi.org/10.1016/j.desal.2019.114077>

This item is brought to you by Swansea University. Any person downloading material is agreeing to abide by the terms of the repository licence. Copies of full text items may be used or reproduced in any format or medium, without prior permission for personal research or study, educational or non-commercial purposes only. The copyright for any work remains with the original author unless otherwise specified. The full-text must not be sold in any format or medium without the formal permission of the copyright holder.

Permission for multiple reproductions should be obtained from the original author.

Authors are personally responsible for adhering to copyright and publisher restrictions when uploading content to the repository.

<http://www.swansea.ac.uk/library/researchsupport/ris-support/>

FUNCTIONAL MATERIALS IN DESALINATION: A REVIEW

Shaheen Fatima Anis^a, Raed Hashaikeh^a, Nidal Hilal^{a, b*}

^a NYUAD Water Research Center. New York University Abu Dhabi, P.O. Box 129188, Abu Dhabi, United Arab Emirates

^b Centre for Water Advanced Technologies and Environmental Research (CWATER), College of Engineering, Swansea University, Fabian Way, Swansea SA1 8EN, United Kingdom

*Corresponding author

Abstract

This paper reviews various functional materials used in desalination. Desalination of the abundant seawater resource has emerged as a promising technology to meet the current fresh water demands. For improved performance, often functional materials such as photocatalysts, electrocatalysts, photothermal materials, sorbents, antibacterial materials and magnetic materials are utilized in thermal, membrane-based and other desalination technologies. With an aim to provide an insight on the existing research on functional materials and the purpose behind using such in desalination, this review collates different research studies of various functional properties and the subsequent materials utilized for those properties. New generation materials such as carbon nanotubes (CNTs) and graphene form a major part, where they exhibit multiple functionalities with improved water transport properties, and thus have been deemed as very attractive enhancers to the desalination technology. Nevertheless, most of the functional materials, such as nano-TiO₂, nano-zeolites, graphene, CNTs and magnetic nanoparticles suffer from several limitations such as specialized synthesis techniques, agglomeration, leaching and environmental and health concerns. This review focuses on such challenges and suggests improvements for enhanced incorporation of these in the desalination technology. Lastly, emerging new technologies, advanced fabrication methods and novel functional hybrid materials are reviewed to equip the readers with the latest research trends. Thus, a comprehensive review is essential which will provide current and future researchers an insight on the importance and significance of utilizing functional materials in various desalination technologies.

Keywords: Desalination, Photocatalysts, Electrocatalyst, Antimicrobial, Magnetic, Antimicrobial, Sorbents.

Contents

1. Introduction	4
1.1 Desalination- a solution to water scarcity	4
1.2 Types of Functional Materials.....	5
2. Photocatalysts.....	11
3. Electrocatalysts	24
4. Photothermal Materials.....	35
4.1 Plasmonic materials	42
5. Magnetic Materials	46
6. Antimicrobial Materials	56
6.1 Antimicrobial Inorganic-Inorganic Hybrid Membranes	72
7. Sorbent Materials	80
8. New Emerging Trends	93
9. Challenges associated with Functional Materials in Desalination	100
10. Conclusion and Future Recommendations.....	110
11. Abbreviations	115
12. References	116

1. Introduction

1.1 Desalination- a solution to water scarcity

Rapid industrialization, urbanization, contamination of available freshwater resources and climate change have all led towards a challenge for providing ample and safe drinking water [1].

A large proportion of the world's population is experiencing fresh water shortages with an alarming scenario where according to the World Health Organization (WHO), about half of the world's population is predicted to live in water-stressed regions by the year 2025. The existing accessible fresh water resources do not match the patterns of the current consumption trends. This has led to the practice of alternative methods such as utilizing desalted seawater or recycling wastewater for efficient water consumption. Desalination of the abundant seawater resource has emerged as a promising technology to meet the current fresh water demands. At present, the Middle East has the largest global desalination capacity (49.1%), followed by North America (16.2%) and South America (13.3%). In total, about 90 millionm³ of water is desalinated each day [2, 3].

The two most prominent desalination categories are thermal and membrane-based desalination processes. Thermal desalination utilizes evaporation and condensation for salt separation, while membrane based desalination processes utilize different types of semi-permeable membranes [4-7] to restrict salt passage. Both thermal and membrane technologies have their prominent place in desalination. For example, thermal desalination plants such as multi-stage flash (MSF) and multiple effect distillation (MED) processes dominate in the Middle East [2], where 70% of total desalination is thermal driven. This is primarily due to high feed salinities which are often

impacted by hydrocarbons and Red Tides. While on the other hand, about 80% of the total desalination plants today are based on reverse osmosis (RO) technology worldwide [8]. Hence, both thermal and membrane-based desalination processes hold immense importance in terms of research advancements and process improvements. In spite of desalination's versatility in meeting fresh water demands and tackling current water scarcity, the process can be energy intensive leading to high energy requirements and considerable running costs [9]. Nevertheless, both thermal and membrane based processes are undergoing extensive research for favorable energetics for lower specific energy consumptions (kWh/m^3). Seawater RO (SWRO) has undergone a credible reduction in energy consumption from 10 kWh/m^3 in the 1900's to about $3\text{-}4 \text{ kWh/m}^3$ at present [10], while thermal desalination requires a large energy input of about 13 kWh/m^3 (for MSF) [2]. With the growing trend in wastewater discharges from both municipal and industrial sources, water pollution is on a rise, leading to a detrimental effect on existing groundwater and seawater quality. Thus, this necessitates optimized thermal systems and desalination membranes. Hence, over the years, many different types of functional materials have emerged in meeting specific desalination requirements [11-14].

1.2 Types of Functional Materials

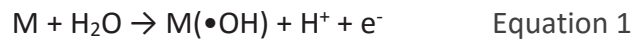
Functional materials may be characterized as those materials which have certain innate properties to be able to perform certain functions of their own. Their classification is usually related to materials with specific properties such as magnetic, electric optical, photocatalytic and others. Such materials may be found in all classes of materials including metals, ceramics and organic materials. Functional materials are known to be applicable in a variety of applications

including energy storage devices [15], as sensors [16], as actuators [17] in water treatment [18] and in many novel electronic devices [19] for medicine, biotechnology, avionics and defense applications. Recent and old review papers have been material oriented, focusing on specific types of functional materials such as cellulosic materials [20, 21], phenolics [22], graphene oxide (GO) [23], metallo-polyelectrolytes [24], carbon-based materials [25, 26] and several others [27-30]. Other review papers have been more application-oriented focusing on a specific application of several functional materials including cancer therapy [31], 3D printing of devices [31], pharmaceuticals [28], photodetectors [32], wastewater treatment [33], catalysis [34] and others [35, 36]. In general, the importance on the advancement of numerous functional materials for diversified applications cannot be stressed further. Desalination holds no exception, whereby significant advancements have occurred during the last decade in this field utilizing functional materials, both in thermal and membrane based systems. For example, recently, CNTs were reported to be used as an electrocatalyst forming the negative electrode in an electrochemical system enabling in situ membrane self-cleaning during desalination [37]. Even though several research papers have been published on numerous functional materials used in desalination [11, 38-41], they have been all targeted towards either a specific functionality or specific materials. A comprehensive review collating the research studies of various functional materials utilized in desalination is essential. This review highlights the functional materials and their respective functions utilized in this field. Through providing an insight on the significance of utilizing such materials in desalination, doors will be open for further improvement for cost effective, efficient desalination of brackish and seawaters.

The types of functional materials that are considered in this review are described below:

- Photocatalysts: these are semiconducting materials which get activated through photon absorption of radiation and consequently stimulate a redox process. Figure 1 shows the photocatalytic mechanism highlighting both oxidation and reduction mechanisms [42]. When light energy falls on the catalyst surface, the valence band electrons may get excited and move to the conduction band of the catalyst, provided the incident light energy is equivalent or greater than the catalyst bandgap. This generates electron-hole pairs with a possibility of participation of these in redox reactions with the compound adsorbed on the photocatalyst [43]. The holes created in the valence band can oxidize donor molecules and react with water molecules to generate hydroxyl ions through the advanced oxidation process. Hydroxyl radicals produced through this oxidation process acts as a strong oxidant enabling chemical reactions leading to pollutant degradation during water purification. The conduction band electrons may react with dissolved oxygen species to form superoxide ions and induce redox reactions. The efficacy of such photocatalytic materials in the desalination field is discussed in detail section 2
- Electrocatalysts: they participate in electrochemical reactions by functioning at the electrode's surface or in some cases might be the actual electrode itself. Electrochemistry provides a versatile and a powerful means for destroying various contaminants in water through a variety of electrochemical procedures [44], among which electrochemical oxidation (EO) is by far the most popular one. Electrocatalysis involves both oxidation and reduction through the direct transfer of electrons in which the electrocatalysts play an important role in assisting in the transfer of electrons between the working electrode and the electrolyte medium. The electrocatalyst avoids a large overpotential hence or otherwise

required in the delivery of electrons. Selective oxidation of organics occurs at the electrodes on which chemisorbed active oxygen is formed, whereas “active oxygen” •OH radicals are physisorbed at the electrodes. The contaminants are thereby completely mineralized by these •OH radicals to harmless gases or inorganic ions. Equation 1 shows the proposed model for the formation of physisorbed hydroxyl radicals where M denotes the electrocatalyst anode [45]. Electrocatalytic materials in desalination membranes are discussed in section 3.



- Photothermal materials: these materials absorb light and convert it to heat energy which can be used for water evaporation in desalination. The conversion is through thermalization and non-radiative recombination of the photo-generated electron–hole pairs. Instead of bulk evaporation, the target is to locally concentrate light absorption and heat generation from the sun to those places where the evaporation rate of the water is the highest. These places are usually the interfaces between air and water. Therefore, exploiting the photothermal effect by localized solar concentration makes thermal desalination an energy-efficient process [46]. Figure 2 shows the schematic diagram of the photothermal conversion. Solar absorption and heat transfer play important roles, whereby it becomes essential for photothermal materials to have optimum optical and thermal properties. Section 4 discusses the utility of such materials in desalination in detail.

- **Magnetic materials:** in general, magnetic materials are those materials which can be either repelled or attracted when placed in a magnetic field. These functional materials find immense importance in desalination as draw solutes in forward osmosis [47], for enhanced selectivity in RO [48], to enhance the performance of solar stills [49] and various other ways as discussed in detail in section 5.
- **Antimicrobial materials:** these functional materials find an important place in desalination, predominantly for antifouling membrane properties. Biofouling is by far one of the major problems in membrane based desalination systems leading to decreased membrane performance, higher energy consumption and membrane degradation over the period of time. Biofouling is referred to the unwanted deposition and growth of biological matter on the membrane's surface. A variety of antimicrobial functional materials have been sought to abate this biofouling problem, discussed in detail in section 6.
- **Sorbent materials:** these functional materials are widely used for absorption and adsorption purposes, with the latter being a predominant method for rejection of salts and other ions from water. Owing to its low cost and simplicity in design together with flexibility, sorption method is an attractive technique in desalination. Particularly, the rejection of solutes by adsorption onto selective adsorbents holds great potential for further research into the field of adsorbent materials, while absorbents hold importance in increasing the water absorption to solar irradiance in solar desalination systems. Adsorption is the tendency of chemical species adhere onto a solid surface. During the process, molecules from either a gas or liquid

phase gets accumulated on a solid surface where it is bound to it by physical and/or chemical interactions. The solid is called the adsorbent while the substance adsorbed at the surface is called the adsorbate [50]. Section 7 details the studies on functional sorbent materials utilized in the desalination field.

With these numerous functional materials utilized in desalination, each one holds its own importance in performing specific functions for treating sea and brackish waters. Many materials provide more than one function and thus can be advantageous in combining multiple functionalities. A good example of such a material is graphene and graphene based composite materials which can act as a sorbent, photocatalyst, electrocatalyst, as a photothermal material and as a photoelectrocatalyst in desalination [51]. This review aims to address functional materials specifically in desalination, highlighting existing methods, materials and new emerging trends with the purpose of instilling new insights into this area for current and prospective researchers.

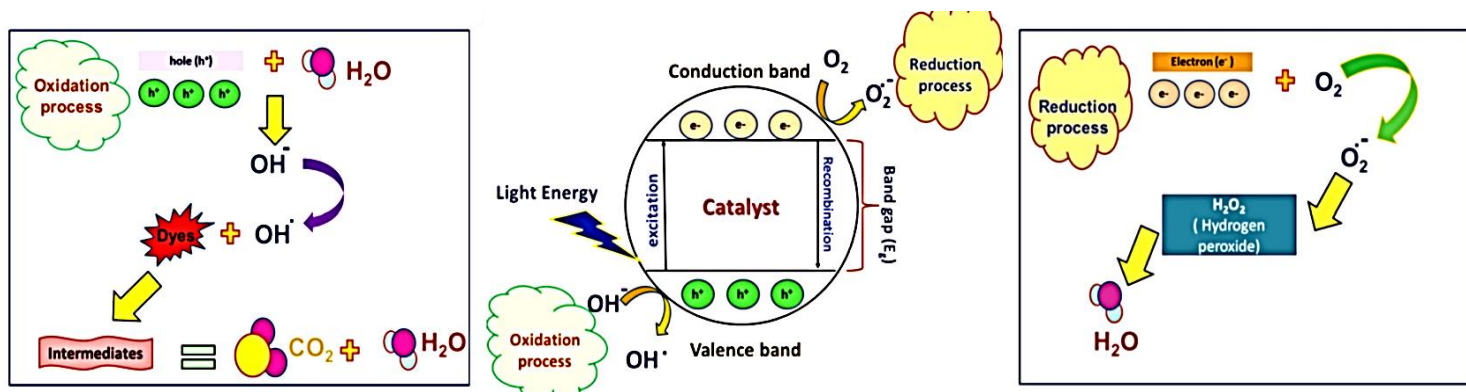


Figure 1: Schematic representation of a photocatalytic mechanism utilizing semiconductor photocatalysts [42]

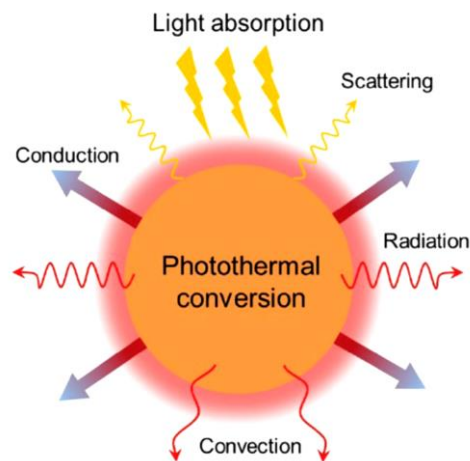


Figure 2: Schematic of photothermal conversion. Reproduced from [52] with permission from The Royal Society of Chemistry

2. Photocatalysts

Photocatalytic materials find great potential in desalination primarily for disinfection and decomposition of detrimental substances under the sun lights containing UV rays. This then helps to control the biofouling problem prevalent in the desalination membranes today. Moreover, a parallel filtration unit coupled with photocatalytic degradation is an ideal setup for seawater desalination containing various organic and inorganic contaminants. Numerous photocatalytic materials have been investigated for this purpose including TiO_2 [53, 54], WO_3 [55], Fe_2O_3 [56], CuS [57], ZnO [58] and various bismuth compounds [59-61]. However, owing to its high adsorption in the ultraviolet (UV) region, and high chemical stability, by far, the most predominant photocatalytic material researched today is titanium dioxide (TiO_2) [62]. Its photocatalytic function helps to decompose organic chemicals and kill bacteria [63] by generating active oxygen species such as OH^\cdot and hydrogen peroxide (H_2O_2) which can destroy the bacterial

cells [64, 65]. Apart from its photocatalytic properties, the hydrophilicity of TiO₂ makes it an attractive material for membrane modification. For instance, the contact angle of the PVDF- TiO₂ membranes was found to be lower, 23°, than the bare PVDF membrane which was reported to be 116.4° [66]. Thus, the synergetic effect of these properties facilitates fouling prevention, promotes water permeability and introduces self-cleaning function on the surface by spreading of water owing to the hydrophilicity [67]. Different factors may affect TiO₂ efficiency including the concentration of the pollutant, duration of light irradiation, depth of light penetration into TiO₂ surface and TiO₂ morphology. Just like other catalytic materials for various catalytic reactions [68-71], results have proven that when used in the nano-form, TiO₂ nanoparticles show improved activity owing to its high surface area in contrast to their bulk form [72, 73]. Nevertheless, immobilization of nano-sized TiO₂ on other substrates [74-76] becomes essential for easier recovery and to prevent leaching. In general, TiO₂ based photocatalytic membranes show improved performances with greater permeate fluxes compared to the neat membranes [77, 78].

Free standing TiO₂ photocatalytic membranes have been reported in several research studies [79-81], however, their usage in desalination is limited due to the challenges associated with the scale up of such membranes. Thus, the most prevalent ones are polymeric- TiO₂ membranes.

Various approaches have been reported for integrating TiO₂ nanoparticles into desalination membranes [82, 83]. However, by far, the most common method reported is self-assembly [84].

For example, Kwak al. [85] designed TiO₂ nanoparticles (~10 nm or less) self-assembled PA TFC membranes through COOH functional group bonding of the aromatic PA layer. Similar salt rejections of ≈96.6%, with a higher water flux of 14.4 gdf was obtained with the TiO₂-TFC membrane compared to 13.2 gdf for the neat TFC membrane, tested at 2000ppm NaCl feed

solution. Figure 3a shows the plots of the survival ratios of *E. coli* bacteria in both the TiO₂ hybrid and the neat TFC membrane under light and dark conditions. Under UV illumination, the survival ratio for the hybrid membrane is the lowest after 4 h of test, while the neat TFC membrane still showed above 40% survival ratio for *E. coli* under the same testing conditions. Kim et al. [86] fabricated the same TiO₂-PA hybrid membrane which also showed superior photo bacterial effect on *E. coli* under UV light illumination, with lesser loss of RO permeability over time (Figure 3b) and an enhanced salt rejection (96%) compared to the neat PA membrane (94.7%). However, the TiO₂ attachment was not strong enough as some of the TiO₂ particles were observed to detach under the RO seven-day operation. Mansourpanahetal et al. [87] reported similar findings where no strong bond was established between the TiO₂ nanoparticles and the polyethersulfone (PES) –OH functional groups. Bae et al. [84] also used an electrostatic self-assembly method between the TiO₂ nanoparticles and sulfonic acid groups on a PES UF membrane's surface. The nanocomposite membrane was seen to maintain a higher stabilized flux of more than 36% of the initial flux compared to the bare PES membrane (20% of the initial flux). In addition, improved rejections were obtained with the composite membrane for a mix feed of membrane bioreactor (MBR) sludge, suspended solids (SS) and soluble chemical oxygen demand (SCOD). Figure 3c shows the rejection profile with increasing molecular weight cut-off (MWCO) of PES which confirms the higher rejection capability of the nanocomposite membrane at each MWCO. Madaeni and Ghaemi [88] fabricated self-cleaning TiO₂ coated TFC membranes through the self-assembly approach. They studied the effects of TiO₂ concentration in membranes, the duration of UV irradiation, the duration of keeping the membranes in water on self-cleaning, presence of SiO₂ particles, and the effect of roughness on the self-cleaning ability. SiO₂ helped in increasing

the surface acidity rendering the membrane ultra-hydrophilic. Membranes immersed in 0.001 and 0.003 wt.% TiO₂ particle solution showed improved self-cleaning property and higher flux. However, with higher percentages at 0.005 wt.% TiO₂ particles, the flux was observed to reduce apparently due to pore blockage. In addition, the self-cleaning property was observed to increase with a longer UV irradiation time until a plateau was reached with no further increment. Similar research studies [78, 89] report low concentrations of TiO₂ in various membranes. In some cases, a higher TiO₂ percentage of 4 wt. % was reported to be an optimum concentration for superior disinfection efficiency [90], while in another study [91], an increase in concentration of the TiO₂ nanoparticles in a hybrid TiO₂-PVDF membrane did not show any significant improvement in its photocatalytic activity. Lee, et al. [82] showed that an increase in TiO₂ concentration up to 5.0 wt. % in PA- TiO₂ membranes led to a slight increase in MgSO₄ rejection with a slight decrease in flux. However, a drastic decrease in salt rejection was observed for concentrations beyond 5.0 wt. %. Figure 3d depicts the change in salt rejection and water flux with a change in TiO₂ loading. Consequently, the mechanical strength of the membranes also significantly decreased with the PA-TiO₂ layer peeling off from the PES support after filtration. In addition, different curing temperatures and its effect on membrane performance were also studied. With an increase in the curing temperature, the rejection was seen to continually increase, however with a decrease in flux. This was attributed to the crosslinking of the polymeric chains at a higher temperature, which provided a dense, rigid membrane structure. Hence, mechanical strength was also seen to improve accordingly. Composite membrane cured at 70°C for 5 min exhibited optimum membrane performance with >95% MgSO₄ rejection and a permeate flux of 9.1 L/m². h. On the contrary, Mansourpanah et al. [87] found that the TiO₂ concentration had no effect on the

desalination performance parameters as the water flux and NaCl rejection showed no significant change on the PES/polyimide (PI) blend membranes.

Various photocatalytic membrane reactors have also been reported, which can combine both the photocatalytic oxidation and membrane filtration processes. A TiO₂ coated membrane may be placed inside a photoreactor or an organic membrane may be submerged in a slurry containing TiO₂ nanoparticles [83, 92]. The effect of hybrid TiO₂ and biomass ash contact time of seawater desalination was studied using a photo reactor equipped with UV light. The result indicated that with an increase in contact time of up to 6 h, the salt concentration gradually decreased by more than 25%. Thus, the hybrid mixture was able to reduce the seawater salinity effectively [93]. Several review papers highlight different aspects of such photocatalytic reactors [94]. For example, Mozia [95] reviewed the pros and cons of photocatalytic membranes in photocatalytic membrane reactors reviewing their flux, permeate quality and membrane fouling. These reactors may help mitigate fouling based on a filtration cake layer owing to the decomposition of the contaminants. In addition, catalyst separation becomes easier or sometimes unnecessary as the membrane could be used as long as the TiO₂ remains active. However, membrane lifetime needs to be assessed and the membrane needs to be exchanged when the catalyst loses its activity.

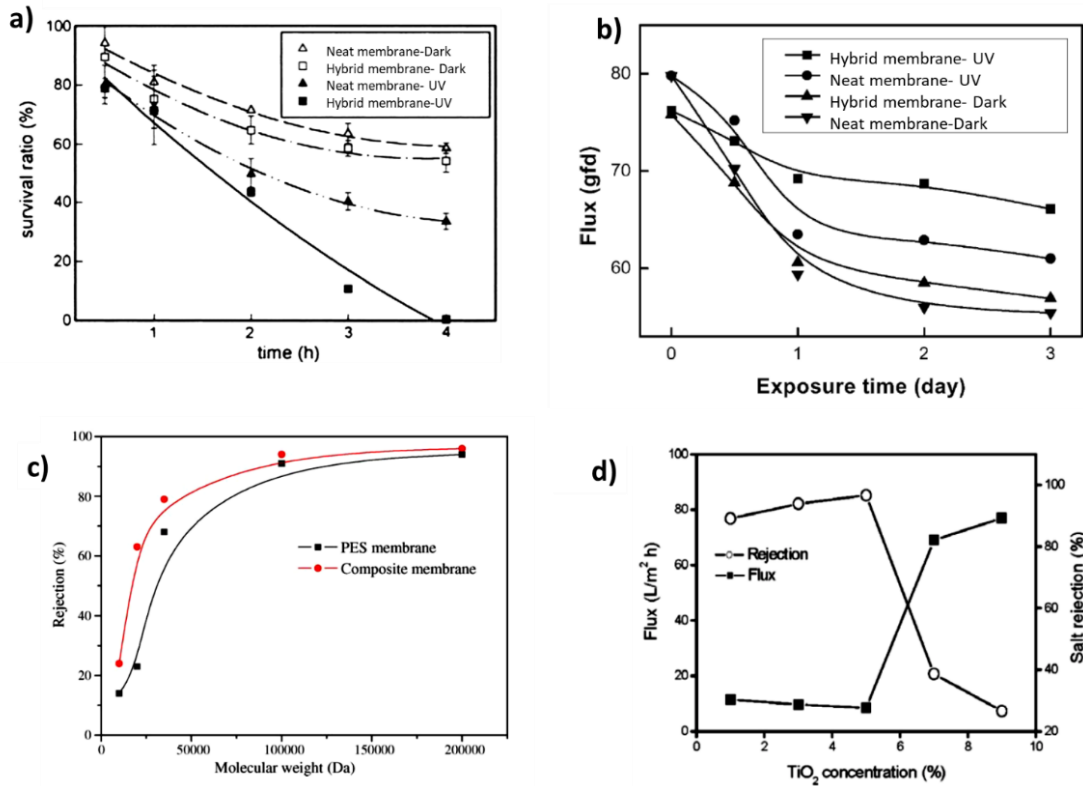


Figure 3: (a) Photocatalytic bactericidal effects of the TiO₂ hybrid and neat aromatic polyamide membranes in the dark and with UV illumination [85]. (b) Water flux of the hybrid and the neat LP membranes with and without UV light after exposure to microbial cells [86]. (c) Rejection profiles of PES and nanocomposite membranes [84] and (d) Effect of TiO₂ concentration on the membrane performance of water flux and MgSO₄ rejection (MgSO₄ concentration was 2000 ppm).

More frequently, TiO₂ is integrated or supported on other materials for enhanced efficiency. Alumina (Al₂O₃) has been widely reported as a support material for photocatalyst immobilization [96, 97]. Djafer et al. [98] fabricated an UF Al₂O₃ supported TiO₂ membrane through slip casting approach whereby defect-free layers of 3μm thickness TiO₂ nanoparticles were coated on the support as shown in Figure 4a. Pure water flux of ~150 L.h⁻¹.m⁻².bar⁻¹ was registered with good photocatalytic degradation of methylene blue. Zhang et al. [99] developed TiO₂ nanotube membranes by grafting TiO₂ into Al₂O₃ MF membrane channels (Figure 4b). Photocatalytic activity was investigated through an in-house filtration setup made with a 250ml glass reactor, in which

the permeate was collected in a beaker and its weight was measured by recording the permeate volume. They observed that placing the light source closer to the photocatalyst membrane enhanced the photocatalytic activity considerably. A lower decrease in membrane flux was observed with the TiO₂ membrane (27%) with a UV irradiation of 11W compared to the dark condition (67%). In addition, 100% rejection was achieved for humic acid for the TiO₂ nanotube membranes [99]. Recently, the trend has shifted towards using photocatalytic materials along with other functional materials for multiple functionalities. For example, Ma et al. [100] integrated membrane separation and photocatalytic bacterial inactivation by fabricating a hybrid Ag–TiO₂/hydroxyapatite (HAP,)/Al₂O₃ composite membrane through a facile two-step approach involving sol–gel method followed by calcination. Figures 4c and 4d show the morphology of HAP-supported Ag–TiO₂ composite as revealed by the TEM and high resolution TEM (HRTEM) images respectively. A 10–30nm thick Ag–TiO₂ layer was observed which covered the HAP particles. A crossflow experimental setup confirmed that Ag–TiO₂ provided photocatalytic degradation of *E. coli* while HAP acted as an efficient bacterial adsorbent. The viable cell count (cfu/ml) for the composite membrane remained fairly low <10¹ compared to the HAP/ Al₂O₃ membrane (>10³) under UV irradiation. Moreover, the *E. coli* membrane flux without UV was reported <200 L.m⁻².h⁻¹, while with UV irradiation, flux >300 <200 L.m⁻².h⁻¹ was achieved. This was owing to the destruction of the bacteria which was responsible for biofouling. A similar potential desalination membrane was reported by Liu et al. [101] where a simultaneous action of blocking and degrading pathogens organic pollutants from water was achieved. They fabricated Ag/TiO₂ nanofiber membranes through electrospinning, followed by vacuum filtration and hot press on the glass fiber support. Electrospinning has emerged as a versatile method to fabricate non-

woven fiber meshes where the process gives flexibility in controlling the fiber composition and morphology [102-104]. Membrane performance by a simultaneous photocatalytic disinfection and membrane filtration was reported, which was carried out through a dead-end filtration setup. Disinfection was evaluated by *E. coli* inactivation under solar irradiation (100 mW/cm^2). The Ag/TiO_2 nanofiber membranes achieved 99.9% *E. coli* inactivation bacteria inactivation under solar irradiation within 30 min [101]. Several other studies report on the design of Ag/TiO_2 and Al_2O_3 supported TiO_2 photocatalytic membranes [105, 106].

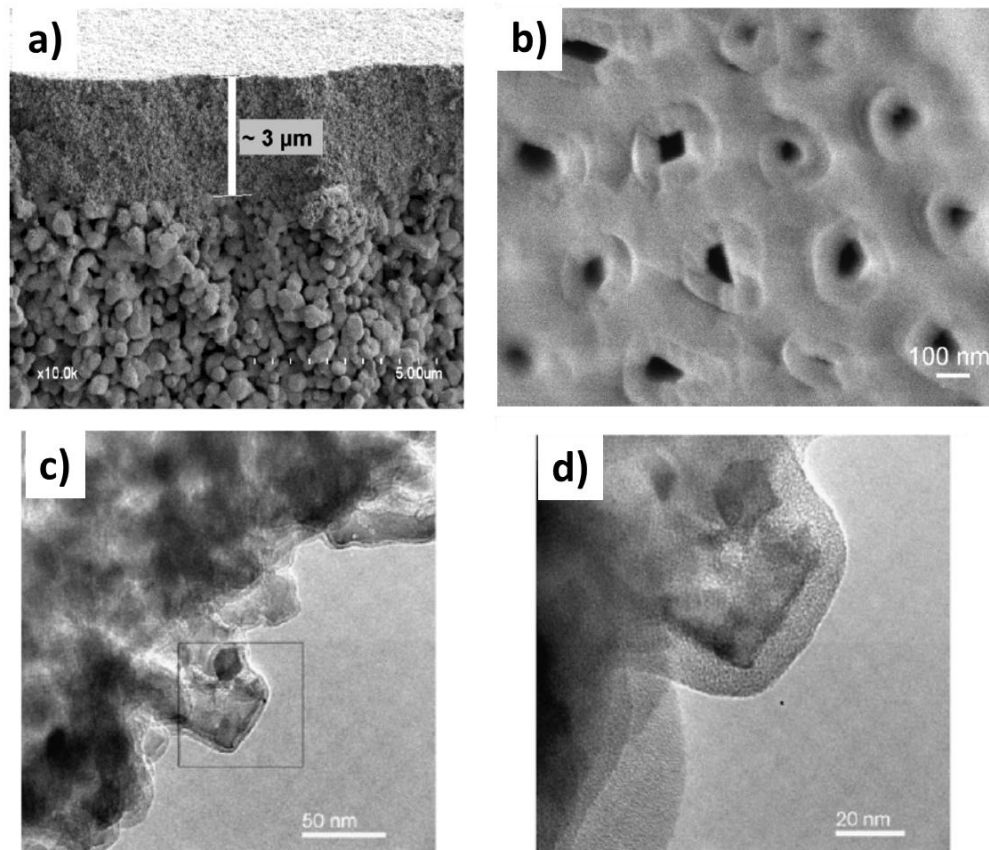


Figure 4: (a) SEM cross-section of a $3\mu\text{m}$ TiO_2 layer deposited on an alumina support [98] (b) SEM image of the TiO_2 nanotube membrane after 2 h of grafting [99], (c) TEM and (d) HRTEM images of HAP-supported Ag-TiO_2 composite [100].

Besides TiO_2 , other semiconductor materials such as ZnO has attracted much interest as photocatalytic materials in various applications due to its excellent disinfectant capability, its hydrophilicity and non-toxicity [107, 108]. In desalination in particular, the material holds immense importance whereby it can form ROS causing bacterial cell penetration and hence killing any bacteria in the water [109]. Patel et al. [110] reported the effect of different photocatalysts on the rate of production of distilled water and its quality using solar desalination. Local water samples from the monsoon season were treated using a solar still with an effective area of $567 \times 660 \times 4 \text{ mm}^3$. The production rate of desalinated water was seen to increase with time, reaching an optimum after 2-3h, and later decreasing during the sunset. A remarkable difference was obtained between the permeate of desalinated water using semiconductor metal oxides and that of without those metal oxides (Table 1), where the TDS and various cation levels were seen to decrease in the presence of the photocatalyst. Recently, Zinadini et al. [111] reported anti-biofouling PES mixed matrix NF membranes made from ZnO/multiwalled carbon nanotubes (MWCNTs) nanocomposite. They coated MWCNTs with ZnO nanoparticles and then blended it in PES casting solution. These composite membranes showed improved pure water flux owing to its increased hydrophilicity by ZnO and CNTs. When illuminated under UV light, the presence of just 0.5 wt. % ZnO/MWCNTs caused degradation of the foulants with improved dye rejection compared to the bare PES membrane. This was attributed to the repulsion effect between nanocomposite membrane and the dye molecules having opposite charges. Hinai et al. [112] compared the antibacterial properties of ZnO nanorods and ZnO nanoparticles incorporated PES membranes. The results showed better performance for the nanorods owing to its higher surface area, compared to the nanoparticles. Owing to the release of Zn^{2+} ions and the formation of ROS

such as H₂O₂ and O₂⁻, 6 wt. % ZnO nanorods/PES membrane was able to successfully inactivate almost 90% E. coli, together with complete inhibition of its regrowth.

Table 1: A comparative study in quality of water with and without photocatalysts [110] (all units are in mg/L except for pH, conductivity is in mmhos.cm⁻¹)

Parameter	Raw water	Desalinated water without using photocatalyst	Desalinated water with photocatalyst		
			MnO ₂	PbO ₂	CuO
pH	8.20	7.1	7.2	7.0	7.1
Conductivity	0.629	0.084	0.038	0.025	0.050
TDS	700	368	48	52	48
Free CO ₂	8	14	6	6	7
Total Alkalinity	157	28	20	12	18
Total Hardness as CaCO ₃	170	16	8	8	6
Calcium	59.7	5.5	2.5	2.5	1.7
Magnesium	5.1	0.5	0.4	0.4	0.4
Fluoride	0.5	0.2	0.3	0.3	0.1
Iron	0.6	0.3	0.3	0.5	0.4
Chloride	42.6	14.2	14.2	14.2	14.2
Sulphate	49.4	20.6	28.8	41.2	32.9
Nitrate	4.5	1.6	2.1	1.2	1.1

Recently, more emphasis is being put into developing new generation photocatalysts, which are not just limited to the UV region of the electromagnetic spectrum, but instead can be utilized in the visible region as well [113]. Liu and coworkers [114] showed that a few-layered vertically aligned MoS₂ films could utilize the whole visible light spectrums (~50% of solar energy). The bandgap of MoS₂ was increased from 1.3 to 1.55 eV. Enhanced electron–hole pair separation was achieved by using a 5nm Cu film on the MoS₂ films, which promoted ROS generation, and hence increased the disinfection rate in water by almost six times. In comparison to TiO₂, the Cu- MoS₂ films gave faster bacterial inactivation under both visible light and sunlight, achieving a water disinfection of >99.999% of bacteria in 20 min. Doping of TiO₂ with certain materials such as nitrogen and palladium [115] can render the material active in the visible range, thus requiring

much lower energy usage. The band gap of TiON thin films was reported to be $\sim 3.00\text{eV}$, compared to TiO_2 thin films with $\sim 3.27\text{eV}$. TiO_2 has been reported to be used in combination with various supports and materials as discussed previously. Many at times, coupling TiO_2 with narrow band gap semiconductors can render the photocatalyst to be to be utilized in the visible region of the spectrum. For example, $\text{TiO}_2/\text{Bi}_2\text{O}_3$ composite photocatalyst may be used for elimination of water contaminants. Bi_2O_3 has a strong absorption in the visible light region and when coupled with TiO_2 , the heterojunction can cause enhanced charge separations [116]. Yet another important material which has emerged as a promising support material for TiO_2 is graphene. In fact, many graphene-based photocatalysts have been developed for water disinfection to date. It is one of the recent smart nanomaterials in the carbon group which has attracted immense attention owing to its exceptionally high surface area ($2630\text{ m}^2\cdot\text{g}^{-1}$), high electrical conductivity ($106\text{ s}\cdot\text{cm}^{-1}$), superior mechanical properties ($\sim 1.1\text{ TPa}$), breaking strengths (42 N m^{-1}), good thermal conductivity, hydrophilicity and excellent optical transmittance ($\sim 97.7\%$) [51]. Table 2 lists some of the advancements on binary and ternary graphene photocatalysts composites. Zeng et al. [117] developed ternary graphene based nanocomposites to facilitate improved charge separation in TiO_2 . Highly dispersed TiO_2 and carbon dots co-decorated rGO (CTR) was synthesized via a hydrothermal approach. TiO_2 -rGO (TR) was also synthesized for comparison purposes. Under solar light irradiation, CTR slurry system reached 1.03 log inactivation of *E. coli* in 60 min compared to only 0.58 log inactivation by TR. These results proved that the enhanced photocatalytic activity of CTR composite was improved by carbon dots. Figure 5a shows the TEM image of untreated *E. coli* cells showing intact and well-preserved membrane cells, while Figure 5b shows bacterial inactivation after solar light irradiation leading to membrane damage and

leakage of interior components. Improved generation of ROS production such as $O_2^{\bullet-}$ and H_2O_2 , together with enhanced charge separation in the CTR photocatalyst led to accelerated photocatalytic bacterial inactivation. Figure 5c depicts a scheme explaining the photocatalytic process in CTR, whereby the electrons from TiO_2 transferred to the carbon dots via rGO nanosheets. These trapped electrons in the carbon dots get donated to the O_2 molecules, forming $O_2^{\bullet-}$ radicals which in turn does the part for bacterial cell membrane damage. In principle, photocatalytic activity may be enhanced through greater light absorption and lesser recombination losses of the photogenerated charge carriers. Apart from doping and integrating them with other semiconductor materials, photocatalytic function may be enhanced by defect engineering, spatial structuring and enhancing the proportion of active facets [118].

Recently, photocatalytic treatment of desalination concentrate was reported. Brine treatment may reduce concentrate volume and can increase water recovery. Lin et al. [119] synthesized Fe-doped TiO_2 nanocomposite thin films on optical fibers using polymer-assisted hydrothermal deposition method. RO concentrates from brackish water and municipal wastewater desalination facilities were investigated to test the photodegradation and photocatalytic efficiency of the nanocomposite under natural sunlight. A wide spectrum of solar irradiation was utilized. The photocatalytic process was also observed to be affected by the pH of the solution due to the adsorption between the dye molecules and catalyst surface, and the redox process of photocatalysis. With no photocatalyst, $\approx 20\%$ Rhodamine B (RhB) degradation was observed due to direct photolysis, while a 69% initial degradation efficiency was achieved with the catalyst. A 19% decline in performance was observed thereafter which remained at $\approx 50\%$ after 10 days of operation owing to the adsorption of RhB molecules onto the photocatalytic fibers. However, the

photocatalyst efficiency was reported to be restored when soaked in ethanol-water solution. Nevertheless, the research on photocatalytic materials in desalination is on a rise with novel materials being developed and tested for improved antifouling and desalination performances.

Table 2: Graphene-based photocatalysts for water disinfection

Reference	Photocatalytic Material	Light Source	Performance
Akhavan et al. [120]	rGO@ TiO ₂ film	Solar	100% inactivation of E.coli.
Liu et al. [121]	GO-TiO ₂ nanorod	Solar	100% inactivation of E.coli.
Gao et al. [122]	GO-ZnO-Ag	Visible	99.99% inactivation of E.coli
Gao et al. [123]	GO-CdS	Visible	100% E.coli and B. subtilis inactivation
Wang et al. [124]	rGO-C ₃ N ₂ -S	Visible	100% E.coli inactivation
Gao et al. [125]	TiO ₂ - GO	UV and Sunlight	Improved MB photodegradation; about 60-80% faster under UV and 3-4 times faster under sunlight.
Zeng et al. [117]	TiO ₂ - C dots/rGO	Solar	1.03 log inactivation of E. coli in 60 min.

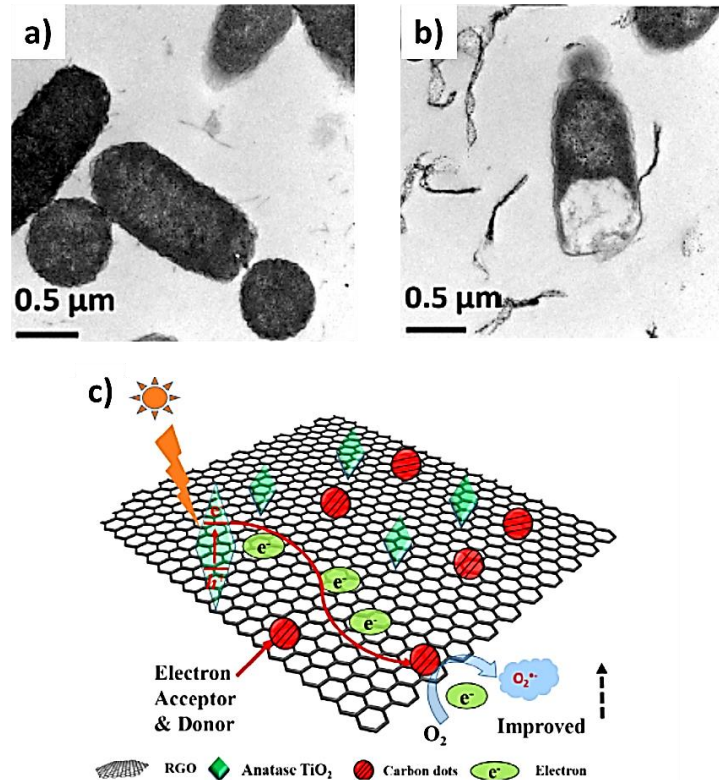


Figure 5: (a) TEM image of untreated E.coli, (b) TEM image of E. coli cells treated by CTR under simulated solar light, and (c) possible electron transfer paths for O₂ reduction by CTR [117]

3. Electrocatalysts

Over the last decade, electrochemistry has offered numerous advances in desalination such as controlling of biofouling [44] and real-time cleaning of membranes for improved membrane lifetime [126, 127]. Mostly, the electrochemical membranes, such as those developed from carbon nanotubes (CNTs) aims at degrading organic and inorganic pollutants through electrochemical oxidation processes, but at the same time, they help in increasing the separation efficiency by the hollow CNT structure leading to smooth passage of water molecules and hindering the passage of ions. CNTs is an emerging nanomaterial which may be used as a filler, or either directly for improved membrane performances. It possesses good mechanical strength,

chemical resistance, ease of functionalization, and a high surface area and an aspect ratio [128]. In addition, these membranes offer energy savings and decreased operational times [39]. Various methods have been reported for the fabrication of electrochemically functionalized CNT membranes, whereby CNTs may be randomly oriented or aligned for close-fitting of CNT pores [129, 130]. Due to its conductive nature, the most exciting application of CNTs as electrocatalysts in desalination has emerged to be as self-cleaning membranes, whereby conductive CNT membranes are employed for membrane based desalination systems for improved performances through fouling control. The membranes are capable of inactivating microorganisms and their conductivity imparts these membranes to clean away the foulants in-situ by application of a voltage during desalination operation. Several recent developments have led to the study of these conductive membranes through electrochemical characterization methods such as electrochemical impedance spectroscopy (EIS) which can help to detect membrane fouling.

Fouling prevention and membrane cleaning through conductive membranes acting as an electrocatalyst in the electrochemical setup may be explained by several mechanisms. Membrane cleaning might occur through direct or indirect oxidation or through bubble formation on membrane surface. Nevertheless, the mechanism largely depends upon the nature of the conductive surface and the type of foulant, and their electrostatic interactions or electrochemical redox reactions at the membrane surface [126]. During electrochemical defouling, the conductive membrane may either be used as an anode or as a cathode in the electrochemical setup. However, the most frequent configuration is as a cathode to prevent CNT oxidation. The foulants may be swept away through hydrogen bubble formation from membrane

surface when the conductive membrane is used as a cathode. Thus, electrocatalytic properties play an important role for optimized electrode performance; lower over potentials are anticipated for hydrogen evolution reaction (HER) and oxygen evolution reaction (OER) so that bubble generation could take place with lower energy requirements [127, 131]. Wu et al. [132] demonstrated that nanobubbles can be used to sweep away the existing foulants, and can also prevent biofouling simultaneously. Voltage was applied between a highly oriented pyrolytic graphite (HOPG) surface as a working electrode, and a counter electrode. On subsequent water electrolysis, hydrogen and oxygen were produced, forming bubbles at the liquid/solid interface. Nanobubble stability and morphology is still a question for open discussion, with only little understanding in this area till date [133]. On surface coverage by nanobubbles, a physical barrier is formed which prevents the foulant coverage on the membrane surface. Atomic force microscopy (AFM) was used to observe the nanobubbles which were produced through electrochemical treatment of the surface for 20 s before bovine serum albumin (BSA) exposure. Protein coverage was seen to decrease by 26–34%, together with removal of the foulant by detachment of the adsorbed protein from the solid–liquid interface. However, through AFM, it was not possible to determine if the nanobubbles were produced either on the protein film, or between the membrane surface and the film. Nevertheless, the protein molecules were seen to wash away with the help of the nanobubbles, while they remained on the areas which was covered with the bubbles. Atomic force microscopy (AFM) was used to observe the nanobubbles which were produced through electrochemical treatment of the surface for 20 s before bovine serum albumin (BSA) exposure. Protein coverage was seen to decrease by 26–34%, together with removal of the foulant by detachment of the adsorbed protein from the solid–liquid interface.

Sun et al. [134] studied defouling mechanisms for aligned CNT membranes. They reported both electrochemical oxidation and electrochemical reduction as effective means for CNT membrane defouling from biomolecules. However, electrochemical oxidation was only applicable a limited number of cycles, whereas bubble generation through electrochemical reduction was reported as a preferred means for a large number of cycles for longer membrane lifetime.

Electrocatalytically active conductive membranes made from CNTs may be used either as self-standing or as mixed matrix membranes. Self-supporting CNT membranes are usually developed as bucky-papers. For example, Rashid et al. [135] studied a range of different nanotubes, multi-walled carbon nanotubes (MWCNTs), amine-functionalized MWCNTs and carboxylic acid-functionalized MWCNTs. For bucky paper synthesis, about 0.038%-0.064% (w/v) of MWNTs were dispersed in various surfactants namely Trix, β -CD and C6S. Following this, the solution was vacuum filtered through a PTFE membrane filter and the bucky paper was washed with Milli-Q water and methanol thereafter. These hydrophilic membranes had contact angles less than 55° and electrical conductivities in the range of 24 to 58 S/cm. The bucky paper dispersed with Trix surfactant gave rejection of almost all major organic contaminants with more than 80% efficiency. However, these membranes usually suffer from irregular pores and pore sizes and a CNT leakage potential posing health risks. Thus, the more popular CNT membranes for self-cleaning application are the mixed matrix membranes in which CNTs are usually dispersed in a polymeric matrix. The electrical conductivity of polymeric membrane may be increased by mixing CNTs, such as that reported by Coleman et al. [136], where they increased the electric conductivity of poly(p-phenylenevinylene-co-2,5-dioctoxy-m-phenylenevinylene) polymer by up

to ten times adding 8 wt.% CNTs. CNT-polymer membranes could exhibit tunable properties which deem that attractive for novel desalination membrane applications. On application of an electrical bias, these membranes could successfully control bacterial inactivation and thus prevent membrane biofouling. Electrically conductive polymer nanocomposite (ECPNC) membrane was reported to be fabricated from carboxyl functionalized MWCNTs. Sodium dodecylbenzene suspended with CNTs was deposited on a PES support layer, after which it was immersed in a 2.0% (w/w) m-phenylenediamine (MPD) solution. This was followed by immersion in 0.15% (w/w) trimesoyl chloride (TMC) dissolved in hexane for 30 s. When connected to a voltage generator (1.5 V square wave, 16.7 mHz), the rate of flux decline of *P. aeruginosa* suspension was observed to be three times lower than the control experiments as shown in Figure 6a, while the flux for non-conductive PNC membrane and the one with no applied voltage saw a drastic decline in flux with time. The red circles in Figure 6a represent membrane flushing points, after which complete flux recovery was achieved for the ECPNC membranes with applied voltage [137]. In an another study, de Lannoy et al. [138] developed electrically conductive UF membranes based on PVA, in which the CNTs were again functionalized with carboxylic acid. The CNT-PVA active layers on cellulose nitrate displayed high electrical conductivity, 20 times more than the bare PVA membrane. Membrane conductivity was observed to increase with CNT concentration, registering a 3.6×10^3 S/m for the maximum CNT concentration of 20 wt. %. However, the membrane with the lowest CNT concentration such as 2 and 5 wt. %, gave the highest amount of solute rejections $\approx 90\%$ as shown in Figure 6b. Pure water flux was found to be 1440 L/m² h at an operating pressure of 5.5 bars. Numerous other studies report on carboxylic

functionalized CNTs for electrically conductive membranes offering potential in desalination membranes [139, 140].

Zhang and Vecitis [141] reported conductive CNT-PVDF membranes for capacitive organic fouling reduction, where the membrane was placed on an UF support and operated as a cathode to create a negative surface charge via capacitive charging for fouling mitigation. A carbon cloth formed an anode for the experiment. Cyclic voltammetry (CV), an electrochemical technique was performed to characterize the Faradic reactivity and non-Faradic capacitance of electrodes. 10ppm polyacrylic acid (PAA) in 0.1–20 mM NaCl solution was used as an electrolyte, over a potential range of –1.2 to 1.2 V (Figure 6c). A very low density absence of any redox peaks indicated that the CNT-PVDF membrane was non-Faradaic. In addition, significantly less back washing time was required compared to the control PES membrane. The mechanism for fouling reduction was suggested to be the potential-induced cathodic negative surface charges which caused an increase in the energy barrier, and thus a decrease in the collision efficiency of the negatively charged foulants with the membrane's surface. Benson et al. [142] developed electrically conductive polyaniline-CNT fabric through electrodeposition. These membranes showed fast ion adsorption and high specific capacitances, rendering them valuable for low-energy desalination processes via CDI. Liu et al. [143] used an electrophoretic deposition (EPD) technique to fabricate CNT-zeolite composite electrodes to integrate the properties of electrical conductivity of CNTs and high adsorption capacity of zeolites. These electrodes were tested for Ca^{2+} rejection by CDI. An optimum concentration between CNTs and zeolite was found to be 1:4, which gave an electrosorption capacity of 25 mg/g for Ca^{2+} under an electrosorption voltage of

2.0 V. In addition, the composite electrodes also showed promising results for magnesium and sodium ions.

A novel in-situ cleaning method via bubble generation through hydrogen evolution was demonstrated by Hashaikeh et al. [37]. An electrically conductive layer of MWCNTs was deposited on a commercial Millipore membrane surface via vacuum filtration. This membrane was tested as a cathode in an electrochemical system with stainless steel counter anode and salt water as an electrolyte. Formation of micro-bubbles at the membrane surface during periodic electrolysis at a voltage of 2 V for 2–3 min helped in sweeping away of CaCO_3 and yeast suspension foulants. Following this study, Lalia et al. [127] fabricated novel electrically conductive carbon nanostructures (CNS)/PVDF membranes through vacuum filtration. Post heat treatment caused PVDF to act as a binder inside the CNS imparting the membrane better mechanical property. Electrolysis led to micro-bubble formation on the membrane surface, resulting in foulant removal. This led to the membrane sustaining higher fluxes through multiple filtration cycles of foulants as compared to those without periodic electrolysis. From Figure 6d, it can be seen that without in-situ cleaning, permeation flux decreased exponentially with time, while after the first electrolysis cleaning, a $20 \pm 2\%$ increase in flux (from 76 to 96%) was observed. Recently, Ahmed et al. [144] reported their work on electrically conductive membranes based on networked cellulose (NC) and CNS fabricated through vacuum filtration. The effect of NC addition in CNS was studied. The bare CNS membrane gave $45 \pm 1\%$ porosity, which decreased to $5 \pm 1\%$ for the CNS-NC membranes. Electrocatalytic activity of the CNS and CNS-NC membranes were compared by coating them on a glassy carbon (GC) electrode. Linear polarization (LP) curves gave the onset potentials for HER for CNS and GC-CNS-NC electrode to be -137 mV and -353 mV

respectively in 0.5 M H₂SO₄. A higher over potential for GC-CNS-NC might be attributed to the inactivity of the NC. Over potentials for OER for GC-CNS and GC-CNS-NC in 0.5 M H₂SO₄ were reported to be 1.04 and 1.18 V respectively. This was reported to be lower than the over potential for platinum working electrode at 1.82V. In addition, NC imparted improved hydrophilicity to the CNS/NC membrane which favored quick regeneration of the electrode surface during electrolysis. CNS-NC membranes gave a rejection of 60% rejection for MgSO₄ and 47% for CaCl₂, with high permeate fluxes of $\geq 100 \text{ L} \cdot \text{m}^{-2} \cdot \text{h}^{-1}$.

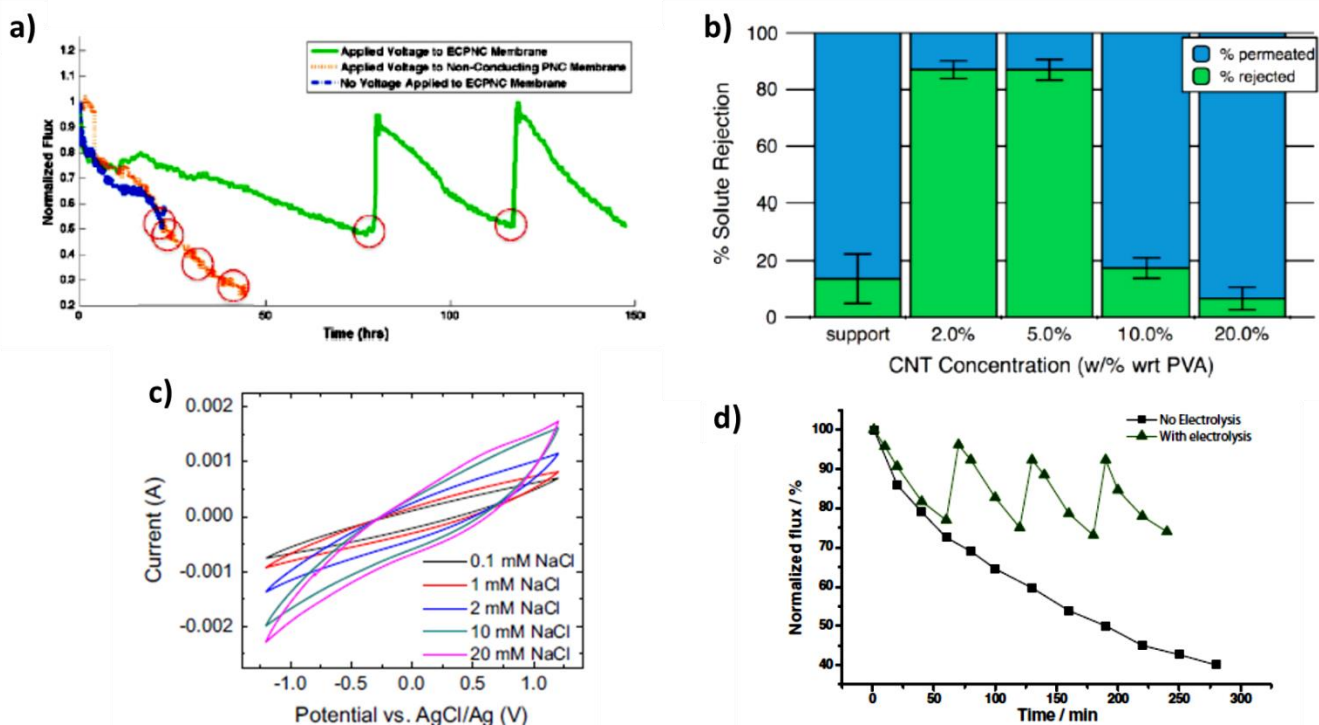


Figure 6: (a) Membrane flux compared for control membrane and ECPNC membranes with and without applied voltage; ECPNC membranes, with applied voltage, demonstrated less flux decline [137], (b) Solute rejection v/s CNT concentration for CNT-PVA membrane; for higher CNT concentration, polymer crystallinity decreases leading to increased membrane permeability [138], (c) CV curves of the conductive CNT-PVDF membranes with a scan rate of 100mVs⁻¹ [141], and (d) Normalized flux v/s time for CNS/PVDF membrane with and without in-situ cleaning using electrolysis.

Besides CNTs, other electrocatalytic materials have also been reported for desalination. Hosseini et al. [145] reported an increase in the electrochemical properties of cation exchange polyvinyl

chloride (PVC) membrane by incorporating zeolite particles in it. An optimum concentration of 8 wt. % zeolites gave a high NaCl selectivity of > 88% and a low amount of electrical resistance of < 6.5 Ω cm². Zeolite concentration beyond the optimum led to a decrease in selectivity and transport number, most probably due to agglomeration issues. Electrochemical desalination is gaining immense importance in desalination batteries [146]. The electrocatalyst electrode materials may be either identical [147] or dissimilar [148]. Desai et al. [149] reported electrochemical desalination of seawater using a zinc|ferricyanide flow battery. Besides desalination, this hybrid battery supplied electrical energy of 10Wh/L. They demonstrated 85% NaCl rejection using 35 g/L NaCl feed. The system registered a high operating voltage of +1.25 V, and a low specific energy consumption of 2.11 Wh/L for 85% salt rejection, together with a flux of 4.7 mol/m²·h. During operation, the discharge half cycle reactions resulted in NaCl rejection from the electrolyte, while the anode was oxidized to Zn²⁺ ions, and the ferricyanide cathode reduced to ferrocyanide. Thus, this resulted in the Cl⁻ ions being drawn into the anolyte tank, and the Na⁺ ions into the catholyte tank through the anion exchange and cation exchange membranes respectively. Before every half cycle, the desalinated water was removed while the Na⁺ and Cl⁻ ions were driven away as brine through cell charging. Figure 7 depicts the desalination battery setup and the processes occurring during discharging and charging. Kim et al. [147] also reported desalination through a similar method, but using similar electrocatalyst electrodes made from copper hexacyanoferrate (CuHCF). Their system used an applied voltage of 0.6 V, which avoided parasitic reactions unlike in CDI. High electrode desalination capacities up to 100 mg-NaCl/g-electrode were observed for 50 mM NaCl influent. Salt rejection through desalination batteries make them applicable for treating high salinity feeds, providing a clear advantage over

the RO technology. Several other studies report on similar, advanced desalination batteries providing a cost-effective seawater desalination option through utilization of electrochemical redox reactions [150, 151].

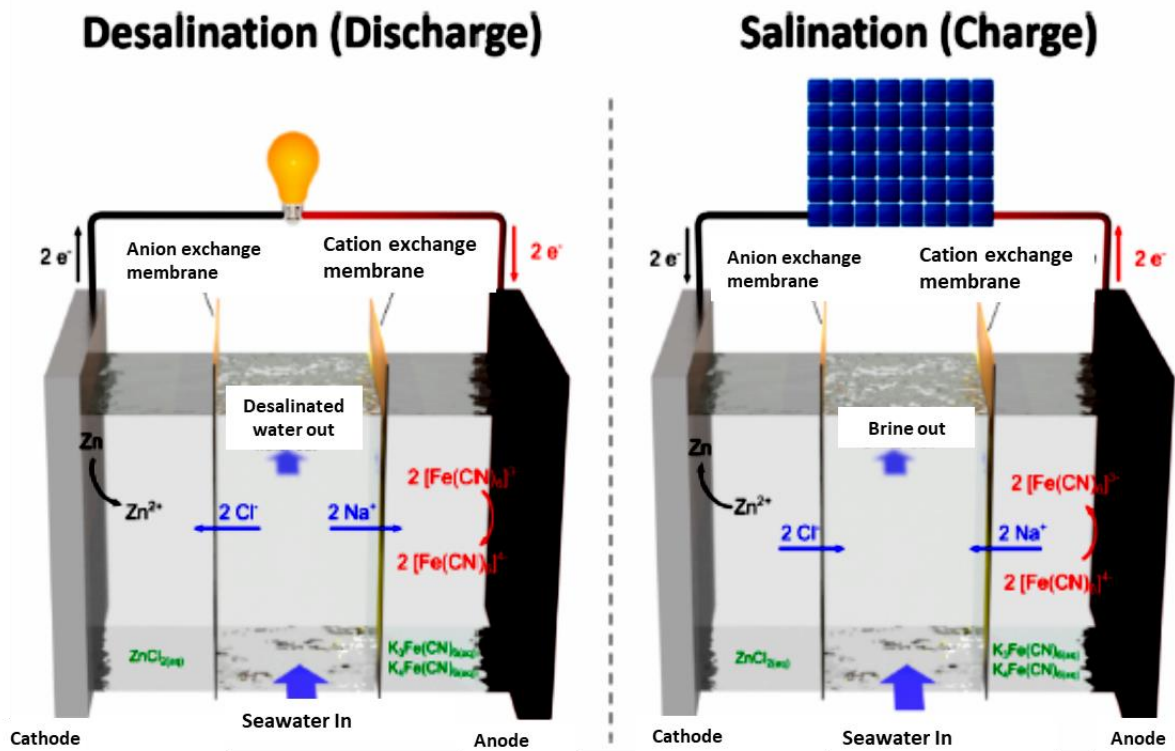


Figure 7: Schematic of the desalination battery operation during desalination (discharge) and salination (charging) [149].

Electrodialysis membranes, widely used for desalination and brine concentration have also been reported for improved membrane properties through incorporation of various functional materials. Highly conductive, selective and fouling resistant ion exchange membranes are continually sought for this application. Bin et al. [152] developed heterogeneous cation exchange membranes from functional polymer powders via a cost-effective hot-press procedure. It was found that the physicochemical and electrochemical properties of the membranes could be

tuned by the resin particle concentration in the membrane matrix. A 1.2g resin concentration showed excellent performance for NaCl desalination, comparable to the commercial Qianqiu® heterogeneous membrane. A decrease in NaCl concentration of 1 M NaCl feed solution to 0.03 M was reported. Besides various functional polymers [153-155], due to its conducting and superior mechanical properties, CNTs have been widely reported for electro dialysis membranes. Hosseini et al. [156] developed mixed matrix ion exchange membranes based on PVC-MWCNTs and studied the membrane potential, ionic permeability of Na⁺ and Ba²⁺ and, ionic flux. Na⁺ selectivity was found to decrease with increasing MWCNTs till 4 wt. %, after which it was reported to increase. The opposite was found for Ba²⁺ ions, where selectivity was first improved with increasing MWCNT concentration till 8 wt. %, and then dropped. For flux, an enhanced ionic flux was obtained for the monovalent ion with increased MWCNT concentration. Anion exchange membranes with improved fouling resistance was reported by Gonzalez et al. [157]. They developed novel nanocomposite membranes by modifying the existing PE commercial membranes by CNTs and iron oxide nanoparticles through solvent-evaporation technique. Improved hydrophilicity led to a 53% and 45% increase in fouling resistance with CNTs (0.6 wt. % loading) and nanoparticles (0.4 wt. % loading) respectively. Moreover, about 50% energy savings were reported due to a lower voltage drop during the experiment. Several review papers have been published on such functional materials critically analyzing their recent developments [158-160]

4. Photothermal Materials

Harvesting solar energy through photothermal conversion is an important pathway for water desalination application. The main factors affecting this conversion are sunlight absorption and thermal management. Hence, coherent materials are anticipated for such a functionality which can avoid superfluous heat losses and at the same time have efficient photon absorption characteristics [52]. Natural solar-to-vapor conversion efficiency is often limited by poor light absorption and other optical losses and thermal losses. This restricts its usage for generating fresh waters at acceptable levels. Numerous studies [161, 162] have been reported on developing high-performance light-to-heat converting materials by designing multi-layer coatings, and tuning the composition of the photothermal materials. Nevertheless, the most important property remains the light harvesting ability of the material. Different configurations may be exploited when using photothermal materials for desalination. A solar simulator is often directed at a solar photothermal material contained in water. These may either be configured as volumetric systems in which the photothermal material is dispersed in the medium, or else as interfacial systems, in which the material might be separated from the bulk. Various photothermal materials have been identified for this purpose including light absorbing nanoparticles [163], monolithic aerogels [164], plasmonic nanoparticles [165], and magnetic particles [166].

Mostly, hydrophobic photothermal materials are sought for saltwater evaporation [167, 168]. A non-wetting surface is capable of repelling water and thus can prevent water infiltration through a membrane in solar desalination. The conversion to heat by the absorbed solar in the photothermal membrane provides local heating at the air-water interface. This localized interfacial heating can help minimize heat losses by the non-evaporative lower part of the bulk water and it also generates a sharp temperature gradient with the same energy input. This leads to evaporation of the water through the membrane pores, following which the vapor can be condensed in a cooler region of the desalination system. Zhao et al. [169] fabricated a trimethoxy(1H,1H,2H,2H-perfluorodecyl)silane modified hydrophobic MXene membrane containing a Ti_3C_2 nanosheet layer. MXenes are 2D carbonitride nanomaterials with a general formula $\text{M}_n\text{X}_m\text{Tx}$. This self-floatable material gave improved light absorption, achieving a solar evaporation rate of $1.31 \text{ kg m}^{-2} \text{ h}^{-1}$ under high salinity conditions of the Bohai Bay seawater. High salt rejection rates of about 99.5% were achieved for Na^+ , K^+ , Mg^{2+} and Ca^{2+} ions as shown in Figure 8a. In addition, improved membrane stability of over 200 hours was registered under one sun irradiation. Yao and Yang [170] synthesized a self-floating, 2D layered alloy based on BiInSe_3 /carbon foam for seawater desalination. It exhibited an evaporation rate of $1.1 \text{ kg m}^{-2} \cdot \text{h}^{-1}$ for 1 sun irradiation. Further, the ion concentrations for Na^+ , K^+ , Mg^{2+} and Ca^{2+} were seen to reduce by four orders of magnitude as compared to as compared to the original seawater, with no visible degeneration in 15 cycles for a 15-day period. These results were attributed to the synergistic effects of exceptional light absorption capability, higher localized interfacial heating, and abundant phonon-assisted decay. Zhu and coworkers [171] synthesized black titania/PVDF with a unique nanocage structure through the self-assembly approach. It's well interconnected

nanograins facilitated heat transfer from titania to water, while the mesoporous structure aided water vapor permeation. A solar-thermal conversion efficiency of 70.9% was achieved under a light irradiation of 1 kW m^{-2} . An evaporation rate of about $1.13 \text{ kg. m}^{-2}. \text{ h}^{-1}$ was achieved, together with a conversion efficiency of 70.9%, which was 1.9 times higher compared to water itself. Seawater from East Sea, China was tested, giving a salinity of almost $\leq 10\text{mg/L}$ for major cations like Na^+ , Ca^+ and Mg^+ . Black titania nanocage durability was studied through repeated cycles, which showed good material durability, with the performance maintaining for more than 10 cycles with each cycle of 5 hours. A metal-ceramic photothermal hybrid was reported by Chen et al. [172] where they demonstrated an increase in desalination efficiency via hydrogen bond destruction based on gold nanoparticles-adsorbed ceramic rods. Illumination with resonant light weakened the strength of interactions within water molecules leading to easy evaporable plasmon-activated water. Their system was 140 % more efficient than untreated water, rendering the photomaterial with great potential for direct contact membrane distillation application. Zhang and co-workers [46] reported a self-healing, hydrophobic photothermal polymer polypyrrole (PPy)/ stainless steel (SS) membrane. Membrane fabrication was achieved by depositing PPy onto a SS mesh substrate. This was followed by fluoroalkylsilane modification to achieve the desirable hydrophobicity. Their results showed a water evaporation rate of $0.92 \text{ kg.m}^{-2}.\text{h}^{-1}$, with a conversion efficiency of about 58% compared to only 24% without a membrane.

Studies have also reported on magnetic photothermal materials. Zeng et al. [166] synthesized hydrophobic, low packing density carbon particles decorated with magnetite (Fe_3O_4) (average size $\approx 500\text{nm}$), through carbonization of poly (furfuryl alcohol) (PFA). Figure 8b shows the TEM

image of a $\text{Fe}_3\text{O}_4/\text{C}$ where some Fe_3O_4 nanoparticles were seen to be embedded in the carbon. A 3.5% NaCl aqueous solution was filled in a 10ml beaker irradiated with a sunlight simulator as shown in the setup in Figure 8c. Light intensity was varied from 1355 to 430 W m^{-2} , while the amount of water evaporated was determined through weight change in the beaker. Different amounts of $\text{Fe}_3\text{O}_4/\text{C}$ particles were spread on the bottom of the beaker to study a change in the light absorbed versus variation in thickness (Figure 8d). With 58 g.m^{-2} (0.023 g) of $\text{Fe}_3\text{O}_4/\text{C}$ particles, the radiation intensity significantly reduced from 1200 W m^{-2} to 100 W m^{-2} , dropping to almost zero with 115 g.m^{-2} (0.045 g) of $\text{Fe}_3\text{O}_4/\text{C}$. Thus, only a small 200 mm (0.045 g) thick layer of $\text{Fe}_3\text{O}_4/\text{C}$ was sufficient to absorb all the sunlight. The difference in intensity reduction with and without salt water was negligible. These floatable particles were able to increase the salt water evaporation by about 130%. Apart from experimental work, solar evaporation was also modelled. Figure 8e compares the experimental and the modelled cumulative amounts of water evaporated. There was close agreement between the two, with only a slight over prediction with the modelling output, primarily because of the increased salinity levels during the end of the test during the experimental work. Similarly, several other hydrophobic magnetic nanoparticles have been developed for solar evaporation including, MnFe_2O_4 , ZnFe_2O_4 and CoFe_2O_4 [173].

Graphene-based photothermal materials have gained considerable interest for solar desalination [174, 175]. Li X et al. [176] developed porous cellulose wrapped in polystyrene foam with a GO film on the top surface. The cellulose provided a 2D water pathway while the GO acted as a solar absorber. The photothermal material was efficient in suppressing thermal losses, which enabled a four orders salinity decrement under an illumination of 1 sun. Recently, Liu et al. [177]

developed a novel bilayered wood-GO structure for potential solar evaporation. The GO layer deposited on the microporous wood provided a high photothermal conversion efficiency with the GO providing a broad optical absorption resulting in rapid temperature increase at the liquid surface. The wood on the other hand served as a thermal insulator confining the photothermal heat and facilitating efficient transport of water from the bulk to the photothermally active space. The composite exhibited a solar thermal efficiency of $\sim 83\%$ under a light power density of 12 kW/m^2 , making it an attractive photothermal material for cost effective, resource limited desalination. Other carbon based photothermal materials such as CNTs have also been identified for this purpose. Yang et al. [178] designed a bilayer Janus absorber through gold nanorod (AuNR) self-assembly onto SWCNT porous films. The combined properties led to enhanced solar spectrum absorption, good photothermal performance, and excellent mechanical integrity. A water evaporation efficiency of about 94% was achieved under a 5 kW m^{-2} solar irradiation. Various seawaters including from the Baltic Sea, World ocean, the Red sea and the Dead Sea were analyzed. Stable desalination performances were achieved for all feeds, giving extremely low salinities of $\approx < 10 \text{ mg. L}^{-1}$. Xu et al. [178] also synthesized Janus absorbers for efficient solar desalination, but using the electrospinning technique. Their developed material had two coatings, a lower hydrophilic polyacrylonitrile (PAN) layer for a water pathway, and an upper hydrophobic carbon black nanoparticles/ polymethylmethacrylate (PMMA) layer for light absorption and salt prevention. An evaporation rate of $1.3 \text{ kg m}^{-2} \text{ h}^{-1}$ was observed, with an energy conversion efficiency of 72% under 1 kW m^{-2} . Salt rejections with 3.5 wt. \% salt water was also studied, with Na^+ , Mg^{2+} , Ca^{2+} , K^+ , and B^{3+} salt concentrations decreasing to below 1.4 mg. L^{-1} , significantly lower than that obtained through RO. A simple, low dose (only 4 g/m^2) CNT-based

floating solar still was investigated for seawater desalination by Gan et al. [179]. The material was layered in the following order: a layer of CNTs to absorb solar irradiation, a polyurethane sponge (PUS) to provide a thermal barrier, and an air laid paper for an efficient water transport channel. Seawater sample from East China Sea was tested for solar evaporation. A reduced salinity from 40,400 $\mu\text{s}/\text{cm}$ to 13.52 $\mu\text{s}/\text{cm}$ was achieved. In addition, a significant decrease in boron concentration was observed, which otherwise requires extensive removal efforts during RO. The concentrations of all major cations (Na^+ , K^+ , Ca^{2+} , Mg^{2+}) and anions (F^- , Cl^- , Br^- , NO_3^- , SO_4^{2-}) originally present in the seawater were seen to decrease to 0.002–2.38 mg/L, well below the range defined by the WHO for safe drinking water.

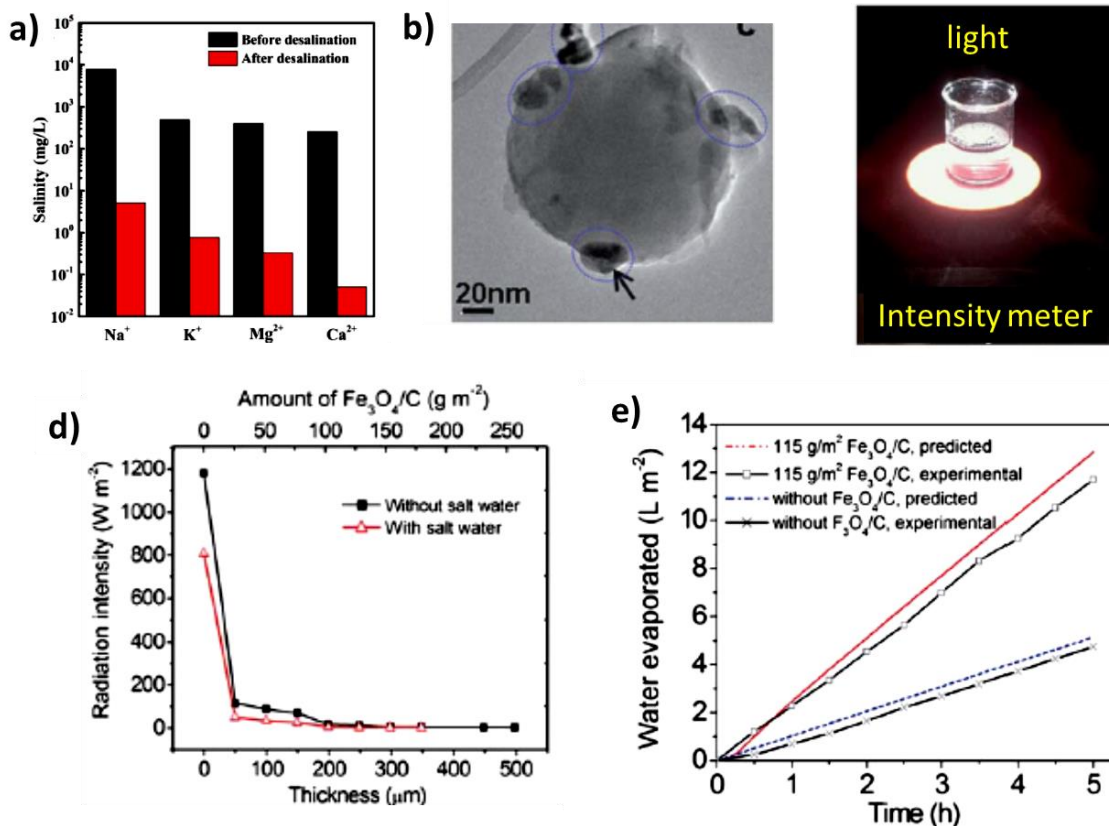


Figure 8: (a) Measured salinity of four primary ions before and after solar desalination, reproduced from [169] with permission from The Royal Society of Chemistry, (b) TEM image of a Fe₃O₄/C particle with the Fe₃O₄ nanoparticles circled in blue, (c) Testing setup, (d) The radiation intensity measured underneath the

beaker versus the weight and thickness of $\text{Fe}_3\text{O}_4/\text{C}$ layer and (e) Experimental and predicted cumulative amounts of water evaporated of salt water. Reproduced from [166] with permission from The Royal Society of Chemistry.

The quest for inexpensive photothermal materials is on a rise, with many research groups focusing on utilizing abundant materials for solar evaporation. For example, Zhu et al. [180] developed an inexpensive cellular carbon sponge with a broad light absorption ability. This novel sponge could soak up water and undergo in situ photothermic vaporization. The capillary action of the sponge was used to confine water, isolating it from the bulk, providing 90% evaporation efficiency. This isolation brought about a 2.5-fold increase in solar-to-vapor conversion, compared to the conventional bulk heating. The sponge could be produced on a large scale through thermal carbonization of a melamine precursor, making it a low-cost method. This technology is beneficial for remote places with poor water supply infrastructures, where production of potable water can be comprehended at an economical cost. Recently, an ultra-low cost cotton based solar evaporation device was developed for seawater desalination to produce drinkable, fresh water [181]. The photothermal material was developed from everyday household materials; cotton cloth was coated with candle soot/ PVDF mixture, after which the cotton cloth was modified using a floating support. This absorber gave a photothermal efficiency of 80% under 1 sun illumination. The rate of water evaporation was calculated to be $0.95 \text{ kg}\cdot\text{m}^{-2}\cdot\text{h}^{-1}$, in contrast to bare water evaporation rate of $0.43 \text{ kg}\cdot\text{m}^{-2}\cdot\text{h}^{-1}$. A homemade solar still was used to study the proficiency of the developed absorber for seawater solar desalination. Very low salinity levels $\approx 121 \text{ mg/L}$, well within the world health organization (WHO) ranges were achieved with the system. This work provided a means of desalinating seawater with low cost,

household materials, more applicable to those parts of the world which lack drinkable water quality.

The light harvesting capability of photothermal materials is the foremost concern in solar evaporation. High absorption may be achieved through tailored material design for both, intensity enhancement and their optical absorption range. One strategy of tuning the optical properties for such materials is by using plasmonic materials as discussed in the next section.

4.1 Plasmonic materials

Plasmonic materials are mostly metallic materials that exhibit negative permittivity. Plasmonics deals with surface plasmon resonance (SPR) which is an electromagnetic (EM) phenomenon. The energy carried by the photons may be transferred to the free electrons called surface plasmons (SPs), at that interface [182]. In Localized SPR (LSPR), one type of SPR, the excited surface electrons oscillate coherently with the incident electromagnetic field. Following this, these electrons then relax through a variety of processes including electron–electron scattering and transferring of energy from the electron gas to the metal lattice via electron–phonon coupling. The latter causes phonon–phonon interactions. This relaxation process converts the kinetic energy of the excited electrons into thermal energy that can be used to rapidly heat up the surroundings of a metal surface. This “green” heat may be utilized in a variety of applications including evaporation of seawater for desalination. One of the main barriers in using plasmonic metal particles as solar absorbers is the limited absorption range only at one or a few LSPR wavelengths [183].

Various advanced fabrication techniques and plasmonic structures have been adopted to overcome the limitations of narrow absorption ranges. Zhou et al. [184] developed aluminium (Al) nanoparticles for plasmon-enhanced solar desalination through a self-assemble approach. Their plasmonic structure consisted of three components: the aluminium oxide membrane (AAM), close-packed Al nanoparticles, and a thin layer of Al on the AAM. Figure 9a highlights the two basic fabrication steps which includes the formation of the nanoporous AAM through anodic oxidation of the Al foil, and the self-assembly of the Al nanoparticles. Such a structure resulted in a strong plasmon hybridization effect, providing an efficient and broad band solar absorption through several mechanisms as studied through finite difference time domain (FDTD) calculations. The close proximity of the Al nanoparticles and the alumina oxide layer induced a distinct redshift widening the LSP resonant modes which gave a broad absorption across the solar spectrum (>96%). Figure 9b depicts the solar desalination experimental set-up used during their study. The plasmonic material was shown to float on the water surface allowing a liquid-vapor phase close to the air-water interface. The steam generated from the air-water interface was condensed in the condensation chamber, while the AAM provided an efficient pathway for water supply and steam flow. To study the competence of the developed plasmonic structure, four different samples with different salinities from the Baltic sea (0.8 wt. %), the Red Sea (4 wt. %), the world ocean (3.5 wt. %), and the Dead Sea (10 wt. %) were used. A significant decrease (~four orders of magnitude) in Na⁺ concentrations were achieved as shown in Figure 9c. the end concentrations were found to be well below the limit specified by WHO and the US Environmental Protection Agency (EPA) for safe drinking standards. This study provided a means of fabricating a low-cost, scalable plasmonic structure for efficient solar desalination.

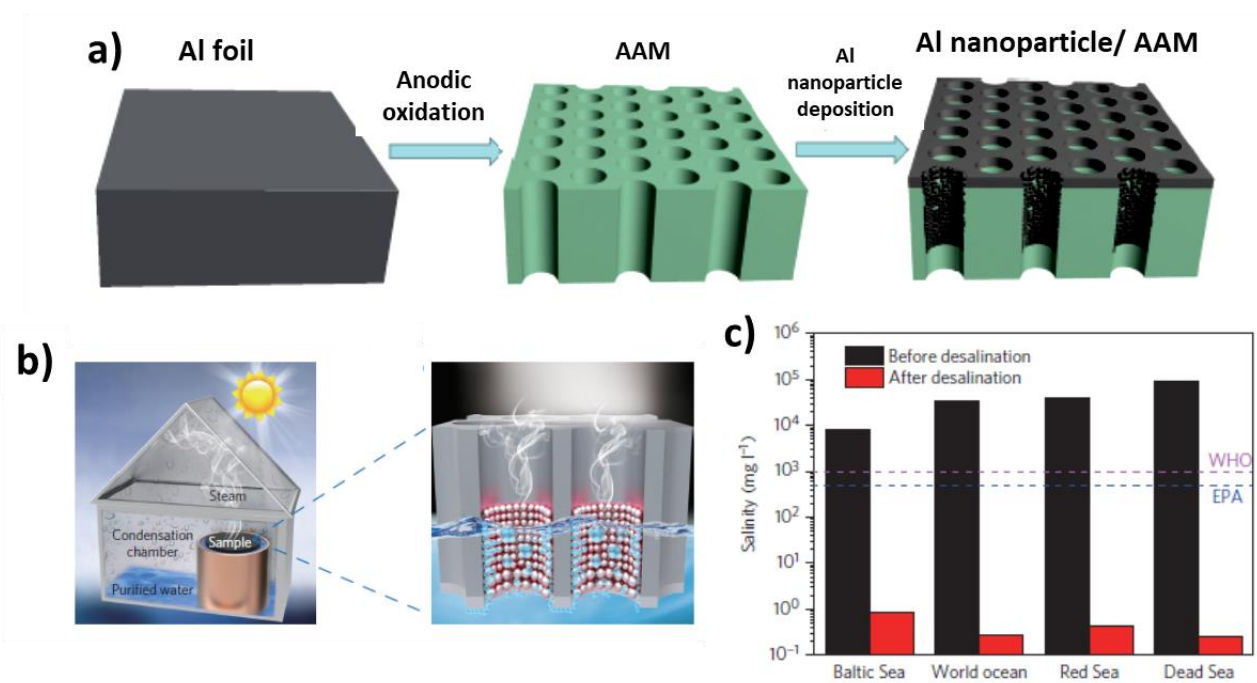


Figure 9: (a) Fabrication process of the plasmonic structure where the Al foil served as the source material for the entire fabrication process: AAM was fabricated by anodic oxidation and the Al nanoparticle/AAM structure was formed after the nanoparticle deposition, (b) Schematic of the experimental set-up and process of the plasmon-enhanced solar desalination, and (c) Measured salinities of the four simulated seawater samples before and after desalination where the dashed colored lines refer to the WHO and EPA standards for drinkable water [184].

Hu and his group [185] also reported on a novel plasmonic material for a large absorption range. They decorated metal nanoparticles of Pd, Au and Ag onto a 3D mesoporous matrix of natural wood. The plasmonic wood exhibited high light absorption ability of $\approx 99\%$ over a broad wavelength range from 200 to 2500 nm. This was attributed to the wood microchannels and the plasmonic effect of the metal nanoparticles. A high solar conversion efficiency of about 85% under a 10 kW m^{-2} was achieved. Zielinski et al. [186] demonstrated a novel technique for fabricating bimetallic Ag/Au hollow mesoporous plasmonic nanoshells which gave superior solar vapor generation. Contrary to the nanoparticles, when exposed to light irradiation, these hollow

nanoshells were reported to generate vapor bubbles from their interior, as well as their exterior. Thus, vapor nucleation was accelerated, facilitating its potential in seawater desalination by rapid, increased salt water evaporation giving a conversion efficiency of 69% under 11 kW m^{-2} . Nevertheless, the nanobubble formation puts constraints on the light irradiation as a highly concentrated light source is required to overcome the threshold energy of bubble formation [183]. Kiriachchi et al. [187] developed a flexible, scalable, low weight, and cost effective plasmonic functionalized Cotton (PFC) nanocomposite containing Au/Ag nanoparticles. This plasmonic material was reported to exhibit a strong solar absorption and an average water evaporation rates of 1.4 and $11.3 \text{ kg m}^{-2} \text{ h}^{-1}$, together with high solar thermal efficiency of up to 94.3% under 8 sun illumination. These results indicated good potential for the Au/Ag-PFC to be used for seawater desalination. Yi and his coworkers [188] reported on a low cost, scalable microporous plasmonic membrane made from black amorphous Al-Ti-O nanostructure, which synergistically combined the plasmonic effects in Al and the high photocatalytic of black TiO_2 , enabling a high solar absorption efficiency of 90.23%. The fabrication of the Al-Ti-O hybrid was brought about by planetary-milling of low-cost precursors of commercial TiO_2 and Al powders. For testing its potential in desalination, flat-sheet microporous PVDF membranes consisting of Al-Ti-O were fabricated through phase-inversion process. The membrane registered a high desalination efficiency of 77.52%, with a water production rate of $\sim 4 \text{ L.m}^{-2}.\text{day}^{-1}$ under 820 W. m^{-2} solar irradiation. Recently, Xu et al. [14] developed Cu nanodots-embedded N-doped graphene urchins. The Cu nanodots were spatially scaffolded in the graphene matrix providing a hybridized localized surface plasmon resonance, which gave an ultra-high light absorption of 99% in the

spectral range of 300–1800 nm. In addition, the graphene provided a favorable water pathway during desalination, achieving 82% desalination efficiency with a fresh water production rate of $\sim 5 \text{ Lm}^{-2}\cdot\text{day}^{-1}$ under solar irradiation. These studies clearly highlight the advances in plasmonic materials in solar desalination for improved absorption ranges and increased desalination efficiencies. Nevertheless, most of the materials are expensive or require high intensity irradiations to facilitate the plasmonic effect.

5. Magnetic Materials

Magnetic fields can positively affect the desalination efficiency [189, 190]. When an external field is applied to a magnetic material, that material can become magnetized to perform one of the many tasks required in desalination. For example, Razmkhah et al. [48] used molecular dynamic simulations to study the effect of magnetic field on desalination efficiency. Strong and weak external fields were applied to a MWCNT. Apart from its conductive nature, CNT membranes find potential in desalination owing to its narrow channels whereby providing an easy passage of water flow. RO process was simulated at a pressure of 25 MPa with and without external fields. An ion rejection of 96% was reported without any field, which increased to 100% after applying the field. Magnetization lead to a complete salt rejection, together with an increased flow rate. This was owed to a more stable hydration shell around the Na^+ ion. Similarly, Alnaimat et al. [189] developed a mathematical model for electromagnetic–mechanical salt removal. They proposed a separator which utilized both magnetic and electrical forces for achieving salt separation. A hard magnet was used to produce a constant magnetic force. The magnetic forces acted in a specific direction within the flow channel. The salt ions were pushed via this magnetic

force accordingly. Their model was useful to study the flow regime inside the separator. A low magnetic force of 0.05×10^{-10} was enough to achieve a separation of 71%.

Various types of magnetic materials have been reported for seawater and brackish water desalination. One of the most studied desalination method's utilizing magnetic particles is forward osmosis (FO). FO uses the osmotic pressure differential ($\Delta\pi$) across a semipermeable membrane as a driving force for water transport across the membrane, unlike the RO process which utilizes hydraulic pressure differences. It therefore results in a concentration of a feed stream and dilution of a draw solution which forms the highly concentrated stream [191]. Studies for new draw solutes are a topic of great interest in recent years [192, 193]. A draw solute should be able to reduce the water chemical potential, and at the same time generate a high osmotic pressure required in FO. Nevertheless, it should be easily separable from the diluted draw solution for regenerative purposes [193]. The latter being a challenge on its own, brings forth numerous studies in this field for ideal draw solutes. Several magnetic nanoparticles have been reported for this purpose. With some surface modifications, these magnetic nanoparticles could generate high osmotic pressures and be easily separated from the draw solution owing to its magnetic functionality in the presence of a magnetic field. This idea was first proposed by the company NanoMagnetics for contaminants removal through FO [194]. Since then, there have been numerous studies highlighting the application of magnetic nanoparticles in FO. Engineered magnetic nanoparticles offer several exciting characteristics [195] such as superparamagnetism, where the nanoparticles can become magnetized up to saturation, and then on removal of the external magnetic field, it can revert back to its 'non-magnetic' interaction. In addition, such materials offer high surface areas and low toxicity. By far, the predominantly reported magnetic

material for this desalination application is magnetite (Fe_3O_4). For example, Ling et al. [196] reported surface modified functionalized Fe_3O_4 magnetic nanoparticles as draw solutes. They used three kinds of organic polymers for this purpose, 2-pyrrolidone, triethylene glycol, and polyacrylic acid (PAA). The organic coated nanoparticles were synthesized through the thermal decomposition method. Amongst the three, PAA coated Fe_3O_4 magnetic nanoparticles gave the highest flux of 10.4-7.7 LMH, while the particles were easily regenerated using a high-gradient magnetic separator. However, the high Mw of the PAA was not sufficient for the high osmotic pressures required for desalination. Thus, Bai et al. [197] reported highly water soluble dextran coated Fe_3O_4 magnetic nanoparticles for brackish water desalination. By using a low molecular weight Dextran polymer ($M_w=1000$), it was possible to generate high osmotic pressures. The high osmotic pressure requirement was met by the organic coating, while the Fe_3O_4 nanoparticles again facilitated an easy recovery via an external magnet field. Dextran particles with two different content percentages were used, 64.44 wt. % and 78.03 wt. %, with an initial draw concentration of 0.5 M. Figure 10a shows the schematic of Fe_3O_4 nanoparticles coated by dextran while Figure 10b demonstrates the separation proficiency of these magnetic nanoparticles. Figure 10b(i) shows well dispersed Fe_3O_4 nanoparticles without any external magnet, while Figure 10b(ii-iii) depicts the separation situation of these nanoparticles at two different concentrations when a magnet was placed at one side of the bottle. It is evident that most of these nanoparticles have collected to the side close to the magnet, thus facilitating recovery.

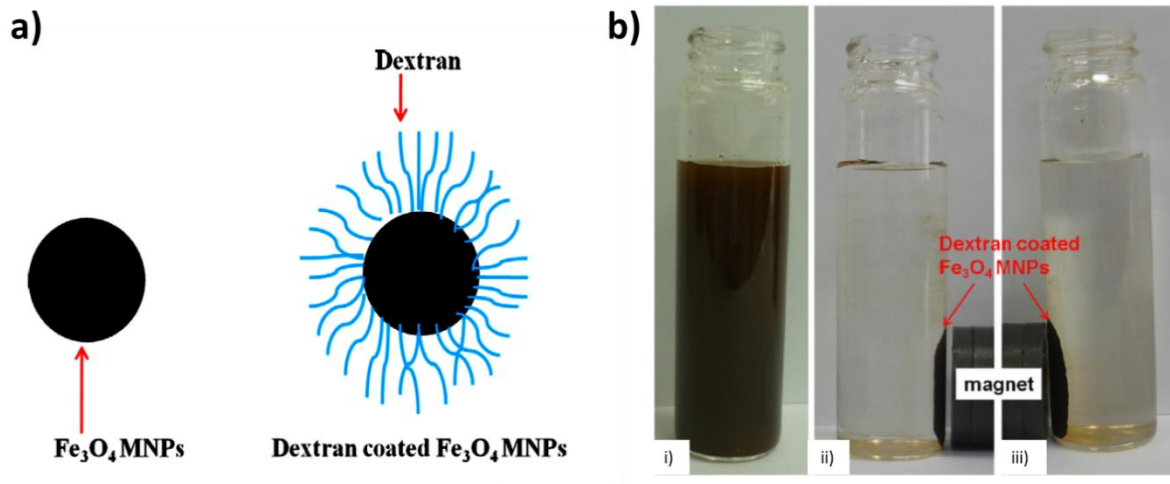


Figure 10: (a) Schematic showing dextran coated Fe_3O_4 magnetic nanoparticles (b) Demonstration of separation of these nanoparticles when (i) the particles are well dispersed in the solution, (ii) the separation situation of these nanoparticles MNP containing with 64.44 wt.% dextran after 10 min and (c) 78.03 wt.% dextran after 15 min. [197]

Numerous other studies report the use of Fe_3O_4 magnetic nanoparticles as FO draw solutes [195, 198-202]. Besides facilitating easy recovery, these magnetic nanoparticles were reported to optimize the water flux during the FO process. For example, Na et al. [195] reported their study using super-hydrophilic, citrate coated Fe_3O_4 nanoparticles. The initial FO pure water flux of 17.3 LMH with 20 mg/L nanoparticles was registered. However, a rapid decline in flux was observed thereafter apparently due to an interaction between the cellulose triacetate (CTA) FO membrane and citrate coated magnetic nanoparticles. The authors proposed a solution to this problem through an introduction of a magnetic field control (MFC) FO module. Two neodymium magnets were used which prevented the citrate coated magnetic nanoparticles from fouling the CTA membrane. Hence, the magnetic field was used to drive away the magnetic nanoparticles from the CTA membrane, resulting in a water flux of 13 LMH with the same concentration of nanoparticles in the draw solution. Even though the resulted flux was lower than the one without

any magnetic force application, it was reported to be stable over the entire period of the experiment. The recovery of these nanoparticles was not reported in their study, however, being an important aspect, it was included in their prospective future research. Dey et al. [199] reported ~9 nm poly sodium acrylate (PSA)-coated magnetic nanoparticles for FO desalination which they termed as smart osmotic draw agents (SMDA). These gave significantly higher osmotic pressures (~30 fold) and water fluxes (~2–3 fold) when compared to the bare polymer counterpart. In addition, the PSA configuration was seen to significantly affect the FO performance. An extended, open conformation was deemed promising owing to the higher number of functional hydrophilic groups available for increased osmotic pressure and FO water fluxes. Figure 11a shows that the PSA-magnetic nanoparticles provided a higher water flux which was retained for about 3 hours during the experiment. In contrast, the PSA draw solute registered much lower flux of about 2 LMH. Figure 11b depicts a significantly improved osmotic pressure of about 11.37 atm for PSA coated particles compared to only 0.4 atm for just bare PSA. Ge et al. [203] reported similar osmotic pressures of ~11–12 atm but with a higher concentration of ~15 wt.% PSA compared to only 0.078 wt. % reported by Dey et al. [199]. Thus, this signifies the importance of using magnetic nanoparticles in coordination with the polymer for enhanced FO performance. Figures 11c and 11d depicts the facile regeneration of the osmotic draw agent. The magnetic nanoparticles were demonstrated to be easily separated with an application of a weak magnetic field applied for 5 min. Draw solutes with nanoparticles with smaller size are usually preferred which can lead to a higher specific area for functionalization. However, small sized magnetic nanoparticles are difficult to be captured using an external magnetic field. Therefore, thermoresponsive polymer PNIPAM has shown great research impact to functionalize magnetic

nanoparticles. When the polymer is heated above its lower critical solution temperature (LCST), it transforms reversibly from hydrophilic to hydrophobic. This transition aids in nanoparticle recovery [204]. Zhao et al. [200] reported the synthesis of thermoresponsive poly(sodium styrene-4-sulfonate)-co-poly(N-isopropylacrylamide) (PSSS-PNIPAM) grafted Fe_3O_4 nanoparticles via ligand exchange. These nanoparticles were reported to be responsive to both temperature and the magnetic field, thus providing a combination of functions. After the FO process, the draw solution was heated above the LCST to allow for improved magnetic capturing through reversible clustering of the particles. 14% of the nanoparticles were found to precipitate out which were directly recycled to the draw solution reservoir. The remaining ones separated through a high gradient magnetic separator (HGMS). Thermoresponsive hydrogels are also gaining research interest as FO draw agents. However, recovery of water from these hydrogels remains a challenge. Amir and coworkers [205] studied a magnetic field-induced heating for recovery of water from swollen hydrogel draw agents. Copolymerization of sodium acrylate and N-isopropylacrylamide was carried out in the presence of Fe_2O_3 of magnetic nanoparticles for the preparation of composite hydrogel particles. Magnetic heating was sought to uniformly generate heat throughout the hydrogel particles minimizing the formation of a dense skin layer commonly formed during the conventional process. It was found that the FO dewatering performance was largely affected by Fe_2O_3 nanoparticle loading. 53% liquid water recovery was achieved by using the magnetic enhanced heating compared to only 7% during conventional heating. Table 3 lists some key findings of the reported magnetic draw solutes in FO.

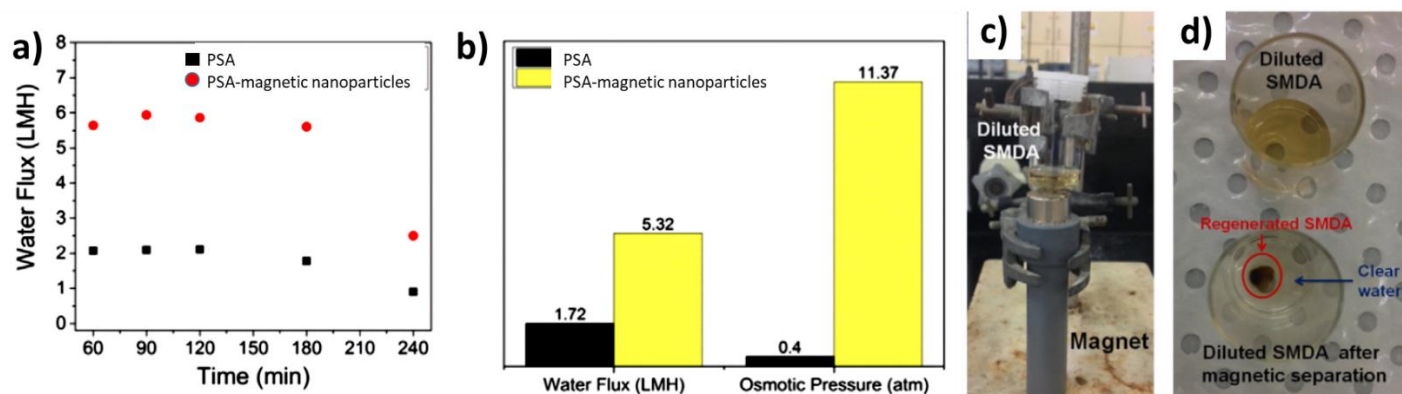


Figure 11: (a) Graph of FO water flux v/s time, (b) comparison of average water flux and osmotic pressures generated by of PSA and PSA coated magnetic nanoparticles (c-d) Magnetic separation of SMDA.

Table 3: List of different magnetic draw solutes and their key findings reported in the literature

Reference	Magnetic Draw Solutes	Key Features
Ling et al. [206]	2-Pyrrolidine, triethylene glycol and polyacrylic acid coated Fe_3O_4 nanoparticles	For the first time, the application of highly hydrophilic magnetic nanoparticles as novel draw solutes in FO was investigated.
Bai et al. [197]	Dextran coated Fe_3O_4 magnetic nanoparticles	High osmotic pressure gradients achieved and demonstration of easy recovery of these magnetic nanoparticles was conducted.
Na et al. [195]	Citrate coated Fe_3O_4 magnetic nanoparticles	A MFC module was studied in which a magnetic field was applied to drive away the magnetic particle from the FO membrane, preventing a dramatic flux decline over the period of time. The proposed MFC FO module was reported to be one of the first device's for increasing water flux using magnetic nanoparticles as draw solutes.
Dey et al. [199]	PSA coated Fe_3O_4 magnetic nanoparticles	Draw solute concentrations as low as ~ 0.13 wt. % demonstrated ~ 30 -fold increase in osmotic pressure and a ~ 2 – 3 -fold increase in FO water flux when compared to the bare polymer draw solute. In addition, the importance of extended, open polymer chain conformation was reported to have a positive impact on the performance compared to the coiled conformation.
Zhao et al. [200]	PSSS-PNIPAM grafted Fe_3O_4 magnetic nanoparticles	Thermoresponsive magnetic nanoparticles were synthesized. Improved capturing of the nanoparticles through reversible clustering on application of heat. Efficient regeneration of the nanoparticles if waste heat is utilized in an industry scale FO unit, lowering the overall cost of the process and hence water production.

Ge et al. [207]	Hydroacid- Fe_3O_4 magnetic nanoparticles	Synthesis through one-pot reaction. Highly dispersing, ionizable abilities for powerful FO draw solutes. High rejections in the post treatment of their regeneration.
Amir et al. [205]	Sodium acrylate and N-isopropylacrylamide- Fe_2O_3 hydrogels	Magnetic heating was used to effectively remove the water from the hydrogels achieving a water recovery rate of 53%.
Ling et al. [208]	Polyacrylic acid and triethylene glycol coated Fe_3O_4 magnetic nanoparticles	A sustainable, integrated FO–UF system for desalination with super hydrophilic magnetic nanoparticles as draw solutes. The agglomeration problem of magnetic nanoparticles recovered by the magnetic fields was overcome by using ultrasonication, hence partially restoring the FO performance.

Besides FO, magnetic materials have been reported to be used in RO. Wang et al. [209] reported a magnetic enhanced coagulation-ultrafiltration process as a pretreatment for seawater desalination through RO. Optimum dosages of FeCl_3 coagulant and Fe_3O_4 magnetic seeds were studied in lab-scale beaker tests. Their results showed that the largest flocculant size of 790.3 μm was obtained at a FeCl_3 dosage of 25.51 mg/L and a Fe_3O_4 dosage of 5.37 mg/L. These dosages were quite low compared to other coagulant dosages. In fact, the dosage of magnetic enhanced coagulation decreased by 1/3, while giving a higher quality permeate with SDI value of 1.40-1.65. Similarly, Jie et al. [210] reported a magnetic flocculation system for turbidity removal as a pretreatment step for seawater desalination. Again, lab-scale beaker tests were designed where optimum dosages of coagulant and magnetite were sought. Their results indicated that when 31.15 mg/L of FeCl_3 was used, 85.9% of turbidity removal was achieved. However, with magnetic enhanced flocculation, turbidity removal rate reached around 92.8% with lower dosages of FeCl_3 (28.74 mg/L) and a magnetite dosage of 6.02 mg/L. RO plants usually suffer from scaling problem, thus reducing the overall plant recovery. For this purpose, antiscalants are widely utilized to inhibit the scaling from prominent scalants such as CaCO_3 , CaSO_4 , and BaSO_4 . However,

antiscalants usually come with disadvantages such as increased potential for biofouling. Thus, many studies have reported the usage of magnetic treatment for scale inhibition [211-214]. Powerful magnetic fields may affect solute properties and produce water with lower hardness, together with control on scaling produced through various scalants. Salman and coworkers [215] reported that the magnetic treatment method (MTM) as an effective way to control scaling in RO desalination plants. Two experiments conducted at the Doha Ro plant to examined the effect of MTM on potable and seawater sources. The results indicated no change in the chemical composition and hardness, however the turbidity of the water was clearly affected. Furthermore, the performance of MTM was compared to that of four different commercial antiscalants used in RO. Three pairs of permanent magnets were used with north and south poles facing towards each other. The magnetic field strength used in the experiment was kept constant at 0.16 T. Feed water was flowed through this field and the procedure was successful in reducing the total suspended solids (TSS). The percentage removal of TSS increased to 39.35% after 6 h from just 8.97% in the first hour. Further, the effect of MTM on BaSO_4 inhibition was found to be stronger than on CaSO_4 or CaCO_3 . Kobe et al. [216] concluded that magnetic field application successfully prevented calcite scaling, where MTM changed the crystal morphology of 90% calcite under a field of 1.22 T. Calcium hydrogen carbonate ($\text{Ca}(\text{HCO}_3)_2$) solutions were prepared by dissolving calcium carbonate in deionized (DI) water. They used X-ray diffraction analysis was to study the change in phase compositions with an applied magnetic field., which confirmed the effect of the density of the magnetic field on the different crystal forms of CaCO_3 . Numerous other studies report on the usage of MTM to control scaling from major scalants [212, 217]. Nevertheless, the use of MTM for scale inhibition still remains in two opinions as some other research studies have

reported to show no prominent effect of using this method for the aforementioned purpose [218-220].

Apart from membrane desalination process, magnetic materials have been utilized in solar thermal evaporation which is a classic method of harvesting solar energy. Wang et al. [221] combined the solar steam generation and magnetic ability to avoid wastage of materials during solar assisted desalination. Reduced graphene oxide (rGO) was decorated on the magnetic nanoparticles and used for treating both seawater and wastewaters. Figure 12a shows the evaporation efficiency of these with different dispersed magnetic nanoparticles. rGO coated Fe_3O_4 nanoparticles gave efficiencies greater than 60% under solar irradiation of 1 kW m^{-2} . Due to Fe_3O_4 , the system could be used in high saline sea and wastewaters, owing to the easier recovery of the magnetic nanoparticles as illustrated in Figure 12b. The Infrared (IR) camera images taken during the process showed that hot zone of the Fe_3O_4 nanoparticle dispersion (left side) moved quickly to the magnet, while the rGO- Fe_3O_4 dispersion (right side) moved slower towards the magnet indicating a more uniform temperature distribution owing to rGO's high thermal conductivity. Sodaye et al. [222] reported magnetic separations for uranium extraction from concentrated brine reject produced from integrated nuclear desalination plants. Usually, the concentrated brines, along with various cations are rejected back to the sea, leading to local degradation of water quality affecting directly the aquatic life. Thus, materials such as uranium may be retrieved from such rejects to be used as a fuel for the integrated nuclear plant. Calixarene- Fe_2O_3 magnetic particles of size $1 \mu\text{m}$ were used with a dosing rate of $1 \text{ cm}^3/\text{L}$ of brine. The magnetic particles were first dispersed in the brine reject and then passed through magnetic

filters, after which the brine was passed on for recovery of other valuables. Uranium was stripped off from these magnetic particles using a solution for recovery. These magnetic functional materials find applications in various areas of desalination from improving desalination performance, to easier recovery of draw solutes in FO and aiding in material recovery from brine rejects.

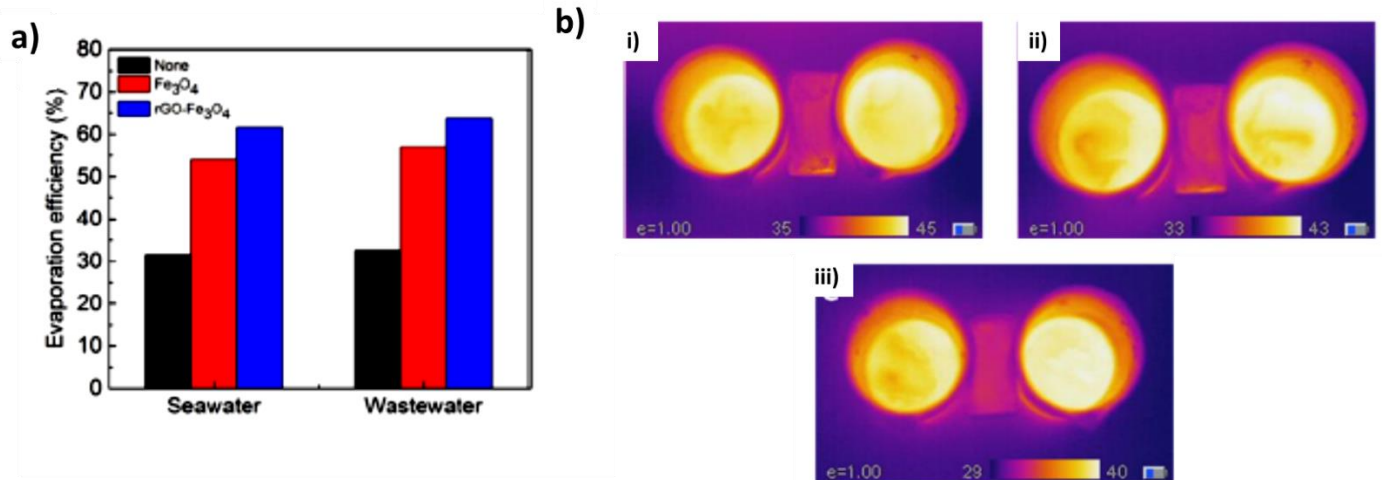


Figure 12: a) Evaporation efficiency of seawater and wastewater with dispersed Fe₃O₄ and rGO-Fe₃O₄ magnetic nanoparticles (b) IR images of the separation process [221].

6. Antimicrobial Materials

Antimicrobial materials are an important class of functional materials largely used to modify the surface of membranes in NF and RO. These materials are found in all classes of materials, organic and inorganic which may have different sizes, shapes, hydrophilicity and biocidal activities [67]. They become necessary to incorporate into membrane materials to prevent the all prevalent biofouling phenomenon which occurs due to the unwanted deposition and growth of biofilms. A biofilm is essentially an assemblage of surface-associated microbial cells enclosed in a matrix of

extracellular polymeric substances (EPS), which are difficult to remove by just gentle washing [223]. These micro-organisms are ubiquitously present in nearly all water systems [224], and they tend to adhere and grow at the expense of nutrients present in the water adversely affecting membrane performance and lifetime. Thus, surface modification of membranes with antimicrobial functional materials becomes essential for improved membrane resistance to active fouling mechanisms [225]. Membrane surface modification is primarily done to retard one or more of the many stages in biofilm formation; bacterial adhesion, microcolony formation, and biofilm maturation. Figure 13 shows a schematic of the antibacterial mechanism, where the biocides can anchor to the bacteria cells via van der Waals forces and cause cell disruption [226]. Secondly, the disruption might also be associated with the metal free ion radicals which can trigger reactive oxygen species (ROS) and cause irreversible cell damage [227]. In numerous cases, the use of negatively charged, more hydrophilic polymers are used to decrease bacterial adhesion [228-231]. Several reviews highlight the prospect of using various polymeric materials for this purpose [67, 232] have been written. However, in this review, the focus is on various antimicrobial materials which can cause inactivation of irreversibly adhered microorganisms. Recently, several engineered nanomaterials have been studied for their strong antimicrobial properties. These include graphene based materials [233], silver (Ag) nanoparticles [234], carbon based materials [235], titanium oxide (TiO₂) [236], gold [237], copper (Cu) [238] and zinc oxide (ZnO) [108].

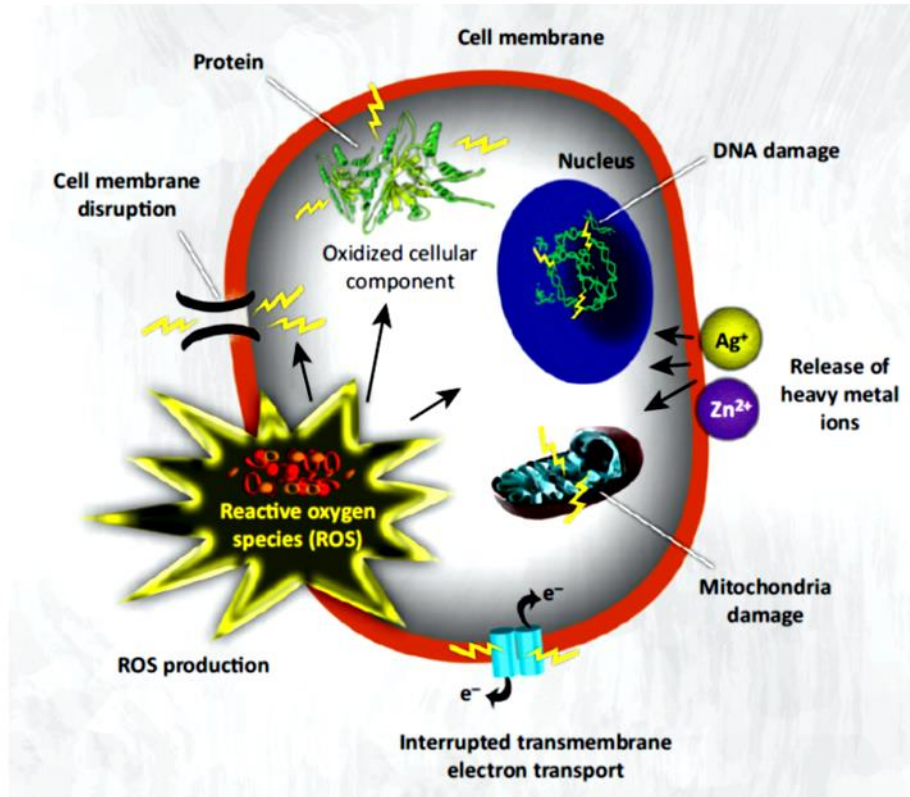


Figure 13: Mechanisms of toxicity of nanoparticles (NPs) against bacteria [226]. Copyright 2012. Reproduced from with permission from Elsevier Ltd.

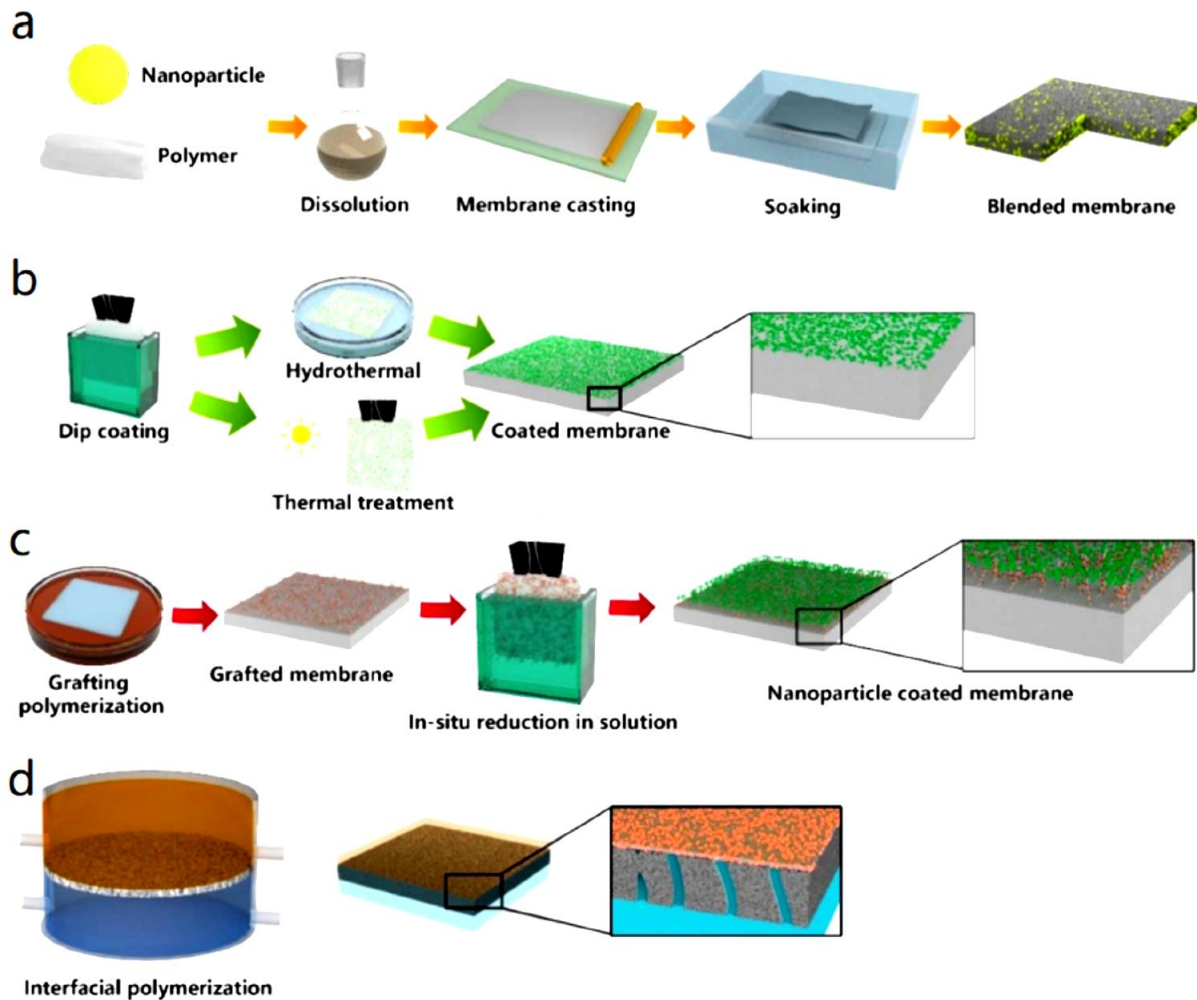


Figure 14: Antibacterial membrane preparation process: (a) Blending (b) surface coating (c) surface grafting (d) interfacial polymerization [239].

The design of antibacterial membranes functionalized with various biocides is significant for efficient biofouling control for maintaining high separation performance. Many different ways may be adopted for fabricating antibacterial membranes. These include blending [240], surface coating [241], in-situ growth [242], self-assembly [243] and interfacial polymerization (IP) [244]. The blending method offers several advantages such as ease of fabrication and broad spectrum of antibacterial activity [245]. Figure 14a highlights the steps for a typical antibacterial membrane produced through the blending approach. Surface coating of antibacterial materials on the

membranes may be achieved through dip coating, spin coating and direct filtration process [246, 247]. Figure 14b depicts a dip-coating process performed by immersion of a substrate into a suspension of antibacterial agents. This process is attractive due to its simplicity and the flexibility of fine-tuning the surface architecture of coatings. However, the coating might be unstable and may require certain functionalization prior to the coating process as shown in Figure 14c. Figure 14d highlights the IP process incorporating antibacterial materials in either the m-phenylenediamine (MPD) or trimesoyl chloride (TMC) component. IP has long been used to fabricate TFC membranes for NF, FO and RO. In a typical IP process, a diamine and a triacylchloride rapidly polymerize to form a polyamide selective layer on top of a support membrane layer. As part of the process, antibacterial nanomaterials can be added in either the aqueous or oil phase prior to the IP process [248]. Other techniques such as layer-by-layer (LBL) self-assembly uses alternative assembly of oppositely charged species [249]. The method allows for precise control of the multilayer structures providing desired functions and thicknesses. Nevertheless, the choice of the fabrication method depends on a case-by-case basis for different materials and in most cases targeted bacteria to be removed. In general, a good membrane should give minimal antibacterial particle aggregation, no leaching and good compatibility with the polymer interface.

Among several antibacterial materials, Ag is the most commonly studied one primarily due to its corrosion resistance, low toxicity and high thermal and chemical stability. The Ag^+ can react with the sulfur and phosphorus present in the waters to form, for example disulphide bonds. This interrupts the electron transport and triggers cell disruption and inhibits DNA replication [250, 251]. Zodrow et al. [252] reported the fabrication of polysulfone (PSf) UF membranes incorporated with nano-Ag. These membranes exhibited antimicrobial properties toward a

variety of bacteria including *E. coli*, K12 and *Pseudomonas mendocina*, and the MS2 bacteriophage. The results showed that 0.9 wt. % of nano-Ag in PSf membrane significantly decreased the growth of *E. coli* on the membrane's surface confirmed through the bacteria colony forming units. Secondly, there was a 94% reduction in the number of *E. coli* attached to the surface compared to the neat PSf membrane mostly due to a decrease in cell viability. Biofilm formation was assessed using *mendocina*, where negligible growth was observed on the Ag-impregnated membrane. Moreover, the nano-Ag incorporation was reported to increase the hydrophilicity of the membrane, hence reducing the potential for other types of membrane fouling. Sawada et al. [242] grafted acrylamide onto a polyethersulfone (PES) hollow fiber membrane, after which silver nanoparticles were then embedded within the a polymer layer through immersion in silver nitrate solution. Improved hydrophilicity with superior antimicrobial properties leading to destruction of more than 99.9% of *E. coli* cells were achieved. Significant research has been put in antibacterial RO membranes incorporated by Ag ions and Ag nanoparticles. For example, Yin et al. [253] fabricated polyamide (PA) TFC membranes by grafting 15nm diameter Ag nanoparticles to its surface via covalent bonding with cysteamine as a bridging agent. Membrane characterization through advanced microscopy analysis revealed Ag nanoparticle immobilization with the antibacterial tests providing no evidence of *E. coli* growth. Figure15 shows no biofilm formation and a relatively clean surface for Ag-grafted TFC after 7 days of biofilm growth test, while biofilm growth was observed on the bare TFC membrane as indicated by the black arrow. In addition, a higher flux of 69.4 ± 0.3 L/m²h was registered for the Ag-TFC membrane compared to 49.8 ± 1.7 L/m²h by the bare TFC. However, a slightly lower salt rejection was obtained with Ag-TFC ($93.6 \pm 0.2\%$) compared to $95.9 \pm 0.6\%$ for TFC membrane.

Rahaman et al. [254] reported a different method for incorporating Ag nanoparticles in RO TFC membranes. They developed novel surface coatings functionalized with Ag nanoparticles for antibacterial effect, and polymer brushes via polyelectrolyte LBL self-assembly for antifouling properties. Commercial RO membranes were spray coated alternatively with poly (acrylic acid) (PAA) and poly (ethylene imine) (PEI)-coated Ag nanoparticles. This coating was further functionalized by grafting hydrophilic polymer. These membranes registered superior salt rejections and low adhesion to E. coli bacteria with improved bacterial inactivation up to 95% within 1h of test. On another occasion, three different membranes (PSf, PES, cellulose acetate (CA)) were made by blending Ag nanoparticles with the polymer matrix prior to phase inversion. The location of Ag nanoparticles in the membrane matrix was found to play a crucial role in Ag⁺ diffusivity. The best performance was that exhibited by the Ag-loaded PSf membranes with almost 100% bacterial growth inhibition due to the release of higher diffusivity of ionic silver from silver nanoparticles near membrane's skin layer [245]. It is preferable to have Ag located near the membrane's surface rather than the bulk to maximize the possibility of direct interactions between the antibacterial agent and the bacteria. Yang et al. [255] fabricated polydopamine (PDA) modified PA RO membranes, followed by in-situ reduction of immobilized Ag ions to Ag nanoparticles on the membrane's surface. Superior antibacterial activity with Bacillus subtilis and E. coli reduction of $62.7 \pm 9.3\%$ and $42.4 \pm 5.7\%$ were respectively obtained together with enhanced salt rejections owing to the generation of Ag nanoparticles at the defect sides. An innovative approach was proposed by Yang et al. [256], whereby they modified both, the RO membrane and its feed spacer with a coating of Ag nanoparticles. The results indicated much better performance of both silver-coated membranes with uncoated spacer and silver-coated

spacer with uncoated membrane compared to the uncoated membrane and spacer. Nevertheless, several other research studies have been reported highlighting the similar effect of Ag on bacterial inhibition restricting biofilm growth on membrane surfaces [257-260]

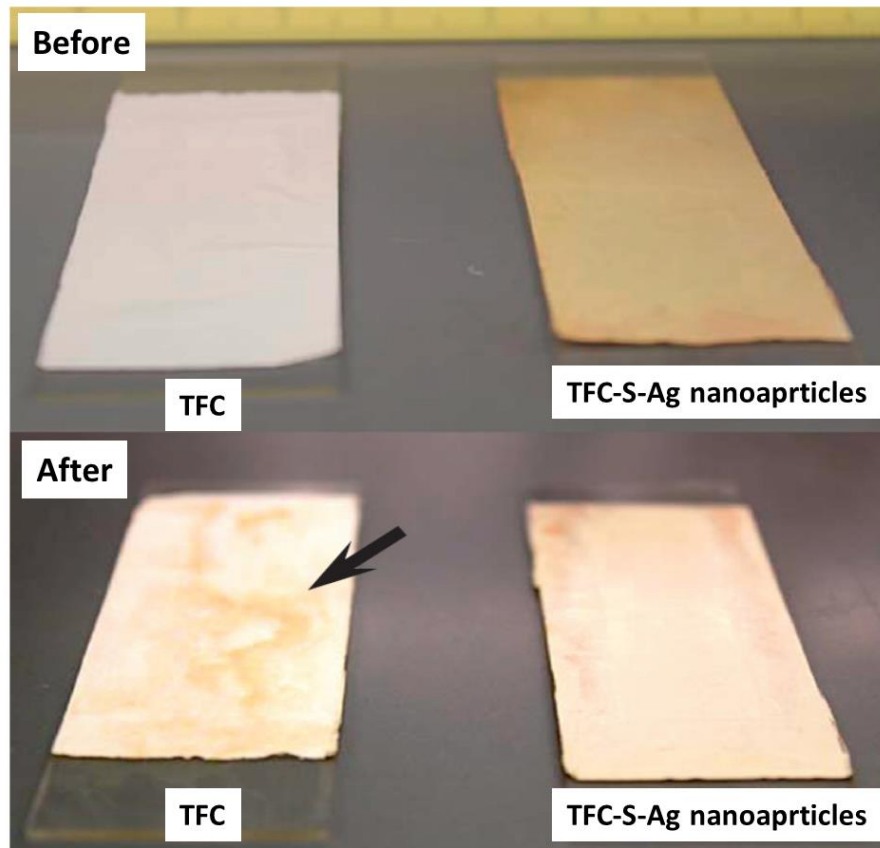


Figure 15: Difference in *E. coli* biofilm growth on TFC and Ag grafted TFC (TFC-S–Ag nanoparticle) membranes after 7 days [253]

Cu-based materials are attractive for their antimicrobial activities against various microorganisms and considerably lower priced than silver [261-264]. Several recent studies highlight the importance of utilizing Cu in antibacterial desalination membranes [265-267]. In contact-mediated mode, hydroxyl radicals are produced that can essentially damage the protein within the bacteria cells [268]. However, while being used in antimicrobial membranes, Cu ions need to be immobilized to prevent their mitigation from the membrane matrix, which would otherwise

contaminate the feed and permeate waters [262, 269-271]. Ben-Sasson et al. [272] developed polyethyleneimine (PEI) -modified Cu nanoparticles-TFC RO membranes through electrostatic interaction. PEI imparted a positive charge to the Cu nanoparticles, which provided an electrostatic functionalization to the negatively charged RO membranes. In addition, the PEI polymer facilitated in stable coverage of the Cu nanoparticles with loadings from 39 to 49 wt. %. Both functionalization and loading was confirmed by advanced characterization techniques such as SEM and x-ray photoelectron spectroscopy (XPS). These membranes led to a significant reduction of 80-95% in the number of attached live bacteria. Ma et al. [273] reported an efficient spray- and spin-assisted layer-by-layer (SSLbL) method to functionalize TFC PA RO membranes with Cu nanoparticles. Enhanced antimicrobial behavior for *E. coli* and *E. faecalis* were reported as shown in Figure 16. The pristine PA membrane was reported to exhibit a rough surface, with increased bacterial deposition over the period of time. However, the modified membrane showed good resistance to bacteria with low CFU/ml during the 6h experimental time.

The current work on TiO_2 is largely focused on its photocatalytic effect to kill bacteria, as discussed previously in section 2. However, many at times, this application becomes limited by the difficulty in introducing UV light to the membrane's surface for TiO_2 activation [85, 90] . Recently, Rasool et al. [274] developed $\text{Ti}_3\text{C}_2\text{T}_x$ -PVDF membranes through vacuum-assisted filtration. These membranes showed good antibacterial properties with a growth inhibition of about 73% against *B. subtilis* and 67% against *E. coli* when compared to the bare PVDF membrane, while about 99% growth inhibition was observed when aged membranes were utilized. Though these membranes were not tested for their desalination capability, it would be

interesting to see their performance for water flux and salt rejections coupled with improved antibacterial performances. ZnO is another antibacterial material which has also been reported for its photocatalytic properties (Section 2). Besides its photocatalytic formation of ROS, the antibacterial mechanism of ZnO Nanoparticles is usually correlated to the or the release of Zn²⁺ ions [275] which can thereafter kill the bacteria by penetrating into its cell membranes. Nevertheless, most of the reported ZnO antibacterial membrane are hybrid forms, discussed in section 6.1. Au nanocomposite membranes also show promising potential for desalination membranes. However, membrane cost will have to be justified in terms of both desalination and antibacterial performances in comparison to cheaper options such as Ag, ZnO and others. Ramdayal and Balasubramanian [237] explored the antibacterial efficacy of solvent cast ultra-stable Au nanoparticles embedded in polyvinyl alcohol (PVA) membranes against *E. coli* and *S. aureus* bacteria. After 12 h of membrane immersion in the bacterial media, inhibition of bacterial growth started with the maximum zone of inhibition of 0.8–1.0 cm against both bacteria. The antibacterial property of Au was reported to be related to the strong bond formation between gold nanoparticles and bacterial electron-donating groups composed of sulfur, oxygen or nitrogen, leading to structural alteration of cell membranes. Nevertheless, most metallic antimicrobial nanoparticles, such as TiO₂, SiO₂, ZnO and Fe₃O₄, are usually functionalized before incorporating them into membranes, to enhance their hydrophilicity [90, 276, 277], while some materials such as graphene, is increasingly being utilized in antibacterial membranes owing to its inherent hydrophilic nature.

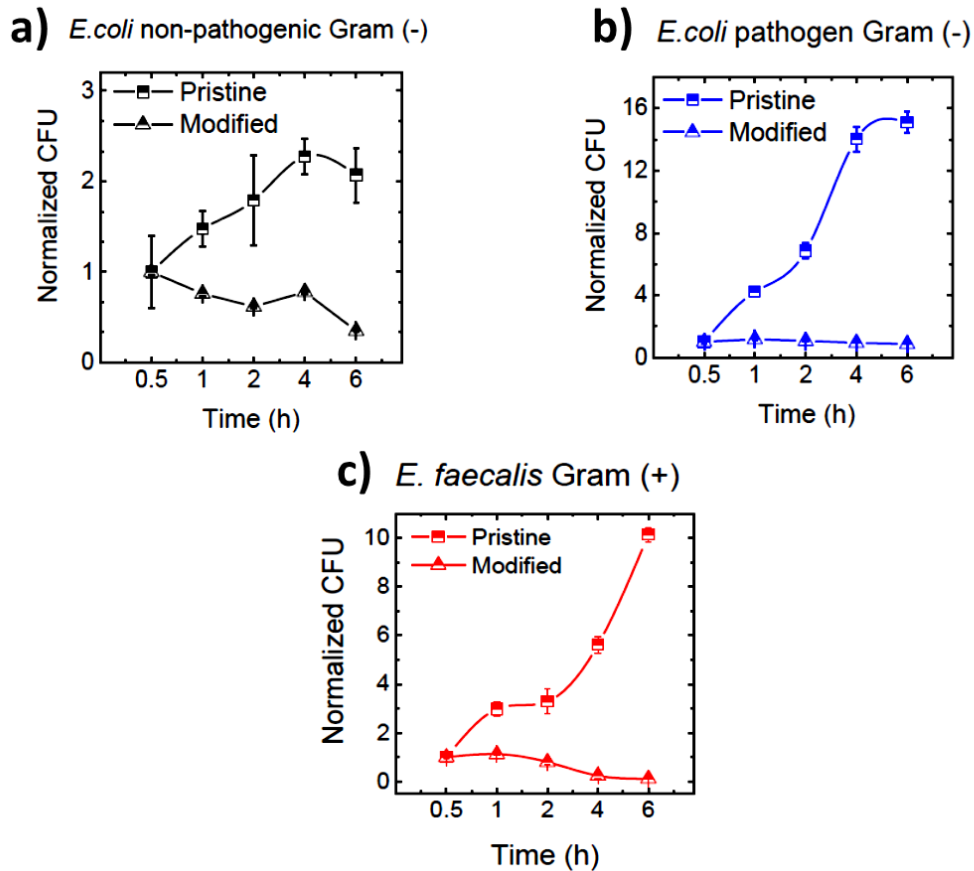


Figure 16: The number of live cells on the pristine and Cu nanoparticle modified membranes for (a-b) *E. coli* and (c) *E. faecalis* bacterial suspensions. [273]

Hydrophilicity is one of the key factors in controlling the antibacterial activity of the membrane. [278]. Hydrophilic membranes are more resistant to bacterial growth due to a hydration layer over the membrane's surface [279]. Therefore, hydrophilic additives, like graphene oxide (GO) make attractive antibacterial materials for biofouling resistant membranes. Graphene based membranes which are gaining importance with significant progress over the last decade [280, 281]. These include graphene, GO and reduced graphene oxide (rGO). Their oxygen containing functional groups and one-atom-thick lamina structure provides superior separation characteristics to antibacterial membranes along with biocidal properties. Similar fabrication

techniques (as discussed above for Ag-based membranes) are applied to develop graphene based antimicrobial membranes. However, by far the most prominent one is based on surface functionalization on polymeric membranes through cross-linking, LBL assembly, covalent immobilization, grafting and in-situ synthesis [282]. GO is reported to induce cell membrane damage facilitated by charge transfer and formation of ROS leading to bacterial inactivation [283, 284]. Choi et al. [285] deposited multilayers of oppositely charged GO and laminated GO nanosheets on TFC PA membranes using the LBL method. Optimization of these layers produced membranes with good chlorine resistance and antifouling resistance to BSA protein. In addition, lower flux reductions of 15% were exhibited compared to the pristine PA membrane (34%) after 12 h of continuous tests. Perreault et al. [280] reported TFC PA membranes functionalized by GO using 1-ethyl-3-[3-(dimethylamino) propyl] carbodiimide hydrochloride and N-hydroxysuccinimide as shown in Figure 17. This imparted improved antibacterial performance to the polymeric membrane lowering the viable *E. coli* cells by 64.5%, while keeping the water flux and salt rejections similar to the bare TFC membrane. In another study, the same research group concluded the importance of GO sheet size on the antimicrobial activity of GO. Smaller sized GO sheets showed higher antimicrobial activity due to higher defect density introduced in GO sheets as size decreases. Recently, Zeng et al. [286] developed amino-functionalized PVDF membranes decorated by GO quantum dots (GOQDs) ranging from 3-20nm on the membrane's surface through the dip coating method. The flux drops over these membranes under an *E. coli*-containing continuous feed indicated only a drop of 24.3% compared to 88.4% of the pristine PVDF membranes. In addition, the GOQD coating effectively inhibited the growth of *E. coli* cells, successfully preventing the formation biofilm on the membrane surface. The metabolic activity

of *E. coli* cells was seen to reduce by 88.9% compared to only 69.2% for 2D GO-PVDF membrane. With an attempt to enhance the microbial resistance, Lu et al. [287] developed vertically aligned GO nanosheets in Polyoxadiazole-co-hydrazide (PODH) polymer through a slow solvent evaporation in the presence of a magnetic field. This led to enhanced exposure of nanosheet edges on the membrane's surface providing more room for antimicrobial activity by reducing the number of viable *E. coli* cells by 71.7% compared to the non-aligned GO nanosheets. A four-layer antibacterial RO membrane was developed by JR et al. [288] by functionalizing a commercial polyamide membrane with PEG, GO, and Au nanostars. The synergetic coupling of these photothermal and antibacterial materials led to a significant decrease in mineral scaling (CaCO_3 and CaSO_4), organic fouling (by humic acid) and biofouling (by *E. coli*). Apart from experimental findings, molecular dynamics (MD) simulations have applied to study the antibacterial effect of graphene on various bacteria. Li et al. [289] studied the interactions of graphene sheets with lipid bilayers. The results showed that graphene sheets entered the microbial cells through spontaneous penetration from its edges. Further, Mao et al. [290] showed that graphene nanosheets with a higher oxidization degree induced more membrane perturbations and cell destructions. Graphene based antimicrobial membranes for desalination application continue to instill interest in researchers due to the material's unique properties offering high separation performance and antibacterial properties [281]. Numerous other studies report on enhanced properties of graphene assisted materials for bacterial inactivation [248, 291-299].

Graphene oxide functionalization → Antimicrobial properties

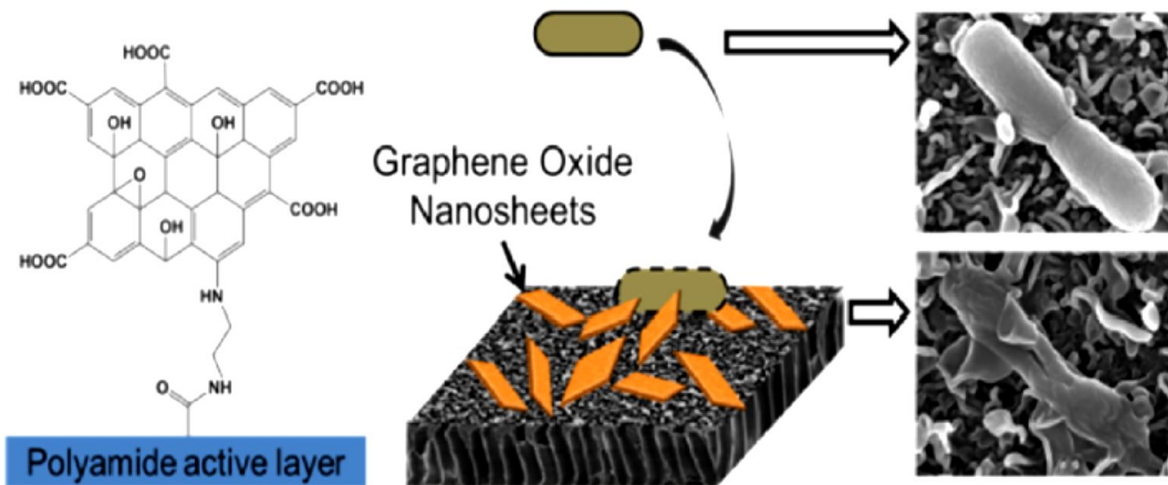


Figure 17: Functionalization of graphene oxide nanosheets onto the TFC membrane. The top SEM image shows normal E.coli cells on the membrane surface while the bottom SEM image shows compromised bacteria cells after membrane functionalization [280]

Besides GO, other carbon-based materials find biocidal applications where they have been successfully tested for bacteria cell destruction and thus incorporated in polymeric membranes for desalination. Kang and co-workers [235] were one of the first ones to report direct evidence of single-walled CNTs (SWCNTs) exhibiting strong antimicrobial activity. The proposed mechanism for this function was bacterial cell death due to cell membrane damage resulting from direct contact with the single-walled SWCNTs. In an another study [300], MWCNTs were shown to exhibit similar behavior, however with some weaker bacterial toxicity in contrast to the SWCNTs. In general, CNTs impose mechanical and oxidative stresses to the surface of the bacteria's cellular membrane. The mechanism includes initial contact between the bacteria and CNTs, then agitation of the cellular membrane, followed by bacterial oxidation depending upon the electronic structure [300-302]. Keeping in mind that the antibacterial activity is strongly dependent upon the direct contact between the CNTs and target micro-organisms, achieving a

uniform and homogeneous CNT dispersion in the solvent is essential during membrane fabrication. One of an early attempt to fabricate CNT-polymer membranes through blending did not register any antibacterial improvements, most probably owing to restricted CNT exposure [303]. From then, numerous studies have come forward to develop antibacterial desalination membranes incorporated with CNTs based on various fabrication techniques. An advanced technique involves the brush grafting of CNTs on polymer chains [202]. CNTs were brush grafted through surface initiated atom transfer polymerization by methyltriethylammonium chloride (MTAC) and poly (ethylene glycol) methyl ether methacrylate (EGMA). Following this, grafted-CNT/PES UF membranes were prepared through the phase inversion technique. The EGMA induced enhanced wettability to the membrane, while the CNTs formed the antimicrobial component. Antimicrobial tests gave almost 99% E. coli and S. aureus bacterial killing while bacterial adhesion (cells per cm²) to the membrane's surface was significantly reduced from 21.5X 10⁷ and 10.3X10⁷ to 5.3X10⁷ and 2.1X10⁷ for E.coli and S. aureus respectively [304]. Kim et al. [305] developed PA RO membranes with oxidized CNTs through IP, coated with poly(vinyl alcohol) (PVA) polymer on its surface. The PA-CNT-PVA membrane showed enhanced mechanical and anti-biofouling properties compared to the bare PA and commercial (LFC-1) membranes. The well-dispersed CNTs in the PA active layer were stabilized by the PVA coatings. Confocal laser scanning microscopy (CLSM) showed the anti-biofouling morphology of the PA, PA-PVA, PA-CNT-PVA, LFC-1 membranes after the antibacterial test (Figure 18a(i-iv)). In Figure 18a, the green spots highlight the live P. aeruginosa cells attached to the membrane's surface. After a continuous test of 24h, a thick and dense biofouled layer can be observed on the PA, PA-PVA and LFC-1 membranes, while negligible biofouling was observed for the PA-CNT-PVA membrane. The cell viability tests shown in Figure

18b further confirmed the enhanced antimicrobial properties of CNTs by damaging the membrane of microorganisms and disrupting their metabolic pathways. Apart from bare CNT-polymeric membranes, more often, CNTs are used in conjunction with other antimicrobial materials such as ZnO [111] and Ag nanoparticles [306-308], for enhanced functional desalination properties. Such hybrid membranes for desalination are discussed in more detail in section 6.1.

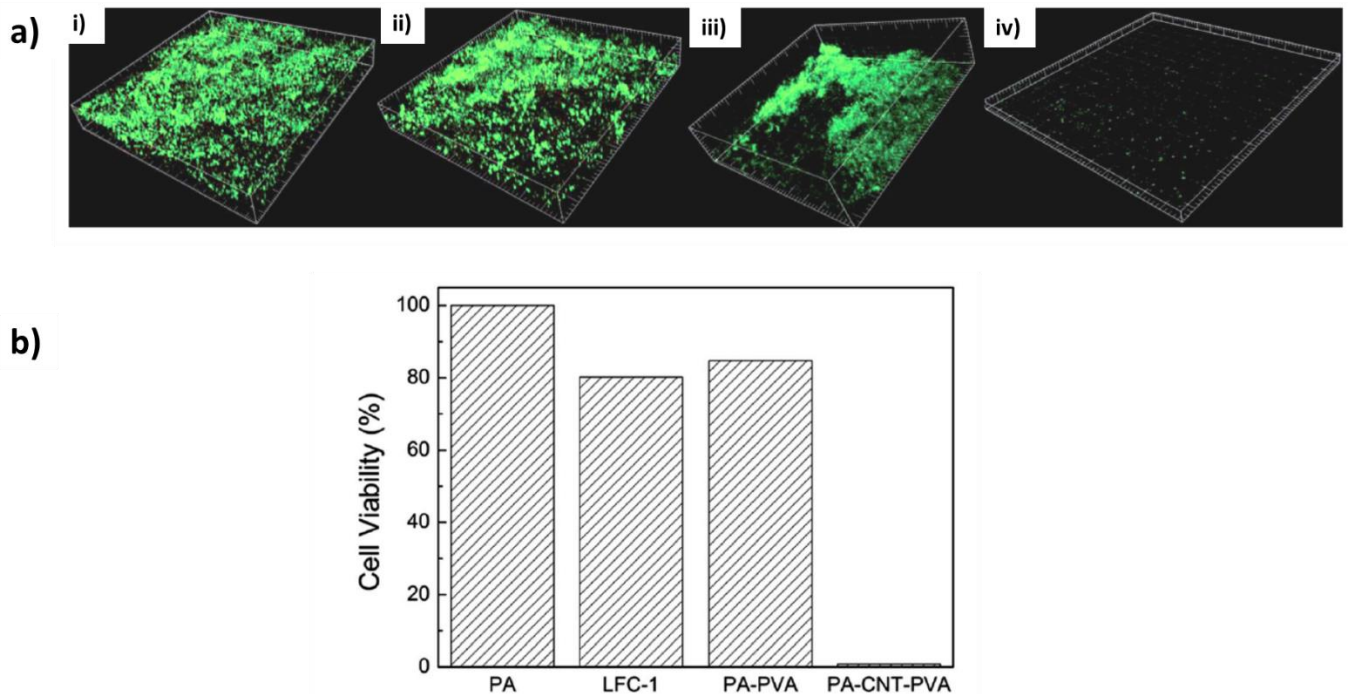


Figure 18: (a) CLSM images of (i) PA, (ii) LFC-1, (iii) PA-PVA0.4, and (iv) PA-CNT0.2-PVA0.2 membranes obtained after 24 h cross-flow test using *P. aeruginosa* as feed solution (b) Cell viability tests for PA, LFC-1, PA-PVA and PA-CNT-PVA membranes, where PA membrane is used as the control standard. (Reproduced from [305], The Royal Society of Chemistry).

Besides inorganic antibacterial materials for desalination, organic materials have also gained importance. These include chitosan [309, 310], Polyzwitterions [311, 312], capsaicin [313, 314] and several others [315-317]. Derived from chitin, chitosan exhibits good antibacterial, non-toxic and biodegradable properties [318-320]. It can bind to the cellular membrane's surface, leading to a loss in bacterial cell structural integrity [321]. More often, chitosan is directly coated on

desalination membranes via crosslinking or electrostatic LBL processes [223,224]. However, despite its advantages of being a low-cost efficient biocide, chitosan usually possesses poor stability and often needs to be tackled carefully under acidic environments [239]. Xu et al. [322] developed capsaicin-mimic antibacterial membranes via the phase inversion method. The membranes were easier to clean in removing the foulants with good antimicrobial properties. In addition, novel organic biocide brushes are increasingly gaining importance for desalination membrane applications, including rhodanine [323], N-acetylcysteine [324], triazine ring [325] and many others [326, 327]. Nevertheless, the most promising antibacterial membranes are hybrid membranes of inorganic materials, with more than one inorganic material facilitating the numerous desalination functions all together. Such membranes are reviewed in detail in the below section.

6.1 Antimicrobial Inorganic-Inorganic Hybrid Membranes

Many at times, metallic ions may be supported on other materials. For example, Ag^+ and Ag nanoparticles have been widely reported to be supported on other carriers such as graphene oxide [328], CNTs [329, 330], halloysite nanotubes (HNTs) [331], SiO_2 [332-334], TiO_2 [335, 336] and zeolites [337, 338]. These support materials are either antibacterial agents themselves such as GO and CNTs, possess photocatalytic properties such as TiO_2 , or have hydrophilic, molecular sieving properties such as zeolites. Hybrid membranes exhibiting antimicrobial properties due Awuah et al. [339] studied the antimicrobial efficacy of Ag-loaded zeolite X on *Escherichia coli* (E.coli), *Staphylococcus aureus* and *Pseudomonas aeruginosa* bacteria. Ag^+ was incorporated into zeolite through an ion-exchange mechanism which resulted in a 2.0 wt. % loading of Ag^+ in the

zeolite framework. The zeolite support was responsible for a constant release of silver ions from the zeolite framework. After 1 hr of testing, no viable cells were detected for any of the three micro-organisms. Liao et al. [338] reported an UF membrane made from PVDF embedded by Ag-loaded NaY particles. The membranes were fabricated through a phase inversion process. A comparison of antibacterial activity was made between neat PVDF and Ag⁺-zeolite-modified PVDF membranes. Apparently no antibacterial activity was observed for neat PVDF membranes, while the composite membranes showed long lasting antibacterial activity against E. coli. In addition, Ag⁺-exchanged NaY zeolite had no influence on the PVDF membrane structure and thus provided high retentions of bovine serum albumin (BSA) above 92%. When tested for pure water flux, a flux of 606 L/m².h was obtained for pure PVDF membranes, while with the addition of Ag⁺-exchanged NaY zeolite particles, the flux was seen to considerably increase to 679 L/m². h. Similarly, Shi et al. [337] reported poly (vinylidene fluoride) hollow fiber membranes embedded with Ag-loaded zeolites. These membranes were fabricated via a wet spinning process via co-extrusion. PVDF and PVP polymers were added to the DMAc solvent and stirred until dissolved. Ag-loaded zeolites were added in the polymer solution and degassed thereafter to remove any air bubbles. The embedding of Ag-loaded zeolites promoted Ag⁺ enrichment and improved antibacterial efficiency when tested on E. coli. More than 95% of the bacteria was killed as confirmed through the antibacterial tests. Bacterial killing was attributed to the direct contact of the bacteria with the Ag⁺-zeolite particles absorbing the Ag⁺ ions [340], which helped inhibition of the enzymes essential for biofouling. Several other research studies [341-343] have been put affront for Ag-loaded zeolite antimicrobial activities deeming for promising desalination membrane applications. One study reported the fabrication of Ag/TiO₂ membranes for FO

desalination, whereby Ag nanoparticles were deposited by a photo-induced growth approach on the surface of commercial cellulose triacetate (CTA) FO membranes. This was followed by TiO₂ self-assembly on the Ag nanoparticles. The experiment did not involve any light irradiation to activate the TiO₂. Thus, TiO₂ in this case did not strictly act as a photocatalyst as discussed in section 2, rather Ag and TiO₂ was reported to synergistically enhance the antibacterial properties of each other lowering the bacterial growth on the hybrid membrane by 11 times compared to the bare CTA membrane without any coating. In addition, a 67–72% recovery of water flux was achieved by these hybrid membranes compared to only 33% by the CTA membrane alone. Thus, TiO₂ played an effective role in decomposing the organic contaminants, facilitating Ag nanoparticle regeneration [105]. Gunawan et al. [306] reported Ag-MWCNTs covalently bonded PAN hollow fiber UF membranes. The MWCNTs helped to minimize water resistance and increased the contact probability between Ag and bacterial cells. In another study, [246] Ag/MWCNTs were deposited on the PAN hollow fiber membranes through filtration under 0.7–0.8 bars. The concentration of bacteria for PAN membranes increased from about 2 X10⁶ CFU/mL to 180 X10⁶ CFU/mL after 18 h of test, while for Ag-MWCNTs-PAN membranes, it took around 80 h to reach a similar bacterial concentration. However, the leaching of Ag ions could not be controlled, and thus Ag nanoparticles had to be replenished for the antibacterial functionality.

Apart from their antibacterial capability, graphene based materials can serve as an efficient support material for various biocidal materials [328, 344, 345]. This flexibility mostly emerges from their multifunctional groups (hydroxyl, carboxyl, epoxy), facilitating easier crosslinking of other agents. Ag nanoparticles on GO has emerged as an attractive composite for enhanced

biocidal ability owing to its synergistic effect [346, 347]. Faria et al. [348] proposed TFC FO membranes functionalized with graphene oxide–silver nanocomposites. The functionalization was achieved by using ethylene diamine to yield amine-terminated surface on the TFC, while GO surface was activated by forming esters as shown by the schematic in Figure 19a. The GO/Ag sheets were covalently linked to the PA layer through the formation of an amide bond between the carboxyl groups of GO and the amine groups on the TFC membrane. For comparison, GO-TFC membranes were also tested for its antimicrobial properties and water permeability. The TFC membrane apparently showed no visible damage on the bacterial cells (Figure 19b), while severe morphological damage was observed for the bacteria cells on the GO/Ag-TFC membrane as highlighted by the white arrows in Figure 19c. These composite membranes exhibited 80% bacterial inactivation against the *P. aeruginosa* bacteria as shown in Figure 19d, when TFC, GO-TFC and GO/Ag-TFC membranes were compared. In addition, the formation of a biofilm during the biofouling experiments showed a rapid decrease in the water flux for pristine membranes compared to both GO-TFC and GO/Ag-TFC membranes (Figure 19e). Wang et al. [349] developed GO-ZIF-8/TFC membranes through the IP method. A uniform distribution of the ZIF-8 zeolite-GO was achieved in the PA layer leading to high desalination performances; a water flux of $40.63 \text{ L m}^{-2} \text{ h}^{-1} \text{ MPa}^{-1}$ and Na_2SO_4 and MgSO_4 rejections of 100% and 77%, respectively. Furthermore, an antimicrobial activity of about 84.3% was registered rendering these membranes as an attractive material for antibacterial desalination membranes. In an another study [350], ZnO was supported on GO and embedded into PSF membrane through the wet phase inversion technique. The study revealed that 0.6 wt. % ZnO–GO nanoparticles embedded membrane successfully inhibited *E. coli* growth due to ROS formation. These membranes were also registered as the most

hydrophilic, compared to other GO-based hybrid membranes based on TiO₂, SiO₂ and Ag nanoparticles [328, 351, 352]. Zhao et al. [331] developed a novel high flux, hybrid antibacterial UF membrane by blending the Ag nanoparticles, HNTs and rGO nanocomposites into PES membrane matrix. HNTs helped in the interlayer expansion of the neighboring rGO sheets and inhibited Ag nanoparticle leaching. These hybrid membranes showed improved antibacterial property of almost 100% E. coli inhibition, with a lower decline in flux of 19.5% compared to 67.3% for pristine PES membranes. Mural et al. [347] developed Ag-rGO/PE-PEO membranes through the melt mixing approach. Antibacterial performance was determined through the loss of viability of bacterial cells by the colony counting method. The colony forming unit (CFU) for E. coli was found to decrease from 3X10⁸ cells in the bare polymeric membrane to 7.5X10⁷ cells in the Ag-rGO-polymeric membrane. Many other research studies have reported on the synergetic effect of Ag-graphene based antibacterial membranes [353-355]. Inorganic-inorganic hybrid antibacterial materials have emerged as a better option for desalination, providing multiple functions, however, their functionalization and incorporation into polymeric matrix is still challenging with several limitations such as agglomeration and leaching. Table 4 highlights some prominent studies on antibacterial membranes over the last five years.

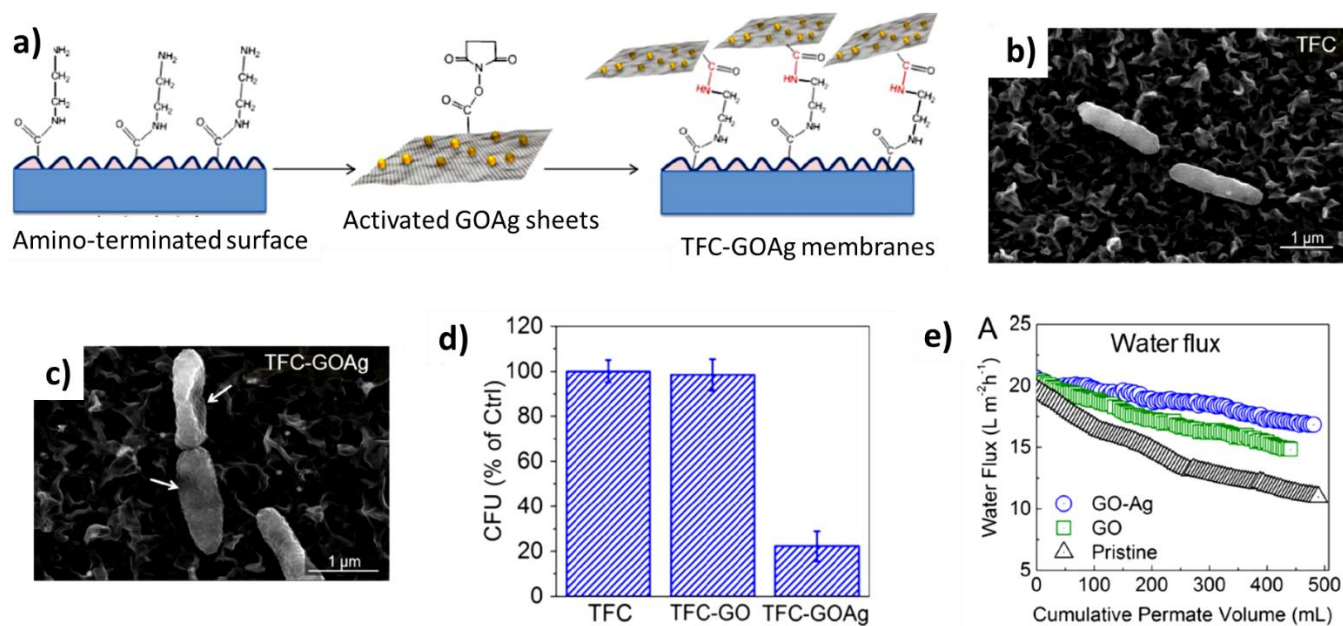


Figure 19: (a) Schematic illustrating the formation of GO/Ag-TFC membrane, (b) SEM image of bacteria cells attached to the TFC-GO membrane (c) SEM image of bacteria cells attached to the GO/Ag-TFC membranes, (d) Viable cells of *P. aeruginosa* after three-hour contact with the surface of pristine and graphene modified membranes and (e) Water flux decline for TFC, GO-TFC and GO/Ag-TFC membranes [348].

Table 4: Prominent studies on inorganic antibacterial membranes during the last 5 years

Reference/ year	Antibacterial material	Membrane type	Fabrication method	Key features
Shi et al. [337], 2014	Ag loaded on zeolite	Dual layer PVDF hollow fibers	Dry jet-wet spinning	>95% of <i>E. coli</i> were killed
Rahaman et al. [254], 2014	Ag nanoparticles-PEI	Commercial TFC RO (SWC4+)	LBL spray coating	Up to 95% inactivation of <i>E. coli</i> attached to the surface within 1 hour of contact time.
Sile-Yuksel et al. [245], 2014	Ag nanoparticles	PSf, PES and CA membranes.	Immersion precipitation	The antibacterial test results showed that the location of Ag nanoparticles in the membrane matrix can change the diffusivity of Ag ⁺ .
Perreault et al. [280], 2014	GO nanosheets	TFC PA RO membrane	Surface functionalization via covalent immobilization	Lowered <i>E. coli</i> cells viability by 64.5% and registered similar salt rejections and water fluxes as bare TFC PA.
Mural et al. [356], 2014	Amine terminated GO (GONH ₂)	Polyethylene (PE)/ Polyethylene oxide (PEO)	Melt blending	High level of <i>E. coli</i> inactivation with superior mechanical strengths.

Chook et al. [346], 2014	Ag nanoparticles-GO	Cellulose membrane	Blending and coagulation	Membrane's porous structure provided significant contact surface for the Ag nanoparticles with the bacteria registering 71.2% and 98.1% bacteria cell inhibition of <i>S. aureus</i> and <i>E. coli</i> respectively.
Kim et al. [305], 2014	Oxidized CNTs	PA, PA-PVA and commercial membranes	IP	Improved mechanical properties, higher salt rejections and excellent anti-biofouling potential.
Rusen et al. [307], 2014	Ag-MWCNTs	PMMA/Commercial membrane	Dip coating	Sandwiched-type structure; good stability of the materials and increased hydrophilicity of the hybrid membranes.
Zhao et al. [331], 2015	Ag nanoparticle-HNTs-rGO	PES UF membrane	Blending	Higher hydrophilicity leading to higher water permeation flux and even attachment of Ag nanoparticles onto rGO leading to improved antimicrobial activity.
Mahmoudi et al. [328], 2015	Ag nanoparticle decorated GO nanoplates	PSf UF membranes	Phase inversion	0.5 wt. % of Ag-GO gave uniform dispersion of the nanoparticles, preventing agglomeration in the polymer matrix with excellent antibacterial properties.
Sun et al. [353], 2015	Ag nanoparticles-GO	Cellulose acetate (CA)	Vacuum filtration	Only 14% of bacterial activity observed after 2 h of antimicrobial test.
Zhao et al. [331], 2015	Ag nanoparticles-HNTs-rGO	PES UF membrane	Blending	A flux drops of only 19.5% with the hybrid membrane compared to 67.3% with pure PES and 100% bacteriostatic rate with <i>E. coli</i> .
Mural et al. [347], 2015	Ag-rGO	PE/PEO	Melt mixing	The CFU mL ⁻¹ decreased to 7.5X10 ⁷ cells from 3.0X10 ⁸ (neat PE/PEO membrane)
Yang et al. [255], 2016	Ag nanoparticles	PA RO membrane	In-situ reduction of Ag ⁺ to Ag nanoparticles by catechol groups in PDA.	Antimicrobial RO membranes with improved salt rejection and similar water permeability compare to control membrane owing to the formation of Ag nanoparticles at defect sites.
Mukherjee et al. [357], 2016	Chitosan	Polyacrylonitrile UF membranes	Surface coating	Strong anti-adhesive property, plus 99.9% rejection efficiency of microorganisms.

Zeng et al. [286], 2016	GOWDs	Amine functionalized PVDF membrane	Dip coating	Metabolic activity of <i>E. coli</i> cells reduced by 88.9% compared to only 69.2% for 2D GO-PVDF membrane.
Wang et al. [349], 2016	ZIF8 onto GO	TFN PA membrane	IP process	Efficient bivalent salt rejection with superior antibacterial property (84.3%).
Li et al. [344], 2016	Ag-GO	PVDF UF membranes	Phase Inversion	Slow release of Ag ⁺ provided remarkable continuous antibacterial activity.
Chen et al. [345], 2016	GO-Ag	PVDF membrane	Non-solvent induced phase inversion	The presence of Ag graphene surface and the action of oxygen functional groups in GO exhibited strong bactericidal activity compared to single GO or Ag nanoparticles.
Yan et al. [304], 2016	Polymer brush grafted CNTs	PES membrane	Phase inversion	Bacterial killing: <i>E. coli</i> and <i>S. aureus</i> : 99%, bacterial adhesion (cells per cm ²): <i>E. coli</i> : 5.3X10 ⁷ (control: 21.5X10 ⁷); <i>S. aureus</i> : 2.1X10 ⁷ (control: 10.3X10 ⁷);
Kim et al. [358], 2016	GO coated with tannic acid	PA RO membranes	IP	The synergistic combination of tannic acid and GO exhibited improved membrane performance with improved water flux, chlorine resistance and antimicrobial properties.
Ma et al. [273], 2016	Cu nanoparticles	TFC PA RO membrane	SSLBL method	Significantly improved anti-biofouling property and easy Regeneration of Cu nanoparticles after depletion through the same SSLBL method.
Huang et al. [298], 2016	GO	Commercial RO membrane	Anchored via azide photochemistry	A 17-fold reduction in biofouling after 24 h of <i>E. coli</i> contact was registered.
Wang et al. [359], 2017	Ag nanoparticles	PAN RO membranes	In-situ reduction of Ag ⁺ to Ag nanoparticles by catechol groups in PDA.	excellent disinfection power, with the membrane exhibited > 7 log reduction for <i>E. coli</i> and > 6 log reduction for <i>B. subtilis</i>
Aani et al. [308], 2017	Ag-MWCNTs	PES UF membrane	Phase inversion	Increase in antibacterial activity with increasing wt. % of Ag-CNTs.
Zhu et al. [267], 2017	Cu-rGO	PAN NF membrane	Co-deposition procedure	Decreased salt retentions due to an increase in membrane

				pore size, however, a reduction in the viable cells to almost 96.4% with the modified membrane.
Ma et al. [265], 2017	Cysteamine- GO- Cu nanoparticles	PA RO membranes	In-situ reduction	A 33% improvement in bacterial inactivation with more robust and durable biocidal properties.
Rasool et al. [274], 2017	Ti ₃ C ₂ T _x	Commercial PVDF membrane	Vacuum-assisted filtration	Bacterial inhibition of about 73% against <i>B. subtilis</i> and 67% against <i>E. coli</i> as compared to the control PVDF membrane.
Faria et al. [348], 2017	Ag-GO	TFC PA FO membrane	Covalent bonding-crosslinking	These composite membranes exhibited 80% bacterial inactivation against the <i>P. aeruginosa</i> bacteria while a much lower water flux decline compared to the pristine TFC membranes.
Lu et al. [287], 2018	Aligned GO nanosheets	PODH membrane	Solvent evaporation in the presence of a magnetic field	Enhanced exposure of nanosheet edges on the membrane's surface led to a significant 71.7% reduction of <i>E.coli</i> cells compared to the non-aligned GO nanosheet membrane.

7. Sorbent Materials

In desalination, sorbent materials are widely used for salt rejection from aqueous solutions. Between adsorbent and absorbent materials, adsorbents are predominantly utilized for this purpose. With a potential to be developed at a relatively low cost, and flexibility and simplicity in process design, operation and maintenance, adsorption has emerged as an attractive technology for salt rejection [360]. The progressive steps involved in the adsorption process include the transport of the ions from the bulk solution to the adsorbent surface; adsorption of the ions at the surface; transport of the ions within the adsorbent sites and then desorption of adsorbed

ions for regeneration purposes [361]. Adsorbents are usually classified based on their chemical composition, particle size distribution, porosity and surface area. Due to their desirable surface area and high adsorption capacity, nano-adsorbents are more attractive than bulk materials, however, they come with their own challenges of recovery, reuse and economic constraints. Hence, natural adsorbents are a more viable option owing to their availability and lower cost [50]. A good adsorbent generally has a high adsorption capacity, high selectivity, favorable kinetics, good mechanical properties, and good stability and reusability [362]. Various adsorbent materials such as zeolites [363], CNTs [364], graphene [365], magnetic adsorbents [366] and bio-adsorbents [367] have been identified for this purpose as summarized in Table 5. Adsorption empirical models are widely used to predict experimental results. Langmuir and Freundlich isotherms are commonly used for investigating single-component systems, while extended and modified Langmuir isotherms were developed to describe the behavior of multi-component adsorption systems [50].

Table 5: Various nano-sorbents for desalination application

Reference	Nanomaterial Sorbent	Performance in Desalination
Sonqishe et al. [368]	Zeolite Y and Zeolite P, Flyash	Nano-sorbents were used for treatment of brine. Zeolite P had higher or similar rejection efficiency than the commercial zeolite Y for K, Ca and Mg ions, but could not remove Na. Fly ash managed to reduce the concentration of Na in brine with good rejection efficiency of Mg.
Wajima et al. [369]	Zeolite Morendite	Natural zeolite was used for seawater desalination for cultivation purposes. 73% Na ⁺ rejection but lower reduction of Cl ⁻ and SO ₄ ²⁻ ions.
Aghakhani et al. [363]	Natural zeolite	Zeolite was used for desalination of natural saline water. Adsorption rate of salinity ions by single and combined forms of five adsorbents was studied.
Xue et al. [370]	Mesoporous LTA Zeolite	Separation of divalent cations, Ca and Mg was investigated. Activation energy for ion exchange was lowered due to the presence of mesopores, leading to a higher exchange rate of Mg ²⁺ compared with the conventional microporous zeolite LTA.
Duke et al. [371]	SAPO-34 and ZIF-8	The SAPO-34 gave negligible water permeation while the ZIF-8 membranes gave 600 kg.m ² .h of water flux,

		however providing unsatisfactory salt rejections of only 6.3%.
Bhadra et al. [372]	CNT immobilized membrane encapsulated in PVDF	Improved desalination efficiency in membrane distillation (MD) with a flux of 19.2 kg/m ² .h and a NaCl salt rejection of 99%.
Mohammadi [364]	CNT sheets	An adsorption capacity of 1.4286 g g ⁻¹ was registered for the oxidized CNTs.
Yang et al. [373]	Plasma-modified ultra-long CNTs (length of 100–200 μm) on mixed cellulose ester	- Superior specific adsorption capacity for NaCl salt. - 400% adsorption capacity by weight - 100% recovery of its initial salt rejection capability after regeneration through simple rinsing by tap water.
Mishra and Ramaprabhu [374]	Functionalized graphene sheets.	Maximum adsorption capacity of 122mg g ⁻¹ for Na.
Wang et al. [375]	functionalized rGO-resol nanocomposite.	Improved electrosorptive removal performance of NaCl, 3.2 mg/g, compared to rGO (1.8 mg/g) and AC (1.5 mg/g).
El- Deen et al. [376]	MnO ₂ -nanorods@graphene	Distinct electrosorptive capacity (5.01 mg/g) and excellent salt rejection efficiency (~ 93%).
Mishra & Ramaprabhu [377]	Flexible carbon fabric supported magnetite MWCNT nanocomposite	1 V DC power supply gave 70% sodium, 67% magnesium, and 73% calcium removal in 20 repeat cycles.

Various studies have compared different adsorbent and absorbent types for salt rejection. Five different adsorbents, peat, AC, zeolite, anionic resin, and cationic resin were compared to remove saline ions from aqueous solutions. 1g of each adsorbent was used in 50 cm³ of brine drainage. All adsorbents were seen to adsorb anions about 1.7 times that of cations, while peat registered the highest adsorption rate of 255.5mg of saline ions amongst the single adsorbents. However, the highest salinity adsorption occurred when a combination of adsorbents was utilized. Cationic resin with peat, zeolite, activated carbon, and anionic resin was more effective than a single form of adsorbent [363]. Ouar et al. [378] reported an experimental yield analysis of groundwater solar desalination using absorbent materials. Black absorbents, such as bitumen, charcoal and Chinese ink were separately added within the absorber plate of conventional solar still. These materials were reported to increase the water absorption of solar irradiance, while playing a significant role of heat storage medium in the solar still. The results showed that

bitumen, charcoal and black ink improved the productivity of the solar still by 25.35%, 18.42% and 6.87% respectively. In addition, their study reported an 18 times decrease in distilled water cost price with solar distillation using a 0.5cm thick bitumen layer compared to other water energy processes.

Specific adsorbent materials have gained special attention to date owing to their multiple material-specific functionalities. For example, due to the valences of silicon and aluminum, the zeolite framework is negatively charged, and thus this creates a high affinity of the structure towards cations leading to a high ion exchange capacity. Thus, this property makes zeolites widely recognized as adsorbents in desalination. In addition, their microporous (pores <2nm) and mesoporous (pores between 2-50nm) structure, and well defined pores deem zeolites suitable for ion selectivity, increasing their performance for salt separation. Several natural and synthetic zeolite types have been reported for this application (Table 5). Wajima et al. [369] reported NaCl rejection from seawater using natural zeolite (morendite) treatment. Na⁺ content was observed to reduce by 73% by natural zeolite, while Cl⁻ and SO₄²⁻ reduction remained minimal. The latter result was expected as zeolite is a cationic exchanger rather than anionic. Wibowo et al. [379] also used natural zeolite (clinoptilolite obtained from Sukabumi, Bandung, Indonesia) as a sorbent material, which they investigated for reducing seawater salinity. Zeolite sorption was enhanced through thermal activation at 225°C for 3 h. A salinity reduction of 3.2ppt, with a 9.14% reduction efficiency was obtained in a single batch process. Safarpour et al. [380] reported surface modification of clinoptilolite using a glow discharge method. they embedded the modified clinoptilolite in the PA layer of the TFC-RO membrane thereafter. Clinoptilolite, 0.01 wt. % imparted improved hydrophilicity and thus a 39% improvement in water flux and an 88%

enhancement in the fouling recovery ratio compared to the pristine PA-TFC membrane. Clinoptilolite was also reported to be incorporated in pervaporation desalination membranes [381]. A high rejection of >97.5% for K^+ and Na^+ , and a 99.99% and 98.52% rejection for Mg^{2+} and Ca^{2+} ions was respectively obtained.

Besides natural zeolites, many synthetic zeolites have been under research interest by various research groups. Xue et al. [370] reported mesoporous LTA zeolite, synthesized using organic functionalized fumed silica as Si source for Mg^{2+} and Ca^{2+} ion exchange. The dual-site Langmuir model suggested that two different kinds of ion-exchange sites were present in the LTA; intrinsic micropores and the established intracrystalline mesopores ca. 3 nm structure. The presence of the mesopores caused a decrease in the activation energy of ion exchange and thus accelerated the Mg^{2+} exchange with Na^+ in the structure. The diffusion rate of hydrated Mg^{2+} was seen to increase in the synthesized LTA by 17.5 times, compared to that of conventional microporous LTA. Thus, mesoporous LTA was deemed as an attractive candidate which could be used in desalination for removing Mg^{2+} . Even though Zeolite LTA is deemed as an effective adsorbent for divalent salt ions, its rejection efficiency for Mg^{2+} is usually low due to the low rate of exchange and narrow pores of LTA. Hence this limits its application in desalination. Dong et al. [382] used another zeolite type, zeolite-Y incorporated in the PA layer of TFC-RO membranes. An optimum loading of 0.15 wt. % showed an increase in water flux from 23.3 to 43.7 gal/ft².day while achieving high salt rejections of 98.8% for a salinity of 16,000 ppm NaCl solution. SAPO-34 and ZIF-8 potential in seawater desalination was explored by Duke and coworkers [371]. They produced these membranes through secondary seeded growth method. Zeolite immersion in seawater caused a release in Al ions which in turn caused ion-exchange by monovalent and

divalent salt cations. Between the two, SAPO-34 gave negligible water flux, while ZIF-8 membranes produced a water flux of 600 kg.m².h with a low salt rejection of 6.3%. Membrane performance could be improved through more robust and inter-grown membranes for RO desalination. Garofalo et al. [383] studied MFI zeolites for vacuum membrane distillation. A permeate flux of 13.7 kg/m².h and a salt rejection of 94.6% was achieved for a 75 g/L brine feed solution. In addition, their 30cm long membranes prepared through the secondary growth method answered to many problems associated with the scale up of pure zeolite membranes for desalination. Nevertheless, scale up of such membranes still remains a challenge for NF and RO where they are difficult to be produced at a large scale owing to the inherent brittleness of the ceramic membranes.

Research on numerous carbon-based materials is on a rise as efficient sorbents for desalination. For example, AC is popular carbanions adsorbent, as well as prominent electrode material for Na and Mg salt rejection [384]. Mendez and Gasco [385] studied the rejection of numerous cations, Ca²⁺, Mg²⁺, Na⁺ and K⁺ using carbon-based materials from anaerobic sewage sludge. These carbonaceous materials were mixed with the salts, NaCl, KCl, CaCl₂ and MgCl₂. Ion efficiency removal was in the order of Mg²⁺ > Ca²⁺ > Na⁺ ~ K⁺. In addition, it was found to increase with solution pH. However, the application of AC as an adsorbent has been extensively studied in wastewater treatment rather than in desalination [386].

Apart from their electrochemical and anti-biofouling properties, CNTS have gained considerable attention due to their excellent adsorption capacities and unique morphological and

physicochemical properties. In addition, CNTs have also shown excellent water permeability and selectivity for in membrane separation processes [41]. They are thus reported to be effective nano-adsorbents. Adsorption of ions into CNTs is largely controlled by the morphology, defects and its active sites. The adsorption of metal cations onto CNTs is largely attributed to the electrostatic attraction and chemical interactions between the ions and the CNT functional groups. The sorption mostly occurs on the CNT internal sites, interstitial channels, grooves and its outside surfaces [387]. Bhadra et al. [372] reported CNT immobilized membrane where PVDF dispersion was used to immobilize the functionalized carboxylated CNTs (c-CNTs). The nanotubes served as a sorbent providing additional pathways for ion transport. These c-CNTs were significantly reported to be more polar than the pristine ones, and hence showed improved desalination efficiency in membrane distillation (MD) with a flux of 19.2 kg/m².h and a 99% NaCl salt reduction. The CNTs were encapsulated in the PVDF which prevented the water and the salt ions from reaching the nanotubes. However, the water vapor permeated through the PVDF were successfully received as the permeate. This mechanism is highlighted in Figure 20. Several surface modification and activation methods have been reported to functionalize CNT surfaces for increased adsorption capacity. [388]. Tofiqhy and Mohammadi [364] investigated desalination of saline water using CNT sheets produced through the chemical vapor deposition (CVD) method. Based on Langmuir isotherm, an adsorption capacity of 1.4286 g g⁻¹ was registered for the oxidized CNTs, which indicated a significant increase in adsorption capacity after the oxidation process. They also studied the efficiency of oxidized CNTs for divalent ion rejection, for which higher adsorption capacity was registered for Mg²⁺ and Ca²⁺ ions [389]. Nevertheless, it was reported by Santosh et al. [390] that solution pH largely affects the adsorption ability of oxidized

CNTs for salt removals. A decrease in pH lowered the adsorption rate, while a pH range of 7–10 is optimum for salt and contaminant rejection. Nevertheless, CNTs have largely been reported for the adsorption of organic and inorganic pollutants in wastewater [391]. However, progressive studies over the years have improved CNT adsorption for various cationic salts through numerous CNT modification methods. Yang et al. [373] reported plasma-modified ultra-long CNTs (length of 100–200 μm) on mixed cellulose ester for superior specific adsorption capacity for NaCl salt. NaCl feed solution was varied for different concentrations, 7000, 3500 and 1700 ppm. The synthesized membranes achieved a 100% recovery of its initial salt rejection capability after regeneration through simple rinsing by tap water. It was found that the total amount of salt removed was relatively independent of the salt concentration and that the ultrahigh adsorption capacity was attributed to the plasma mediated conversion of the outer layers of the ultra-long CNTs to an amorphous network. Figure 21a shows the SEM image where only a few salt crystals were observed on the pristine CNTs surface as compared to the plasma modified CNTs (Figure 21b), where a significantly higher density of NaCl crystals were found to be adsorbed. Figure 21c shows the TEM image of the modified CNTs where the NaCl crystal lattice was clearly identified being embedded in the CNTs. Thus, the mechanism of salt rejection was proven to be adsorption instead of salt rejection as in RO and NF membrane systems. The modified CNTs were immersed in static 0.02M NaCl water with different masses (in mg). Figure 21d shows the specific adsorption results, which gave 400% adsorption capacity by weight. The adsorption capacity of 160 mg plasma modified CNT membrane in different salt concentration was also evaluated. The Langmuir adsorption isotherm fitted well for the adsorbed salt as a function of the final solution concentration, as shown in Figure 21e.

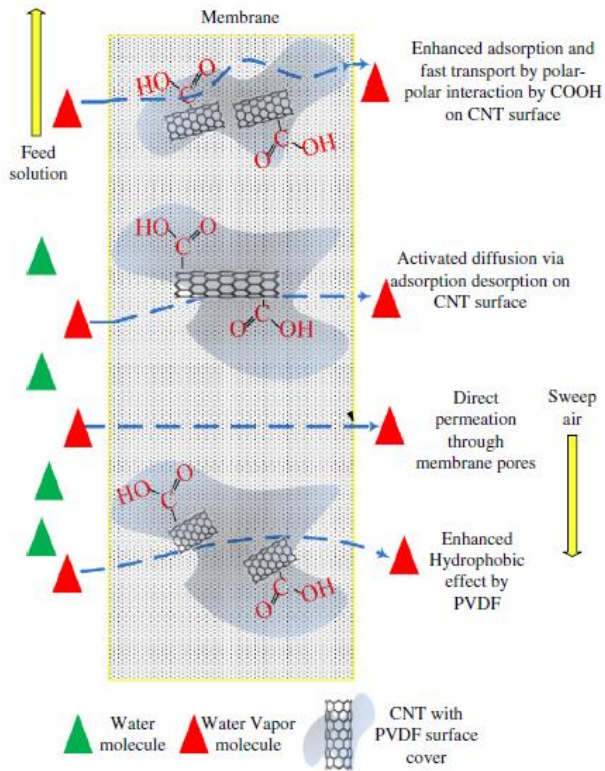


Figure 20: Mechanism action of c-CNTs in MD [372]

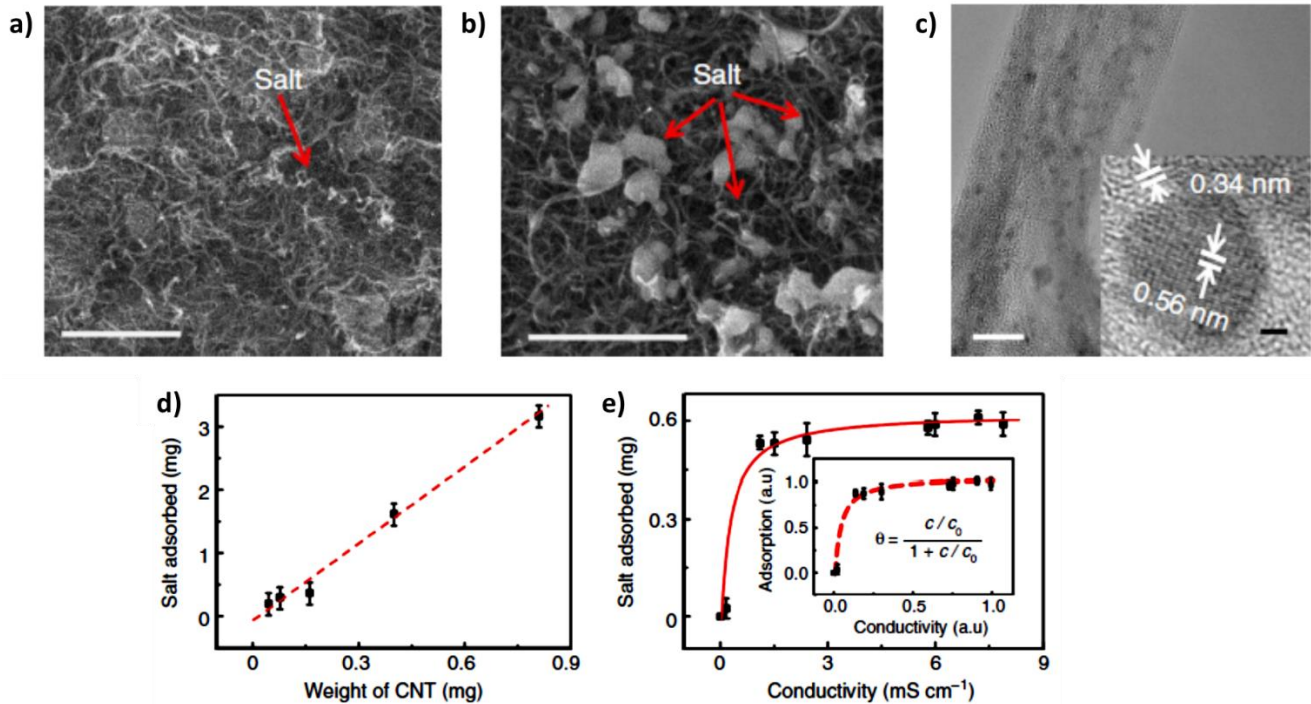


Figure 21: (a) SEM image of pristine CNTs after the adsorption reached saturation; scale bar, 1 μm . (d) SEM image of plasma modified CNTs after the adsorption reached saturation; scale bar, 1 μm . (c) TEM image confirming the NaCl nanocrystals in the modified CNTs; scale bar, 1 nm (d) Salt adsorbed by plasma-modified CNT membranes with different CNT masses in 0.02M NaCl solution and (e) 160 mg of CNT membranes in salt water with different conductivities; the inset in shows the Langmuir isotherm equation fitting plot, where y is the mass of salt adsorbed, c is the normalized conductivity of solution at equilibrium and c_0 is the Langmuir adsorption constant.

Graphene is an ideal absorbent owing to its non-corrosive property, high surface area (theoretically about $2630\text{m}^2\cdot\text{g}^{-1}$), and the presence of oxygen-containing functional groups [365]. The latter being an important aspect, whereby the metal ions tend to adsorb onto these functional groups. Several variables affect the adsorption capacity of graphene including its oxygen-containing groups, ionic strength and pH. Usually, lowering the pH decreases graphene's adsorption capacity. With a high solution pH, the negatively charged graphene due to deprotonation of carboxyl and hydroxyl groups, attracts the positively charged metal ions, leading to enhanced adsorption capability. Figure 22 depicts different methods in which

graphene may be utilized as adsorbents for metal ion removal from aqueous solutions [365]. Computational modelling results have suggested that nanoporous graphene membranes can achieve extremely high water permeability reaching $4000 \text{ L}\cdot\text{m}^2\cdot\text{h}^{-1}\cdot\text{bar}^{-1}$, with about 3 times the salt rejection attained by the present commercial RO membranes [392]. Mishra and Ramaprabhu [374] exfoliated the GO for synthesizing graphene sheets. These graphene sheets were functionalized by the hydrophilic functional groups of $-\text{COOH}$, $-\text{C}=\text{O}$, and $-\text{OH}$ its surface. These were in turn studied for simultaneous separation of both Na and Arsenic rejections. The maximum adsorption capacities for arsenate, arsenite and sodium was found to be at 142, 139 and 122 mg g^{-1} . Besides cationic species, graphene has also been reported for the removal of anionic species such as Cl^- , PO_4^{4-} and F^- from aqueous solutions. The mechanism of anion adsorption is related to the anion- π interactions [365]. Graphene also makes an ideal material for CDI electrodes where electrosorption of ions plays an important role in desalination. Due to the tendency of graphene to agglomerate, an initial attempt to use rGO as a CDI electrode resulted in a low Na^+ electrosorption of only about 1.85 mg g^{-1} [393]. Wang et al. [375] synthesized functionalized rGO-resol nanocomposites (rGO-RF), which they used as an electrode material for CDI. rGO-RF showed better electrosorptive rejection performance of NaCl, 3.2 mg/g when compared to rGO (1.8 mg/g) and AC (1.5 mg/g). This difference was attributed to the higher surface area of rGO-RF, $406.4 \text{ m}^2 \cdot \text{g}^{-1}$, resulting in a higher NaCl uptake. El-Deen et al. [376] developed a novel one-pot synthesis method for MnO_2 -nanorods@graphene. First, graphite was converted into graphene through vigorous oxidation in the presence of manganese sulfate, after which reduction under microwave irradiation led to the formation of MnO_2 -nanorods. These CDI electrodes revealed distinct electrosorptive capacity (5.01 mg/g) and excellent salt rejection

efficiency ($\sim 93\%$). Faisal et al. [394] developed 3-D lamellar structured nitrogen-doped graphene/CNT via a thermal annealing process. The nitrogen doping into the graphitic network rendered the CDI electrode with a high surface area, enhanced the conductivity, greater pore volume, and an improved interface between the electrolyte and electrodes this in turn helped in accelerated salt adsorption, giving superior capacitive deionization of 440 F. g^{-1} at a current density of 1 A. g^{-1}). Numerous other research studies report improved CDI electro materials for enhanced salt adsorption [395, 396].

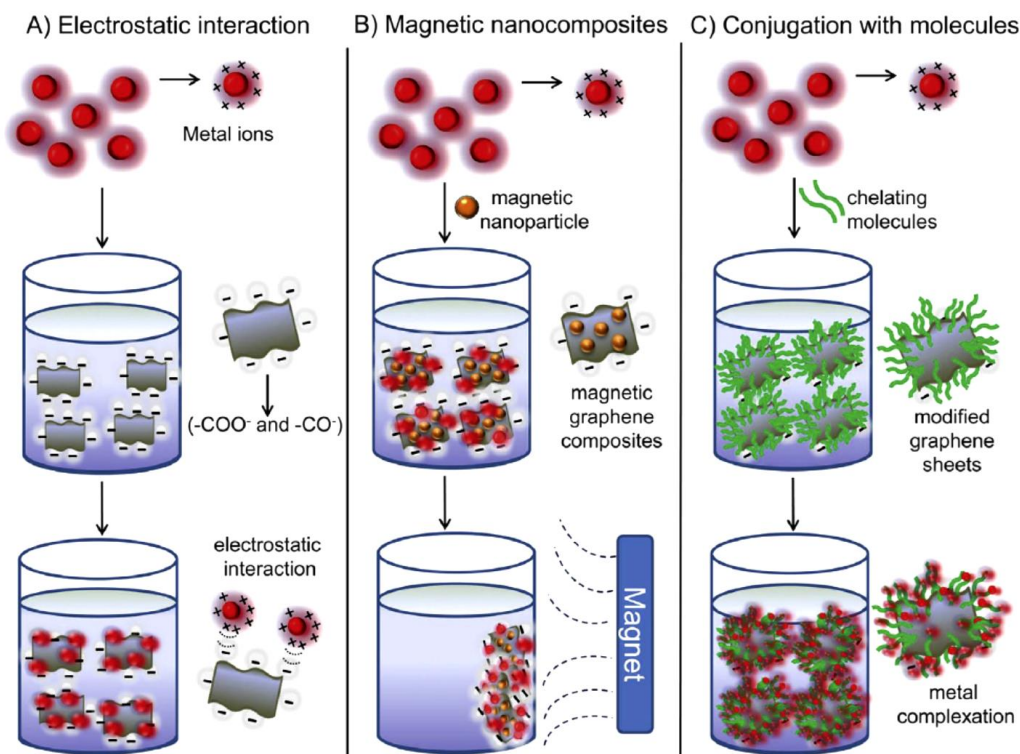


Figure 22: Main strategies to apply graphene-based materials as adsorbents for metal ion removal (A) electrostatic interaction; using non-modified graphene, GO or rGO, (B) magnetic attraction; Graphene sheets can be functionalized with magnetic nanoparticles to improve adsorption capacity and (C) synergetic effect between the chelating properties of the organic molecules and adsorption capacity of the graphene sheets. Reproduced from [365] with permission from The Royal Society of Chemistry.

There are also studies reported on the use of magnetic adsorbents. Mishra & Ramaprabhu [377] developed a new type of super capacitor based on flexible carbon fabric supported magnetite MWCNT nanocomposite for desalination of seawater. 1 V DC power supply was enough to remove 70% sodium, 67% magnesium, and 73% calcium in 20 repeat cycles. Lehmann et al. [366] reported the recovery of high-purity magnesium solutions from 1st stage SWRO brines by Mg(OH)₂ adsorption on 10 g Fe/L Fe₃O₄ magnetic seed particles, which were thereafter separated by magnet-assisted gravity forces. High purity (>97% purity) Mg-solutions were obtained leading to reduced cost of Mg production compared to commercial products. Other desalination adsorbents include low-cost adsorbents such as those derived from agricultural and biological wastes, synthetic and bio-polymers, industrial by-products, and modified natural materials [50].

Adsorbents are also used in thermal desalination processes, whereby the technology uses a highly porous adsorbent to power the sorption cycle. The components usually involve an evaporator, adsorbent beds and a condenser. Silica gel, owing to its high affinity towards water vapor is predominantly used for this purpose. The silica gel adsorbs the vapor generated in the evaporator and the silica gel in another bed could be regenerated by a heat source. This helps to regenerate the water vapor which otherwise would be purged into the atmosphere. This system can essentially be integrated with multiple-effect distillation where operational temperature ranges may be extended for improved system performance ratio [397]. Recently, Askalany et al. [398] reported composite of 1-ethyl-3-methylimidazolium methane sulfonate ionic liquid in Syloid AL-1FP silica. This material showed extraordinary water vapor sorption. At ionic liquid loadings of >1.8 wt. %, the composite registered a type III isotherm, but with an

increased dependence between temperature and the adsorbed water. The latter made the material applicable for thermal desalination, where 60 wt. % 1-ethyl-3-methylimidazolium methane sulfonate in 40 wt. % silica provided an optimum combination and gave 1.7 times purer water than the currently used nanoporous sorbents. However, natural silicate based adsorbents usually offer poor performance, which might be enhanced by amine grafting [399].

8. New Emerging Trends

In the quest for improved desalination performances, different fabrication approaches, new concepts, systems and novel composite functional materials are continuously being developed and reported. Many at times, numerous processes are combined for efficient desalination performances. For example, the process of adsorption membrane filtration (AMF), combining an adsorption process with membrane separation technology is considered as a promising alternative for water process applications. This integrated process has been reported for boron rejection, but may be extended for salt rejection [400] for cost effective desalination process requiring lower operating pressures in the membrane process unit. Besides system integration and upgrades, various functional materials are continually being optimized, while new ones are being developed.

Following the seriousness of fouling effects, improvements in antibacterial materials are gaining much research interest. Jiang et al. [401] reported in-situ Ag nanoparticles photocatalytic synthesis by crumpled GO-TiO₂ membranes for antimicrobial membranes. Their effort was

directed towards regenerating the antimicrobial activity over extended operation times. GO-TiO₂ membranes were first prepared through vacuum filtration onto a PES support. These membranes were then placed in 15 mg/L AgNO₃ solutions under UV light irradiation for a relatively fast and efficient in-situ Ag nanoparticle (particle size of 40 to 120 nm) synthesis. The percentage of attached live cells of *B. subtilis* and *E. coli* was reported to decrease from 100% to ca. 3 log for both bacteria. However, a decrease in antimicrobial functionality was observed due to Ag⁺ dissolution over time. Post-functionalization through crosslinking, grafting or coating usually reduces the antibacterial effectiveness. Therefore, recently, mussel-inspired polydopamine (PDA) coating has received great research interest due to its strong adhesive properties to various substrates. With the help of various functional groups such as amine, catechol, and imine, the PDA coatings immobilize the multifunctional nanomaterials for enhanced antibacterial properties [402]. In addition, knowing PDA's capability of reducing Ag⁺ to Ag nanoparticles, various studies focus on the in-situ synthesis of Ag nanoparticle coatings onto PDA-modified membranes [403, 404]. Huang et al. [403] in-situ immobilized Ag nanoparticles onto a PSf UF membrane through Ag⁺ reduction using Ag(NH₃)₂OH via PDA deposition. The PDA layer provided good adhesion on the UF membrane, facilitating Ag⁺ reduction on the surface, and a uniform Ag nanoparticle distribution without any pore blockage. Nanoparticle morphology was regulated by varying the Ag(NH₃)₂⁺ ion concentration, directly impacting the membrane hydrophilicity and permeate flux. When compared with the bare PSf membranes, the Ag-PDA-PSf UF membranes showed a higher water flux, and a lower flux decline over time for BSA filtration. An increase of 35% in the pure water flux was registered, 336 L m⁻² h⁻¹ for the Ag-PDA-PSf UF membranes.

Further, surface modification with PDA increased the membrane's hydrophilicity, and led to only a 17% flux decline after biofouling, compared to 45% with the pristine membranes.

Another antibacterial material which is gaining interest are hydrogels. An electro-responsive supramolecular GO hydrogel was reported using redox-active ruthenium (Ru) complexes as non-covalent cross-linkers. When an electric field was applied, like any hydrogel, these were able to switch their physical properties by changes in the Ru ion oxidation states. The dead bacteria were unable to attach to the hydrogels, making their killing and removal easier, thus facilitating hydrogel regeneration. Therefore, GO-hydrogels showed strong antibacterial activity and thus were deemed as an interesting potential for desalination where the adsorbed bacteria in the GO hydrogel based membranes could be inactivated by a high voltage electric pulse [405]. Biocatalytic antibacterial membranes has attracted increasing attention due to the unique benefit of using various enzymes in the polymer matrix for biofilm inhibition [406]. Enzyme immobilization onto a membrane has emerged as an effective strategy to improve membrane's activity and reusability [407]. Zhao et al. [408] immobilized lysozyme onto halloysite nanotubes (HNTs) via covalent bonding. These biocatalytic HNTs were then mixed with the with PES matrix for membrane preparation. Lysozyme was also reported to be immobilized onto GO, which were then mixed with PES to fabricate antibacterial membranes via phase inversion method [409]. The incorporation of GO significantly enhanced the mechanical strength and the hydrophilicity giving increased water flux, together with improved antibacterial activity against *E. coli*.

Microbial desalination cells (MDC), a newly developed technology is gaining importance whereby desalination is usually coupled with microbial fuel cell process and renewable energy production [410]. Various cell configurations have been reported, but in general, an MDC unit consists of anode and cathode chambers, with a desalination chamber in the middle created by inserting an anion-exchange membrane (AEM) and a cation-exchange membrane (CEM) on either side. The anode chamber acts to degrade the organic contaminants for wastewater treatment and energy generation, the middle chamber for salt removal from seawater, while the cathode chamber completes the electrical loop. The electrode and the exchange membrane material plays a yet important role, and thus needs careful consideration before selection. For example, in the air cathode MDC configuration, it was possible to reduce water salinity by 63% using carbon cloth electrode with platinum catalyst [411]. Cobalt tetra-methoxyphenylporphyrin and activated carbon can also be reported for this purpose [412]. The use of biocathode catalysts is also becoming increasingly popular. Wen et al. [413] used biocathode MDC of carbon felt and bacterial catalysts. Salt removal by 92% was achieved with a total desalination rate of 2.83 mg/h. Improvements in salt removal were reported by using a carbon supported silver-tin dioxide composite cathode electrocatalyst. The electrochemical studies through CV and LP revealed much superior reduction kinetics of the electrocatalyst compared to no catalyst. Increased desalination efficiency of $72.6 \pm 3.0\%$ was achieved for a NaCl concentration of 20 g/L. Moruno and coworkers [414] reported sulfonated sodium poly(ether ketone) cation exchange membranes and quaternary ammonium chloride poly(2,6-dimethyl 1,4-phenylene oxide) anion exchange membranes. (AEM). A high desalination rate with a $78.6 \pm 2.0\%$ of salinity reduction was achieved for Pacific Ocean seawater, which was higher than the commercial membranes. Such studies on optimized electrocatalysts

and ion exchange membrane materials for desalination through MDC is a subject of continuous research [415].

New research trends in magnetic nanoparticles for desalination are also on a rise. Recently, efforts have been focused on developing light-responsive magnetic nanoparticles. Draw solutes for FO may be generated by external stimuli, such as sunlight which provides a renewable and low-cost energy source. Light-responsive heterodimers composed of Fe_3O_4 magnetic nanoparticles, with plasmonic Ag nanoparticle coated PNIPAM polymers were reported [416]. Fe_3O_4 seeds were used to facilitate Ag nanoparticle growth the growth for heterodimer formation. Subsequently, PNIPAM was added to functionalize the Ag nanoparticles and also to provide thermo-sensitivity. Owing to the plasmonic effect, Upon sunlight irradiation, the Ag nanoparticles could absorb energy [417], and the inter-band absorption mechanism caused most of the absorbed light to be transformed into heat. This led to localized heating around the heterodimers, causing an increase in the LCST of PNIPAM, which made the polymer chains collapse and hence aggregate. Thus, thermoresponsive Fe_3O_4 nanoparticles were transformed into photoresponsive Ag- Fe_3O_4 heterodimers. On removal of the solar source, below the LCST of PNIPAM, the heterodimers re-dispersed in the aqueous solution. Nevertheless, the aggregation facilitated magnetic separation, and hence reduced the energy consumption. Nemati et al. [13] developed magnetic nickel ferrite (NiFe_2O_4) nanoparticles modified by a novel hydrogel based on 2-acrylamido-2-methyl propane sulfonic acid (HAMPS) for cation exchange membranes. Membrane permselectivity for Na^+ , membrane potential, and transport numbers showed improved trends. Membrane flux was increased from 13.07 to 27.7%.

Conventional solar stills usually suffer from low desalination productivity. Hence, increased attention is being put in utilizing functional nanoparticle modified solar stills. Nanoparticles may enhance thermal characteristics of the feed water by increasing the surface area for heat transfer. Gupta et al. [418] used 0.12 wt. %, CuO nanoparticles for this purpose. The modified still was compared with the conventional one, which showed that the former produced 3445 ml/m²-day, compared to the conventional one at 2814 ml/m²-day for a water depth of 5cm. the overall thermal efficiency was also improved from 24.8% to 37.4 % for the modified one. In addition, the estimated water cost for the modified still was calculated to be Rs. 0.40/L, compared to Rs 0.51/L for the conventional. Thus, higher total fixed cost for modified still with nanoparticles was compensated by its high productivity. Chen et al. [49] reported enhanced solar stills by using magnetic CNTs modified from Fe₃O₄. The magnetic particles facilitated with easier recoveries, along with improved heat utilization saline water evaporation. The evaporation efficiency was seen to increase with an increase in nanofluid concentration. With only a small 0.04 wt. % of Fe₃O₄/CNT, almost 100% solar energy absorption was achieved. However, highly saline waters >1000ppm might not be suitable due to adverse effects on suspension stability of these nanofluids. Thus, these novel, recoverable magnetic nanofluids require extensive research output for high salinity feed feasibility.

Commercial desalination membranes are usually made from dense synthetic polymeric films. However, novel biomimetic materials such as aquaporin (AQP) has gained increased attention for desalination membranes, where these pore-forming proteins mimic the ability of lipid bilayers

in biological cells. AQP may form water channels that can selectively transport water molecules, concurrently excluding the salt cation species. This property has made AQP an exciting alternative for low energy seawater desalination membranes [41]. Kumar et al. [419] suggested the idea of incorporating AQP into desalination membranes. They developed amphiphilic triblock-polymers (ABP) containing the bacterial water-channel protein AQP. They showed that such membranes had great potential in desalination, and can achieve a two-fold increase in water permeability compared to conventional RO membranes. Zhong et al. [420] fabricated AQP-ABM upon CA substrate. The NF membrane with AQP: ABA ratio of 1:50 gave a water permeability of $34.19 \pm 6.90 \text{ L/m}^2 \text{ h bar}$ and a NaCl rejection of $32.86 \pm 9.12\%$. This high water flux indicated a three-fold increase compared to other state-of-the art NF membranes[421]. Numerous literature reviews detail the advancements of AQP-based membranes [422, 423]. Nevertheless, AQP represents an ideal material for ultra-pure water production. However, numerous limitations such as identification of appropriate support materials, range of operating conditions, membrane fouling resistance and cost considerations are yet to be extensively researched before commercializing these. At present Various studies are undergoing to mimic such biological channel AQP systems. For example, Li et al. [424] introduced hydrophilic groups in CNT interiors rather than its exteriors to mimic the AQP channels. It was shown that 100% desalination could be achieved with such a material, with a reasonable flux of about 13 times that of the present commercial membrane. The charged functional groups such as $-\text{NH}_3^+$ or $-\text{COO}^-$ when added in CNT interior, could block same charged ions outside consequently attracting oppositely charged ions into the pore.

Self-assembled materials in nanostructured polymeric membranes is a topic of considerable interest for more than a decade. High selectivity membranes owing to narrow pore size distribution are possible resulting from the equilibrium self-assembly technique [5]. Usually, reactive small molecules, with molar mass of either <1 kDa self-assemble into lyotropic or thermotropic liquid crystalline mesophases or molecules with a molar mass > 10 kDa self-assemble into mesophases, structurally similar to small molecule systems [425, 426]. Liquid crystalline mesophases are often polymerized or cross-linked before their subsequent membrane fabrication for improved robustness. Efforts are largely focused on molecular design for the development of scalable directed self-assembly methods for vertically oriented cylindrical pores in thin films. Orientation control and scalability might be achieved using magnetic fields in both small and block copolymer systems [427]. Peinemann et al. [428] for the first time combined self-assembly with non-solvent-induced phase separation (NIPS) for a scalable route to produce thin film membranes incorporated with vertically oriented pores. However, the resulting pore size distribution was broader than that produced in equilibrium self-assembly processes. However, improved selectivity and flux recoveries were achieved when compared to the conventional UF membranes [429]. Thus, this method holds great potential for improved desalination membranes made from self-assembled nanostructured polymeric materials.

9. Challenges associated with Functional Materials in Desalination

Undoubtedly, functional materials play an important role in various desalination technologies, without which major desalination processes would either register low performance or high water production costs. However, such materials come with their own challenges and limitations, either at their synthesis stage, their difficulty to characterize or to integrate in with desalination technologies. Nevertheless, recent advancements and research studies are continually sought to overcome these limitations. This section highlights the challenges associated with various functional materials discussed in this review, together with techniques and methods (if any) to overcome them.

The most common type of photocatalytic membranes in desalination are those comprising of MMMs with the photocatalytic filler either embedded in the polymer matrix or the material coated on the active side of the membrane. In both cases, during operation, the stability of the polymer under continuous UV irradiation is a question of great concern. Rahimpour et al. [89] reported no apparent damage in PES membranes after 4h filtration experiments under UV light illumination due to similar feed rejections with and without light irradiation. However, other studies such as those by Song et al. [78] reported a structural damage in TiO_2 -PVDF-PEG membrane after 12h irradiation. Consequently, the removal rate of natural organic matter was seen to decrease, while the flux increased with time. Interestingly, their membrane structure remained intact until 8h of irradiation, thus clearly signifying the dependence on the duration of light irradiation on membrane performance. This also hints the importance of carrying out tests for longer duration to study the effects of UV irradiation on the structure and long-term stability of polymeric membranes.

Besides membrane stability, another challenge with photocatalytic materials such as nano-TiO₂ are the health and environmental risks associated with it. Although bulk TiO₂ is inert and has been reported to have negative impacts, the same is not true for nanoscale TiO₂. When immobilized onto a substrate, it may not adversely affect human health, however, nano-TiO₂ could potentially have health impacts for researchers exposed to its dust. Nevertheless, human health implications for using nano-TiO₂ are still uncertain, requiring extensive investigations into its impact in order to regulate the use of nano-TiO₂ for photocatalytic water purification. Other technical challenges include photocatalytic system optimizations and modelling predicting long-term stability of such systems.

The choice of fabrication process also affects the functionality of various materials, such as the antibacterial efficiency of desalination membranes. Blending, for example, enhances the homogeneous dispersion of inorganic fillers in the polymer matrix increasing the interfacial affinity between the two [430], however, an inherent disadvantage of this method is that most of the filler particles might not be in direct contact with the bacteria, hence reducing the biofouling resistance [431]. A significant loss of antibacterial and antiviral activity was reported for Ag⁺-PSf UF membranes fabricated from the phase inversion process [252]. XPS analysis indicated concentrations of 0.034 mg/L of Ag⁺ in the permeate that was filtered at a rate of 0.004 mL/cm²/s. Thus, a successful fabrication technique is essential to allow for sufficient release of silver ions for antibacterial activity, while at the same time preventing a rapid depletion of silver. Improved nano-Ag incorporation may be achieved by concentrating the particles on the selective membrane layer or anchoring it for its slow release. Another approach might be to encapsulate the Ag in another substance for a constant, slow release rate [432]. Nevertheless,

regeneration of Ag might be brought about by the reduction and deposition of silver salts, such as AgNO_3 [433]. Water chemistry is yet another parameter which may affect membrane performance. Silver toxicity to *E. coli* was reported to be altered by common water constituents such as chloride, phosphate and sulfides which were shown to affect silver solubility. In some cases, where cysteine was present, bacterial cell damaged was seen to be reversed [252].

When using functional nanoparticles, such as CNTs, nano-metal oxides and even graphene, the foremost challenge in utilizing these is their agglomeration issue. Due to their high surface area and charge density, nanoparticles tend to agglomerate, hence compromising on their accessibility to active sites [434]. Dey and Izake [199] reported a total water flux decrease of 21% due to magnetic nanoparticle agglomeration in PSA-coated Fe_3O_4 FO polymer draw agents. Numerous other studies have documented the decrease in desalination performance due to magnetic nanoparticle agglomeration during its regeneration process. Figure 23 shows the gradual decline in water flux (<10%) after each FO cycle performed with three different feed solutions of DI water, saline water and simulated seawater. This was attributed to the loss of Fe_3O_4 nanoparticles grafted with PSSS-PNIPAM during regeneration [200]. An integrated UF-FO system was proposed by Ling et al. [208]. The role of the UF unit was to regenerate the magnetic draw solute. When compared with a magnetic separator, the separator showed nanoparticle agglomeration unlike the UF. Though ultrasonication was initially proposed for this problem, but the magnetic properties of the nanoparticles may be compromised, leading to deterioration and jeopardizing regeneration efficiency in magnetic fields. The novel FO–UF system gave enhanced recovery efficiency of nanoparticle draw solution, marking its potential for seawater and brackish

water desalination. Another possible solution is to introduce hydrophobic sites on the particles, which can help prevent agglomeration during regeneration in the presence of a magnetic field. A weaker magnetic field might be applied in this case, alleviating the agglomeration issue. Nevertheless, synthesis of such nanoparticles may be complex, and results showed that only about 50% recovery was achieved using such hydrophobic magnetic particles, while the rest had to be recovered through NF [193]. Although smaller nanoparticles are usually preferred in FO draw solutes, it was reported that nanoparticles below 11nm were difficult to be separated and recovered even under a strong magnetic field. In addition, a uniform particle distribution is desirable for efficient regeneration via a membrane process, something which is again quite a challenge [193]. Chou et al. [119] developed Ag-loaded CA hollow fiber membranes through an in-situ synthesis method. Poly (vinyl pyrrolidone) (PVP) was used as a reductant for in-situ Ag nanoparticle preparation. An even distribution of the particles, as well as effective prevention of agglomeration was obtained attributed to the nitrogen atom in the PVP [435].

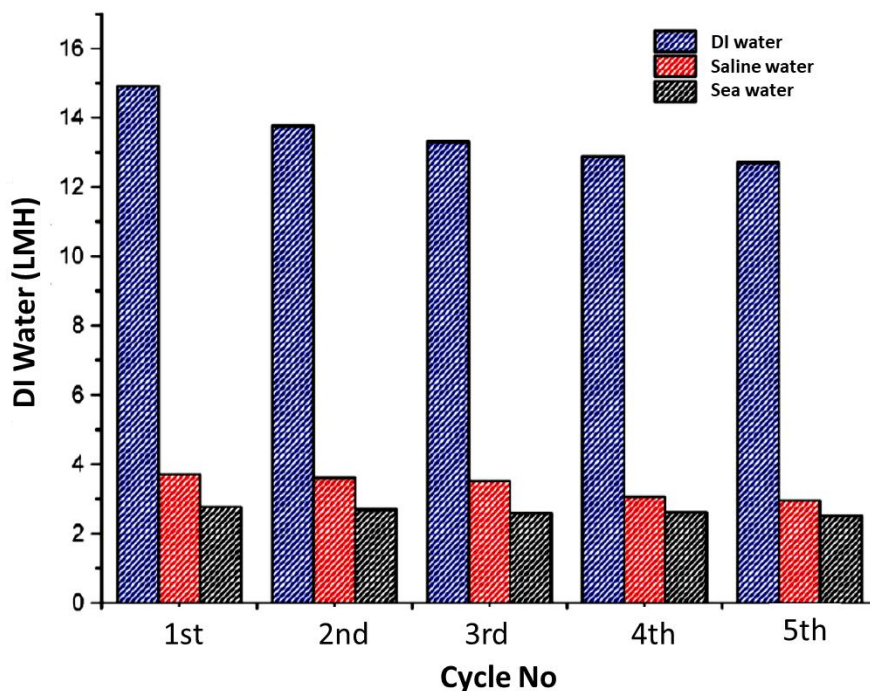


Figure 23: Water fluxes for the various feed solutions after each cycle after regeneration using Fe_3O_4 magnetic nanoparticles grafted with PSSS-PNIPAM draw solute. Reprinted with permission from Zhao et al. [200], Thermoresponsive magnetic nanoparticles for seawater desalination, ACS Applied Materials and Interfaces, Copyright (2013) American Chemical Society.

Graphene, in most solvents, easily aggregates. The aggregation of graphene layers leads to a contaminant reduction by impaired surface accessibility and interaction. With its potential to be developed further, there is a strong focus to overcome aggregation of graphene and GO during the synthesis of graphene-based membranes [436, 437]. Thus, to overcome this technological bottleneck, graphene-based membranes have been modified with various functional groups such as carboxyl, hydroxyl and ketones. The introduction of such hydrophilic groups has enhanced graphene dispersion and decreased agglomeration [51]. Apart from agglomeration, graphene, GO and rGO synthesis is still a challenging process. Specialized synthesis techniques are often required, often questioning their reproducibility. Thus, new, simple ways of fabricating such materials are required for improved structure, size, reproducibility and properties. In addition,

for utilizing its high desalination performance by its various functional features, graphene-based membranes need to be produced on a large, commercial scale, something which is still under research till date. Further, graphene toxicity is another limitation which needs to be addressed before the membrane material can be commercialized. Its toxicity on human health and the ecosystem are still being extensively investigated, with only slight successes in these areas.

Similar to graphene, CNTs also suffer from analogous limitations of agglomeration and poor dispersion in solvents. Kim et al. [305] reported a decrease in antibiofouling property of PA-CNT-PVA membranes with increased CNT loadings, primarily due to aggregated CNT clusters. The agglomeration of CNTs also affects its adsorption properties, thus lowering its efficiency for contaminant adsorption [438], complicating the membrane synthesis process. CNT agglomeration and its close-fitting bundles is usually attributed to CNTs low dispersity in most media, primarily due to the strong π - π interactions and van der Waals forces among CNTs [439]. This tendency increases from MWCNT to SWCNT as one decreases the number of graphitic layers of CNTs [440]. This limitation might again be overcome by functionalization CNTs for improved dispersion properties [441]. Another challenge in fabricating CNT-based functional desalination membranes is their reproducibility, and most of the time its specialized synthesis techniques involving adequate dispersion, infusions and the usage of various solvents and chemicals [442]. Nevertheless, these challenges are continually being sought to take advantage of CNTs unique properties such as its excellent hydrophilicity, mechanical strength and superior biofouling resistance.

Similar to graphene and CNTs, zeolite nanoparticles have proved their functionality in various desalination technologies including RO, pervaporization, electrodialysis and MD. They provide high salt rejections with incredibly improved water flux owing to their shape selectivity and nanoporous interconnected channels. However, they too suffer from limitations similar to as posed by graphene and CNTs which include agglomeration, leaching and synthesis reproducibility. Zeolite-embedded TFC membranes usually take longer IP times than the conventional TFC membranes [382]. In addition, their agglomeration usually leads to interstitial defects. Kim et al. [443] used a polymer network as a temporary barrier to prevent zeolite aggregation during calcination after dispersion. Agglomeration in electrodialysis during high zeolite loadings usually leads to decrement in electrical conductivity, selectivity and ionic permeability [145]. In a NF and RO, zeolite-based membranes are often reported for decreased membrane flux and salt rejections with increased salinity levels [381, 383]. However, continuous efforts are being made to overcome these limitations, whereby zeolite agglomeration problem is given consideration at a large scale for optimized membrane performances. Nevertheless, because zeolites are majorly used as catalysts for various applications [444], it is worth mentioning that numerous efforts have been made in the catalytic field to prevent zeolite nanoparticle agglomeration [434], from which the desalination industry can benefit and inculcate those ideas and methodologies during zeolite-based membrane development.

Though ABM-AQP represent new, advanced class of functional materials, one major limitation for ABM is its stability for industrial (and large scale) desalination, and hence its scale-up. Most of the reported research studies on such materials is limited to small membrane areas due to

highly specialized synthesis techniques. Following this limitation, a new approach for fabricating ABM was developed by Zhao et al. [445], where they soaked PSf support into MPD containing AQP-based proteoliposomes. Regular procedure was followed thereafter, whereby TMC was introduced for IP. AQP containing vesicles provided preferential water paths through the PA rejection layer, enhancing the water permeability significantly. These membranes provided good mechanical stability for long run periods up to several months, together with stable rejections and fluxes. In addition, a 40% increase in water permeability was reported compared to the commercially available brackish water RO membrane (BW30). Further, compared to the commercial seawater RO membrane, SW30HR, permeate flux in an order of magnitude higher was achieved, clearly indicating the potential of AQP-based membranes in desalination for industrial applications. Thus, commercializing such membranes would require more research input towards finding novel ways of fabricating AQP membranes on a large scale with synthesis reproducibility.

Furthermore, environmental risk and public health impact due to nanomaterial leaching in permeate water is a major concern. Many studies highlight the potential of Ag⁺ leaching from MMMs. Ag-ion leaching to the medium was reported to be assessed by atomic absorption spectroscopy (AAS), which showed about 56% leaching from the zeolite support [340]. In addition to secondary pollution, gradual leaching adversely affects the antibacterial activity of the membrane. This problem is extended to various other functional materials including CNTs, graphene, nano-metal oxides and zeolites. These aspects need critical analysis and should be regularly assessed by environmental agencies for regulatory purposes. A safety guideline can be advantageous which can develop new policies for functional nanomaterial usage in desalination.

Until and unless their health impacts are fully understood and documented, the application of several novel functional nanomaterials in largescale water desalination is hindered in the near future. Following this urge, it is highly likely that this challenge will inspire several researchers towards the health and safety study on these materials in water desalination technologies.

future.

Table 6: Pros and Cons, and suggested research directions of various types of functional materials

Functional Material	Advantages	Limitations	Suggested Improvements: future research prospects
Photocatalysts	Efficient way of organic contaminant degradation and disinfection of seawater and brackish waters; when integrated with desalination membranes, it can help reduce biofouling for improved salt rejections and permeate fluxes.	<ul style="list-style-type: none"> -Popular photocatalysts such as TiO₂ can only be used in the UV range, not utilizing the full solar spectrum. -Need for a light source near the photocatalyst puts limitations on its placement and design of experimental/pilot setup. 	Extensive research is needed in the area of dual or multiple semiconductor photocatalysts for bandgap engineering which can make use of a broader range of the solar spectrum.
Electrocatalysts	<ul style="list-style-type: none"> -Self-cleaning membranes for fouling control application in desalination. -Improved membrane lifetime and less decline in water flux over time. -Electrochemical desalination batteries providing a cost-effective seawater desalination option through utilization of electrochemical redox reactions. 	<ul style="list-style-type: none"> -Environmental and health concerns of using CNTs based membranes for self-cleaning. -Leaching issues. 	Immediate need for comprehensive research regarding environmental, economic and performance feasibility for a long term usage.
Photothermal materials	<ul style="list-style-type: none"> -Sustainable sources leading to cheaper options utilizing solar energy. -Permeate waters with low salinity levels owing to evaporation-condensation of water vapor leading to improved health standards. -Possibilities of combining the functionalities of photothermal materials with other such as photocatalysts for bifunctional applications. 	<ul style="list-style-type: none"> - Conversion efficiencies are often limited by optical and thermal losses limiting water production levels. - lack of experimental and computational studies for deep understanding of photothermal mechanism. 	<ul style="list-style-type: none"> - Advanced nanomaterials should be tailored for unique electronic and optical properties to display localized surface plasmonic effects. - Synthesis of low-cost, sustainable, well-controlled nanostructures.

Magnetic materials	-Facilitates easier recovery, thus increases prospects for regeneration and reuse. -Improves FO performance with respect to flux increase.	Agglomeration problem in magnetic nanoparticles leading to decline in desalination efficiency over a period of time.	Tailored magnetic separators with tunable magnetic strengths for improved nanoparticle recovery and reuse.
Antimicrobial materials	-Inhibits and controls biofouling -When supported on certain materials such as zeolites, improved membrane performance may be achieved owing to dual functionality.	-leaching -antibacterial materials might be unstable and require careful post treatment or grafting for improved functionality. -Reproducibility	The use of polyelectrolytes to avoid leaching problems and development of advanced support materials for better immobilization for controlled leaching.
Sorbents	-lower operating and maintenance cost compared to other salt rejection techniques. - Flexibility and simplicity in process design and operation.	-Recovery and regeneration of nano-sorbents still remains a challenge. -Agglomeration problems	Development of integrated systems combining adsorbents and desalination membranes for

10. Conclusion and Future Recommendations

In order to overcome the fresh water scarcity, functional materials have led to a novel and innovative solution in seawater desalination for improved desalination performances. Most of the photocatalytic, antimicrobial, sorbent, electrocatalytic, photothermal and magnetic materials comprise of new generation nanomaterials such as CNTs, graphene, zeolites, novel metal oxide nanoparticles and AQP. The incorporation of such materials for desalination technology is a challenge in itself owing to material reproducibility, specialized synthesis techniques, scale up and environmental and health concerns. This review has detailed several roles of various functional materials in thermal and membrane-based desalination processes,

with their pros and cons. Existing studies, their challenges, novel methods and potential improvements were highlighted. Table 6 provides an overview of the several advantages and disadvantages associated with each type of functional material. Suggested improvements and future research directions are also provided.

Research studies on photocatalytic materials such as free standing TiO_2 and supported TiO_2 membranes were reviewed. Studies with and without photocatalyst materials for water desalination were highlighted showing a striking difference in total TDS, total alkalinity, conductivity free CO_2 and total hardness with and without MnO_2 , PbO_2 and CuO photocatalysts. In addition, recent developments on novel materials utilizing a broad solar spectrum ($\approx 50\%$) were discussed. Further, electrocatalyst role in fouling prevention and membrane self-cleaning applications during desalination were reviewed. Conductive membranes used under an electrochemical setup are usually attractive for such purposes. Electrochemical mechanisms depend upon the nature of the conductive surface and the type of foulant, and their electrostatic interactions with the membrane surface. The review also focused on novel devices such as desalination batteries and the electrocatalysts used for such technologies. Various hydrophobic photothermal composites used in seawater desalination were reviewed, including magnetic and low cost photothermal materials. This was further followed by recent studies on plasmonic materials in solar desalination including Al, Pd, Au and Ag nanoparticles, their advanced fabrication techniques and recent research trends for enhanced salt rejection and water productivity. Functional magnetic materials such as Fe_3O_4 were given special consideration, being widely utilized in FO draw solutes and RO for efficient particle separation. Various research

studies on antimicrobial materials and their fabrication methods were reviewed for NF and RO membrane surface modification to prevent biofouling phenomenon. Being the widely researched antimicrobial materials, Ag and graphene were given special consideration, along with their hybrid composites with the material being supported on a support layer such as CNTs, zeolites or TiO₂ for efficient and controlled release of ions. Research studies on natural and synthetic zeolites such as morendite, LTA and MFI were reviewed in greater detail for their sorbent properties whereby salt separation is achieved through adsorption of the salt ions onto its surface. Carbon-based materials such as CNTs and graphene were also reviewed for this functional property in desalination.

Many materials such as CNTs and graphene can perform more than one function and thus can be utilized for multifunctional purposes. However, their synthesis, agglomeration problems and health concerns still need extensive research for commercial feasibility. Apart from conventional functional materials, this review has highlighted new emerging trends such as hybrid processes, novel composite materials and new technologies which can provide further insight to researchers in this field on the upcoming trends and the dire need for continuous improvements in functional materials in desalination.

Based on the review in this paper, future recommendations which may answer several questions pertaining to functional materials current limitations on synthesis, fabrication and integration in desalination are highlighted below:

- Most of the functional materials in desalination are nano-scale. Apart from the composition of their building blocks, the properties of nanomaterials also depend upon their nano-scaled structure. Therefore, this calls for a deep understanding of the various nanomaterials such as CNTs, graphene, mixed nano-oxides and others for an interdisciplinary collaboration between the fields of materials science, physics, chemistry, engineering and biology.
- Many functional materials such as plasmonics, sorbents and magnetic materials are widely used in other industries including the electronics and catalysis industry. Researchers should take advantage of the progress made on such materials in other fields. For example, advanced research is underway on zeolites as catalysts, where their new combinations, synthesis techniques and modification methods are explored. Those advances could be beneficial for the desalination industry in answering many of the existing limitations such as agglomeration, choice of support materials, leaching problems and novel hybrid materials.
- Besides investing in improving existing functional materials for thermal and membrane-based desalination, future research should also focus on developing novel hybrid functional materials with improved new strategies for incorporating them in desalination.
- Even though functional materials are prominently utilized in various desalination technologies, very few studies report on their cost considerations. Many at times, the

high cost of certain nanomaterials and their integration with the desalination technology might not be justified with respect to the end water product.

- Zeolite-based membranes offer numerous functionalities in desalination. However, much research is needed to explore the properties of various zeolite types by introducing other metal ions in its structure. This could lead to multi-functional properties beneficial in terms of cost improvement and desalination performance. For example, photocatalytic materials such as nano-TiO₂ could be supported on LTA or zeolite-Y and used as sorbents providing simultaneous photocatalytic activity for biofouling prevention.
- Leaching of antibacterial ions such as Ag has been a major challenge. Research on new support materials is required for controlled discharge of such ions to prevent antimicrobial degradation over time. One solution is to use polyelectrolytes which can help prevent nanoparticle leaching from a polymer substrate. Other potential approaches include improved coating stability and optimized membrane morphology and structures.
- Agglomeration is one major limitation with functional nanoparticles. This limitation could be addressed by shaping the nanoparticles in a wire, string or fiber form for both agglomeration prevention and increased accessibility to the active sites for improved photocatalytic, electrocatalytic, magnetic and sorbent functionalities.
- Magnetic nanoparticles are prevalently utilized as FO draw solutes. There is a much dire need for an evaluation of the energetic and economic feasibility of magnetic

nanoparticles in FO. Thus, besides developing new magnetic draw solutes, research should also be directed towards comprehensive, robust lifecycle analyses for utilizing such materials.

- To avoid magnetic nanoparticle agglomeration, one research direction is to develop tailored magnetic separators with tunable magnetic strengths. This could provide a solution for both agglomeration and magnetic nanoparticles recycling in the FO process.
- For mixed matrix membranes such as those involving filler functional nanoparticles embedded in a polymeric matrix, there is a dire need for interface optimization for improved functionality. A mismatch often leads to poor desalination performances by not providing sufficient interaction between the matrix and the filler. Specialized fabrication techniques for blending and coating may provide a solution to this challenge in fabrication.
- The use of green functional materials, biodegradable polymers and environmental friendly systems is highly recommended. Though this aspect is seldom stressed upon, with the on-going global environmental crisis, much attention should be spurred in focusing future research towards sustainable functional materials.

11. Abbreviations

CNTs	Carbon nanotubes
RO	Reverse Osmosis
MSF	Multi stage flash
NF	Nanofiltration

GO	Graphene oxide
rGO	Reduced graphene oxide
EO	Electrochemical oxidation
MWCNT	Multi walled carbon nanotube
FO	Forward osmosis
PAA	Polyacrylic acid
MFC	Magnetic field control
CTA	Cellulose triacetate
PSA	Poly sodium acrylate
HGMS	High gradient magnetic separator
UF	Ultrafiltration
MTM	Magnetic treatment method
EPS	Extracellular polymeric substances
PVDF	Poly (vinylidene fluoride)
E. coli	<i>Escherichia coli</i>
IP	interfacial polymerization
MPD	phenylenediamine
TMC	trimesoyl chloride
PA	Polyamide
PES	Polyethersulfone
CA	Cellulose acetate
PE	Polyethylene
PEI	Polyethyleneimine
PAN	Polyacrylonitrile
PVA	Poly (vinyl) alcohol
SEM	Scanning electron microscopy
CDI	Capacitive deionization
NIPS	Non-solvent-induced phase separation

12. References

- [1] M. Elimelech, W.A. Phillip, The future of seawater desalination: energy, technology, and the environment, *science*, 333 (2011) 712-717.
- [2] S.F. Anis, R. Hashaiekh, N. Hilal, Reverse osmosis pretreatment technologies and future trends: A comprehensive review, *Desalination*, 452 (2019) 159-195.
- [3] P.S. Goh, A.F. Ismail, N. Hilal, Nano-enabled membranes technology: Sustainable and revolutionary solutions for membrane desalination?, *Desalination*, 380 (2016) 100-104.
- [4] S.F. Anis, B.S. Lalia, R. Hashaiekh, Controlling swelling behavior of poly (vinyl) alcohol via networked cellulose and its application as a reverse osmosis membrane, *Desalination*, 336 (2014) 138-145.
- [5] J.R. Werber, C.O. Osuji, M. Elimelech, Materials for next-generation desalination and water purification membranes, *Nature Reviews Materials*, 1 (2016) 16018.
- [6] P.S. Goh, A.F. Ismail, A review on inorganic membranes for desalination and wastewater treatment, *Desalination*, 434 (2018) 60-80.
- [7] Z. Yang, X.-H. Ma, C.Y. Tang, Recent development of novel membranes for desalination, *Desalination*, 434 (2018) 37-59.
- [8] R. Valavala, J. Sohn, J. Han, N. Her, Y. Yoon, Pretreatment in Reverse Osmosis Seawater Desalination: A Short Review, *Environmental Engineering Research*, 16 (2011) 205-212.
- [9] J. Schallenberg-Rodríguez, J.M. Veza, A. Blanco-Marigorta, Energy efficiency and desalination in the Canary Islands, *Renewable and Sustainable Energy Reviews*, 40 (2014) 741-748.
- [10] G. Amy, N. Ghaffour, Z. Li, L. Francis, R.V. Linares, T. Missimer, S. Lattemann, Membrane-based seawater desalination: Present and future prospects, *Desalination*, 401 (2017) 16-21.
- [11] A.A. Mayyahi, B. Deng, Efficient water desalination using photo-responsive ZnO polyamide thin film nanocomposite membrane, *Environmental Chemistry Letters*, 16 (2018) 1469-1475.

- [12] P. Formoso, E. Pantuso, G. De Filpo, F. Nicoletta, Electro-conductive membranes for permeation enhancement and fouling mitigation: A short review, *Membranes*, 7 (2017) 39.
- [13] M. Nemati, S.M. Hosseini, F. Parvizian, N. Rafiei, B. Van der Bruggen, Desalination and heavy metal ion removal from water by new ion exchange membrane modified by synthesized NiFe₂O₄/HAMPS nanocomposite, *Ionics*, (2019).
- [14] J. Xu, F. Xu, M. Qian, Z. Li, P. Sun, Z. Hong, F. Huang, Copper nanodot-embedded graphene urchins of nearly full-spectrum solar absorption and extraordinary solar desalination, *Nano Energy*, 53 (2018) 425-431.
- [15] B. Peng, J. Chen, Functional materials with high-efficiency energy storage and conversion for batteries and fuel cells, *Coordination Chemistry Reviews*, 253 (2009) 2805-2813.
- [16] J. Herbert, *Ferroelectric transducers and sensors*, CRC Press, 1982.
- [17] Y.F. Zhang, N. Zhang, H. Hingorani, N. Ding, D. Wang, C. Yuan, B. Zhang, G. Gu, Q. Ge, Fast-Response, Stiffness-Tunable Soft Actuator by Hybrid Multimaterial 3D Printing, *Advanced Functional Materials*, (2019) 1806698.
- [18] I. Ali, New Generation Adsorbents for Water Treatment, *Chemical Reviews*, 112 (2012) 5073-5091.
- [19] S.E. Lyshevski, *MEMS and NEMS: systems, devices, and structures*, CRC press, 2002.
- [20] M. Giese, M. Spengler, Cellulose nanocrystals in nanoarchitectonics-towards photonic functional materials, *Molecular Systems Design and Engineering*, 4 (2019) 29-48.
- [21] T. Keplinger, X. Wang, I. Burgert, Nanofibrillated cellulose composites and wood derived scaffolds for functional materials, *Journal of Materials Chemistry A*, 7 (2019) 2981-2992.
- [22] M.A. Rahim, S.L. Kristufek, S. Pan, J.J. Richardson, F. Caruso, Phenolic Building Blocks for the Assembly of Functional Materials, *Angewandte Chemie - International Edition*, 58 (2019) 1904-1927.
- [23] Q. Liu, G.-R. Xu, Graphene oxide (GO) as functional material in tailoring polyamide thin film composite (PA-TFC) reverse osmosis (RO) membranes, *Desalination*, 394 (2016) 162-175.
- [24] T. Zhu, Y. Sha, J. Yan, P. Pageni, M.A. Rahman, Y. Yan, C. Tang, Metallo-polyelectrolytes as a class of ionic macromolecules for functional materials, *Nature Communications*, 9 (2018).
- [25] M. Baibarac, P. Gómez-Romero, Nanocomposites based on conducting polymers and carbon nanotubes: From fancy materials to functional applications, *Journal of Nanoscience and Nanotechnology*, 6 (2006) 289-302.
- [26] J.P. Paraknowitsch, A. Thomas, Functional carbon materials from ionic liquid precursors, *Macromolecular Chemistry and Physics*, 213 (2012) 1132-1145.
- [27] Y.K. Mishra, R. Adelung, ZnO tetrapod materials for functional applications, *Materials Today*, 21 (2018) 631-651.
- [28] K.M. Hutchins, Functional materials based on molecules with hydrogen-bonding ability: Applications to drug co-crystals and polymer complexes, *Royal Society Open Science*, 5 (2018).
- [29] I.E. Oflyand, G.I. Dzhardimalieva, Molecular design of supramolecular polymers with chelated units and their application as functional materials, *Journal of Coordination Chemistry*, 71 (2018) 1272-1356.
- [30] T. Kato, J. Uchida, T. Ichikawa, T. Sakamoto, Functional Liquid Crystals towards the Next Generation of Materials, *Angewandte Chemie - International Edition*, 57 (2018) 4355-4371.
- [31] W.H. Chen, G.F. Luo, X.Z. Zhang, Recent Advances in Subcellular Targeted Cancer Therapy Based on Functional Materials, *Advanced Materials*, 31 (2019).
- [32] C. Xie, F. Yan, Flexible Photodetectors Based on Novel Functional Materials, *Small*, 13 (2017).
- [33] E. Eroglu, C.L. Raston, Nanomaterial processing strategies in functional hybrid materials for wastewater treatment using algal biomass, *Journal of Chemical Technology and Biotechnology*, 92 (2017) 1862-1867.
- [34] H. Jia, J. Cao, Y. Lu, Design and fabrication of functional hybrid materials for catalytic applications, *Current Opinion in Green and Sustainable Chemistry*, 4 (2017) 16-22.
- [35] F.K. Kessler, Y. Zheng, D. Schwarz, C. Merschjann, W. Schnick, X. Wang, M.J. Bojdys, Functional carbon nitride materials-design strategies for electrochemical devices, *Nature Reviews Materials*, 2 (2017).
- [36] J. Weiss, P. Takhistov, D.J. McClements, Functional materials in food nanotechnology, *Journal of Food Science*, 71 (2006) R107-R116.
- [37] R. Hashaikeh, B.S. Lalia, V. Kochkodan, N. Hilal, A novel in situ membrane cleaning method using periodic electrolysis, *Journal of Membrane Science*, 471 (2014) 149-154.
- [38] J. Zhu, J. Hou, Y. Zhang, M. Tian, T. He, J. Liu, V. Chen, Polymeric antimicrobial membranes enabled by nanomaterials for water treatment, *Journal of Membrane Science*, 550 (2018) 173-197.

- [39] S. Ali, S.A.U. Rehman, H.-Y. Luan, M.U. Farid, H. Huang, Challenges and opportunities in functional carbon nanotubes for membrane-based water treatment and desalination, *Science of The Total Environment*, 646 (2019) 1126-1139.
- [40] A.M.A. Abdelsamad, A.S.G. Khalil, M. Ulbricht, Influence of controlled functionalization of mesoporous silica nanoparticles as tailored fillers for thin-film nanocomposite membranes on desalination performance, *Journal of Membrane Science*, 563 (2018) 149-161.
- [41] Y.H. Teow, A.W. Mohammad, New generation nanomaterials for water desalination: A review, *Desalination*, 451 (2019) 2-17.
- [42] R. Saravanan, F. Gracia, A. Stephen, Basic principles, mechanism, and challenges of photocatalysis, in: *Nanocomposites for Visible Light-induced Photocatalysis*, Springer, 2017, pp. 19-40.
- [43] K. Kumar, A. Chowdhury, Use of Novel Nanostructured Photocatalysts for the Environmental Sustainability of Wastewater Treatments, in: *Reference Module in Materials Science and Materials Engineering*, Elsevier, 2018.
- [44] A. De Battisti, C.A. Martínez-Huitle, Chapter 5 - Electrocatalysis in Wastewater Treatment, in: C.A. Martínez-Huitle, M.A. Rodrigo, O. Scialdone (Eds.) *Electrochemical Water and Wastewater Treatment*, Butterworth-Heinemann, 2018, pp. 119-131.
- [45] C.A. Martínez-Huitle, L.S. Andrade, Electrocatalysis in wastewater treatment: recent mechanism advances, *Química Nova*, 34 (2011) 850-858.
- [46] L. Zhang, B. Tang, J. Wu, R. Li, P. Wang, Hydrophobic Light-to-Heat Conversion Membranes with Self-Healing Ability for Interfacial Solar Heating, *Advanced Materials*, 27 (2015) 4889-4894.
- [47] Q. Ge, M. Ling, T.-S. Chung, Draw solutions for forward osmosis processes: developments, challenges, and prospects for the future, *Journal of membrane science*, 442 (2013) 225-237.
- [48] M. Razmkhah, F. Moosavi, M.T.H. Mosavian, A. Ahmadpour, Does electric or magnetic field affect reverse osmosis desalination?, *Desalination*, 432 (2018) 55-63.
- [49] W. Chen, C. Zou, X. Li, H. Liang, Application of recoverable carbon nanotube nanofluids in solar desalination system: An experimental investigation, *Desalination*, 451 (2019) 92-101.
- [50] M.A. Alaei Shahmirzadi, S.S. Hosseini, J. Luo, I. Ortiz, Significance, evolution and recent advances in adsorption technology, materials and processes for desalination, water softening and salt removal, *Journal of Environmental Management*, 215 (2018) 324-344.
- [51] M.R. Gandhi, S. Vasudevan, A. Shibayama, M. Yamada, Graphene and Graphene-Based Composites: A Rising Star in Water Purification-A Comprehensive Overview, *ChemistrySelect*, 1 (2016) 4358-4385.
- [52] L. Zhu, M. Gao, C.K.N. Peh, G.W. Ho, Solar-driven photothermal nanostructured materials designs and prerequisites for evaporation and catalysis applications, *Materials Horizons*, 5 (2018) 323-343.
- [53] S. Yang, J.-S. Gu, H.-Y. Yu, J. Zhou, S.-F. Li, X.-M. Wu, L. Wang, Polypropylene membrane surface modification by RAFT grafting polymerization and TiO₂ photocatalysts immobilization for phenol decomposition in a photocatalytic membrane reactor, *Separation and Purification Technology*, 83 (2011) 157-165.
- [54] Y. Zhang, D. Wang, G. Zhang, Photocatalytic degradation of organic contaminants by TiO₂/sepiolite composites prepared at low temperature, *Chemical Engineering Journal*, 173 (2011) 1-10.
- [55] H. Lee, J. Choi, S. Lee, S.-T. Yun, C. Lee, J. Lee, Kinetic enhancement in photocatalytic oxidation of organic compounds by WO₃ in the presence of Fenton-like reagent, *Applied Catalysis B: Environmental*, 138-139 (2013) 311-317.
- [56] Z. Miao, S. Tao, Y. Wang, Y. Yu, C. Meng, Y. An, Hierarchically porous silica as an efficient catalyst carrier for high performance vis-light assisted Fenton degradation, *Microporous and Mesoporous Materials*, 176 (2013) 178-185.
- [57] V.K. Gupta, D. Pathania, S. Agarwal, P. Singh, Adsorptional photocatalytic degradation of methylene blue onto pectin-CuS nanocomposite under solar light, *Journal of Hazardous Materials*, 243 (2012) 179-186.
- [58] S. Liu, X. Wang, W. Zhao, K. Wang, H. Sang, Z. He, Synthesis, characterization and enhanced photocatalytic performance of Ag₂S-coupled ZnO/ZnS core/shell nanorods, *Journal of Alloys and Compounds*, 568 (2013) 84-91.
- [59] Y. Huo, Z. Xie, X. Wang, H. Li, M. Hoang, R.A. Caruso, Methyl orange removal by combined visible-light photocatalysis and membrane distillation, *Dyes and Pigments*, 98 (2013) 106-112.
- [60] J. Wang, Y. Yu, L. Zhang, Highly efficient photocatalytic removal of sodium pentachlorophenate with Bi₃O₄Br under visible light, *Applied Catalysis B: Environmental*, 136-137 (2013) 112-121.

- [61] X. Xiao, R. Hu, C. Liu, C. Xing, X. Zuo, J. Nan, L. Wang, Facile microwave synthesis of novel hierarchical Bi₂O₃Br₁₀ nanoflakes with excellent visible light photocatalytic performance for the degradation of tetracycline hydrochloride, *Chemical Engineering Journal*, 225 (2013) 790-797.
- [62] S. Sakka, Chapter 11.1.2 - Sol-Gel Process and Applications, in: S. Somya (Ed.) *Handbook of Advanced Ceramics (Second Edition)*, Academic Press, Oxford, 2013, pp. 883-910.
- [63] A. Mills, S. Le Hunte, An overview of semiconductor photocatalysis, *Journal of Photochemistry and Photobiology A: Chemistry*, 108 (1997) 1-35.
- [64] Y. Kikuchi, K. Sunada, T. Iyoda, K. Hashimoto, A. Fujishima, Photocatalytic Bactericidal Effect of TiO₂ Thin Films: Dynamic View of the Active Oxygen Species Responsible for the Effect, 1997.
- [65] S. Gelover, L.A. Gómez, K. Reyes, M. Teresa Leal, A practical demonstration of water disinfection using TiO₂ films and sunlight, *Water Research*, 40 (2006) 3274-3280.
- [66] S.-J. You, G.U. Semblante, S.-C. Lu, R.A. Damodar, T.-C. Wei, Evaluation of the antifouling and photocatalytic properties of poly(vinylidene fluoride) plasma-grafted poly(acrylic acid) membrane with self-assembled TiO₂, *Journal of Hazardous Materials*, 237-238 (2012) 10-19.
- [67] R.R. Choudhury, J.M. Gohil, S. Mohanty, S.K. Nayak, Antifouling, fouling release and antimicrobial materials for surface modification of reverse osmosis and nanofiltration membranes, *Journal of Materials Chemistry A*, 6 (2018) 313-333.
- [68] B. Zhuman, Saepurahman, S.F. Anis, R. Hashaiekh, Obtaining high crystalline ball milled H-Y zeolite particles with carbon nanostructures as a damping material, *Microporous and Mesoporous Materials*, (2018). <https://doi.org/10.1016/j.micromeso.2018.06.041>.
- [69] S.F. Anis, A. Khalil, G. Singaravel, R. Hashaiekh, A review on the fabrication of zeolite and mesoporous inorganic nanofibers formation for catalytic applications, *Microporous and Mesoporous Materials*, 236 (2016) 176-192.
- [70] S.F. Anis, G. Singaravel, R. Hashaiekh, NiW/nano zeolite Y catalysts for n-heptane hydrocracking, *Materials Chemistry and Physics*, 212 (2018) 87-94.
- [71] S.F. Anis, R. Hashaiekh, Electrochemical water splitting using nano-zeolite Y supported tungsten oxide electrocatalysts, *Journal of Nanoparticle Research*, 20 (2018) 47.
- [72] X.Z. Li, H. Liu, L.F. Cheng, H.J. Tong, Photocatalytic Oxidation Using a New Catalyst TiO₂ Microsphere for Water and Wastewater Treatment, *Environmental Science & Technology*, 37 (2003) 3989-3994.
- [73] Z. Liu, X. Zhang, S. Nishimoto, M. Jin, D.A. Tryk, T. Murakami, A. Fujishima, Highly Ordered TiO₂ Nanotube Arrays with Controllable Length for Photoelectrocatalytic Degradation of Phenol, *The Journal of Physical Chemistry C*, 112 (2008) 253-259.
- [74] N. Daneshvar, D. Salari, A. Niaei, M.H. Rasoulifard, A.R. Khataee, Immobilization of TiO₂ Nanopowder on Glass Beads for the Photocatalytic Decolorization of an Azo Dye C.I. Direct Red 23, *Journal of Environmental Science and Health, Part A*, 40 (2005) 1605-1617.
- [75] H. Uchida, S. Hirao, T. Torimoto, S. Kuwabata, T. Sakata, H. Mori, H. Yoneyama, Preparation and Properties of Size-Quantized TiO₂ Particles Immobilized in Poly(vinylpyrrolidinone) Gel Films, *Langmuir*, 11 (1995) 3725-3729.
- [76] C.H. Ao, S.C. Lee, Enhancement effect of TiO₂ immobilized on activated carbon filter for the photodegradation of pollutants at typical indoor air level, *Applied Catalysis B: Environmental*, 44 (2003) 191-205.
- [77] C.P. Athanasekou, G.E. Romanos, F.K. Katsaros, K. Kordatos, V. Likodimos, P. Falaras, Very efficient composite titania membranes in hybrid ultrafiltration/photocatalysis water treatment processes, *Journal of Membrane Science*, 392-393 (2012) 192-203.
- [78] H. Song, J. Shao, Y. He, B. Liu, X. Zhong, Natural organic matter removal and flux decline with PEG-TiO₂-doped PVDF membranes by integration of ultrafiltration with photocatalysis, *Journal of Membrane Science*, 405-406 (2012) 48-56.
- [79] X. Zhang, A.J. Du, P. Lee, D.D. Sun, J.O. Leckie, TiO₂ nanowire membrane for concurrent filtration and photocatalytic oxidation of humic acid in water, *Journal of Membrane Science*, 313 (2008) 44-51.
- [80] S.P. Albu, A. Ghicov, J.M. Macak, R. Hahn, P. Schmuki, Self-Organized, Free-Standing TiO₂ Nanotube Membrane for Flow-through Photocatalytic Applications, *Nano Letters*, 7 (2007) 1286-1289.
- [81] J. Liao, S. Lin, N. Pan, S. Li, X. Cao, Y. Cao, Fabrication and photocatalytic properties of free-standing TiO₂ nanotube membranes with through-hole morphology, *Materials Characterization*, 66 (2012) 24-29.
- [82] H.S. Lee, S.J. Im, J.H. Kim, H.J. Kim, J.P. Kim, B.R. Min, Polyamide thin-film nanofiltration membranes containing TiO₂ nanoparticles, *Desalination*, 219 (2008) 48-56.

- [83] S. Leong, A. Razmjou, K. Wang, K. Hapgood, X. Zhang, H. Wang, TiO₂ based photocatalytic membranes: A review, *Journal of Membrane Science*, 472 (2014) 167-184.
- [84] T.-H. Bae, I.-C. Kim, T.-M. Tak, Preparation and characterization of fouling-resistant TiO₂ self-assembled nanocomposite membranes, *Journal of Membrane Science*, 275 (2006) 1-5.
- [85] S.-Y. Kwak, S.H. Kim, S.S. Kim, Hybrid Organic/Inorganic Reverse Osmosis (RO) Membrane for Bactericidal Anti-Fouling. 1. Preparation and Characterization of TiO₂ Nanoparticle Self-Assembled Aromatic Polyamide Thin-Film-Composite (TFC) Membrane, *Environmental Science & Technology*, 35 (2001) 2388-2394.
- [86] S.H. Kim, S.-Y. Kwak, B.-H. Sohn, T.H. Park, Design of TiO₂ nanoparticle self-assembled aromatic polyamide thin-film-composite (TFC) membrane as an approach to solve biofouling problem, *Journal of Membrane Science*, 211 (2003) 157-165.
- [87] Y. Mansourpanah, S.S. Madaeni, A. Rahimpour, A. Farhadian, A.H. Taheri, Formation of appropriate sites on nanofiltration membrane surface for binding TiO₂ photo-catalyst: Performance, characterization and fouling-resistant capability, *Journal of Membrane Science*, 330 (2009) 297-306.
- [88] S. Madaeni, N. Ghaemi, Characterization of self-cleaning RO membranes coated with TiO₂ particles under UV irradiation, *Journal of Membrane Science*, 303 (2007) 221-233.
- [89] A. Rahimpour, S.S. Madaeni, A.H. Taheri, Y. Mansourpanah, Coupling TiO₂ nanoparticles with UV irradiation for modification of polyethersulfone ultrafiltration membranes, *Journal of Membrane Science*, 313 (2008) 158-169.
- [90] A. Rahimpour, M. Jahanshahi, B. Rajaeian, M. Rahimnejad, TiO₂ entrapped nano-composite PVDF/SPES membranes: Preparation, characterization, antifouling and antibacterial properties, *Desalination*, 278 (2011) 343-353.
- [91] R.A. Damodar, S.-J. You, H.-H. Chou, Study the self cleaning, antibacterial and photocatalytic properties of TiO₂ entrapped PVDF membranes, *Journal of hazardous materials*, 172 (2009) 1321-1328.
- [92] S. Feroz, F. Al Siyabi, j.j. Dumanan, S. Al-Saadi, Application of Solar Nano Photocatalysis in Treatment of Seawater, 2014.
- [93] R. Isha, N.H. Abd Majid, A Potential Hybrid TiO₂ in Photocatalytic Seawater Desalination, *Advanced Materials Research*, 1113 (2015) 3-8.
- [94] D.F. Ollis, Integrating photocatalysis and membrane technologies for water treatment, *Annals of the New York Academy of Sciences*, 984 (2003) 65-84.
- [95] S. Mozia, Photocatalytic membrane reactors (PMRs) in water and wastewater treatment. A review, *Separation and Purification Technology*, 73 (2010) 71-91.
- [96] A. Alem, H. Sarpoolaky, M. Keshmiri, Titania ultrafiltration membrane: Preparation, characterization and photocatalytic activity, *Journal of the European Ceramic Society*, 29 (2009) 629-635.
- [97] P. Liu, H. Liu, G. Liu, K. Yao, W. Lv, Preparation of TiO₂ nanotubes coated on polyurethane and study of their photocatalytic activity, *Applied Surface Science*, 258 (2012) 9593-9598.
- [98] L. Djafer, A. Ayril, A. Ouagued, Robust synthesis and performance of a titania-based ultrafiltration membrane with photocatalytic properties, *Separation and Purification Technology*, 75 (2010) 198-203.
- [99] X. Zhang, A.J. Du, P. Lee, D.D. Sun, J.O. Leckie, Grafted multifunctional titanium dioxide nanotube membrane: Separation and photodegradation of aquatic pollutant, *Applied Catalysis B: Environmental*, 84 (2008) 262-267.
- [100] N. Ma, X. Fan, X. Quan, Y. Zhang, Ag-TiO₂/HAP/Al₂O₃ bioceramic composite membrane: Fabrication, characterization and bactericidal activity, *Journal of Membrane Science*, 336 (2009) 109-117.
- [101] L. Liu, Z. Liu, H. Bai, D.D. Sun, Concurrent filtration and solar photocatalytic disinfection/degradation using high-performance Ag/TiO₂ nanofiber membrane, *Water Research*, 46 (2012) 1101-1112.
- [102] S.F. Anis, R. Hashaikeh, Electrospun zeolite-Y fibers: Fabrication and morphology analysis, *Microporous and Mesoporous Materials*, 233 (2016) 78-86.
- [103] S.F. Anis, G. Singaravel, R. Hashaikeh, Electrospun Ni-W/zeolite composite fibers for n-heptane hydrocracking and hydroisomerization, *Materials Chemistry and Physics*, 200 (2017) 146-154.
- [104] S.F. Anis, B.S. Lalia, G. Palmisano, R. Hashaikeh, Photoelectrochemical activity of electrospun WO₃/NiWO₄ nanofibers under visible light irradiation, *J Mater Sci*, 53 (2018) 2208-2220.
- [105] A. Nguyen, L. Zou, C. Priest, Evaluating the antifouling effects of silver nanoparticles regenerated by TiO₂ on forward osmosis membrane, *Journal of Membrane Science*, 454 (2014) 264-271.
- [106] Y.-F. Lin, K.-L. Tung, Y.-S. Tzeng, J.-H. Chen, K.-S. Chang, Rapid atmospheric plasma spray coating preparation and photocatalytic activity of macroporous titania nanocrystalline membranes, *Journal of Membrane Science*, 389 (2012) 83-90.

- [107] A. Sirelkhatim, S. Mahmud, A. Seeni, N.H.M. Kaus, L.C. Ann, S.K.M. Bakhori, H. Hasan, D. Mohamad, Review on Zinc Oxide Nanoparticles: Antibacterial Activity and Toxicity Mechanism, *Nano-Micro Letters*, 7 (2015) 219-242.
- [108] S. Javdaneh, M.R. Mehrnia, M. Homayoonfal, Engineering design of a biofilm formed on a pH-sensitive ZnO/PSf nanocomposite membrane with antibacterial properties, *RSC Advances*, 6 (2016) 112269-112281.
- [109] K.R. Raghupathi, R.T. Koodali, A.C. Manna, Size-Dependent Bacterial Growth Inhibition and Mechanism of Antibacterial Activity of Zinc Oxide Nanoparticles, *Langmuir*, 27 (2011) 4020-4028.
- [110] S.G. Patel, S. Bhatnagar, J. Vardia, S.C. Ameta, Use of photocatalysts in solar desalination, *Desalination*, 189 (2006) 287-291.
- [111] S. Zinadini, S. Rostami, V. Vatanpour, E. Jalilian, Preparation of antibiofouling polyethersulfone mixed matrix NF membrane using photocatalytic activity of ZnO/MWCNTs nanocomposite, *Journal of Membrane Science*, 529 (2017) 133-141.
- [112] M.H. Al-Hinai, P. Sathe, M.Z. Al-Abri, S. Dobretsov, A.T. Al-Hinai, J. Dutta, Antimicrobial activity enhancement of poly (ether sulfone) membranes by in situ growth of ZnO nanorods, *ACS omega*, 2 (2017) 3157-3167.
- [113] Feroz S. Treatment of Saline Water by Solar Nano Photocatalysis. *Synth Catal.* 2017, 2:1.
- [114] C. Liu, D. Kong, P.-C. Hsu, H. Yuan, H.-W. Lee, Y. Liu, H. Wang, S. Wang, K. Yan, D. Lin, P.A. Maraccini, K.M. Parker, A.B. Boehm, Y. Cui, Rapid water disinfection using vertically aligned MoS₂ nanofilms and visible light, *Nature Nanotechnology*, 11 (2016) 1098.
- [115] Q. Li, W. Liang, J. Ku Shang, Enhanced visible-light absorption from PdO nanoparticles in nitrogen-doped titanium oxide thin films, *Applied physics letters*, 90 (2007) 063109.
- [116] P.Y. Ayekoe, D. Robert, D.L. Goné, TiO₂/Bi₂O₃ photocatalysts for elimination of water contaminants. Part 1: synthesis of α - and β -Bi₂O₃ nanoparticles, *Environmental Chemistry Letters*, 13 (2015) 327-332.
- [117] X. Zeng, Z. Wang, N. Meng, D.T. McCarthy, A. Deletic, J.-h. Pan, X. Zhang, Highly dispersed TiO₂ nanocrystals and carbon dots on reduced graphene oxide: Ternary nanocomposites for accelerated photocatalytic water disinfection, *Applied Catalysis B: Environmental*, 202 (2017) 33-41.
- [118] A.B. Djurišić, Y.H. Leung, A.M. Ching Ng, Strategies for improving the efficiency of semiconductor metal oxide photocatalysis, *Materials Horizons*, 1 (2014) 400-410.
- [119] L. Lin, H. Wang, H. Luo, P. Xu, Photocatalytic treatment of desalination concentrate using optical fibers coated with nanostructured thin films: impact of water chemistry and seasonal climate variations, *Photochemistry and photobiology*, 92 (2016) 379-387.
- [120] O. Akhavan, E. Ghaderi, Photocatalytic Reduction of Graphene Oxide Nanosheets on TiO₂ Thin Film for Photoinactivation of Bacteria in Solar Light Irradiation, *The Journal of Physical Chemistry C*, 113 (2009) 20214-20220.
- [121] J. Liu, L. Liu, H. Bai, Y. Wang, D.D. Sun, Gram-scale production of graphene oxide–TiO₂ nanorod composites: towards high-activity photocatalytic materials, *Applied Catalysis B: Environmental*, 106 (2011) 76-82.
- [122] P. Gao, K. Ng, D.D. Sun, Sulfonated graphene oxide–ZnO–Ag photocatalyst for fast photodegradation and disinfection under visible light, *Journal of hazardous materials*, 262 (2013) 826-835.
- [123] P. Gao, J. Liu, D.D. Sun, W. Ng, Graphene oxide–CdS composite with high photocatalytic degradation and disinfection activities under visible light irradiation, *Journal of hazardous materials*, 250 (2013) 412-420.
- [124] W. Wang, J.C. Yu, D. Xia, P.K. Wong, Y. Li, Graphene and g-C₃N₄ nanosheets cowrapped elemental α -sulfur as a novel metal-free heterojunction photocatalyst for bacterial inactivation under visible-light, *Environmental science & technology*, 47 (2013) 8724-8732.
- [125] Y. Gao, M. Hu, B. Mi, Membrane surface modification with TiO₂–graphene oxide for enhanced photocatalytic performance, *Journal of Membrane Science*, 455 (2014) 349-356.
- [126] F. Ahmed, B.S. Lalia, V. Kochkodan, N. Hilal, R. Hashaikeh, Electrically conductive polymeric membranes for fouling prevention and detection: A review, *Desalination*, 391 (2016) 1-15.
- [127] B.S. Lalia, F.E. Ahmed, T. Shah, N. Hilal, R. Hashaikeh, Electrically conductive membranes based on carbon nanostructures for self-cleaning of biofouling, *Desalination*, 360 (2015) 8-12.
- [128] Ihsanullah, Carbon nanotube membranes for water purification: Developments, challenges, and prospects for the future, *Separation and Purification Technology*, 209 (2019) 307-337.
- [129] G. Gao, Q. Zhang, C.D. Vecitis, CNT–PVDF composite flow-through electrode for single-pass sequential reduction–oxidation, *Journal of Materials Chemistry A*, 2 (2014) 6185-6190.

- [130] C.D. Vecitis, M.H. Schnoor, M.S. Rahaman, J.D. Schiffman, M. Elimelech, Electrochemical Multiwalled Carbon Nanotube Filter for Viral and Bacterial Removal and Inactivation, *Environmental Science & Technology*, 45 (2011) 3672-3679.
- [131] S.F. Anis, B.S. Lalia, A.O. Mostafa, R. Hashaikeh, Electrospun nickel–tungsten oxide composite fibers as active electrocatalysts for hydrogen evolution reaction, *J Mater Sci*, 52 (2017) 7269-7281.
- [132] Z. Wu, H. Chen, Y. Dong, H. Mao, J. Sun, S. Chen, V.S.J. Craig, J. Hu, Cleaning using nanobubbles: Defouling by electrochemical generation of bubbles, *Journal of Colloid and Interface Science*, 328 (2008) 10-14.
- [133] X.H. Zhang, N. Maeda, V.S. Craig, Physical properties of nanobubbles on hydrophobic surfaces in water and aqueous solutions, *Langmuir*, 22 (2006) 5025-5035.
- [134] X. Sun, J. Wu, Z. Chen, X. Su, B.J. Hinds, Fouling Characteristics and Electrochemical Recovery of Carbon Nanotube Membranes, *Advanced Functional Materials*, 23 (2013) 1500-1506.
- [135] M.H.-O. Rashid, S.Q.T. Pham, L.J. Sweetman, L.J. Alcock, A. Wise, L.D. Nghiem, G. Triani, M.i.h. Panhuis, S.F. Ralph, Synthesis, properties, water and solute permeability of MWNT buckypapers, *Journal of Membrane Science*, 456 (2014) 175-184.
- [136] J.N. Coleman, S. Curran, A. Dalton, A. Davey, B. McCarthy, W. Blau, R. Barklie, Percolation-dominated conductivity in a conjugated-polymer-carbon-nanotube composite, *Physical Review B*, 58 (1998) R7492.
- [137] C.-F. de Lannoy, D. Jassby, K. Gloe, A.D. Gordon, M.R. Wiesner, Aquatic Biofouling Prevention by Electrically Charged Nanocomposite Polymer Thin Film Membranes, *Environmental Science & Technology*, 47 (2013) 2760-2768.
- [138] C.F. de Lannoy, D. Jassby, D.D. Davis, M.R. Wiesner, A highly electrically conductive polymer–multiwalled carbon nanotube nanocomposite membrane, *Journal of Membrane Science*, 415-416 (2012) 718-724.
- [139] D. Lawrence Arockiasamy, J. Alam, M. Alhoshan, Carbon nanotubes-blended poly(phenylene sulfone) membranes for ultrafiltration applications, *Applied Water Science*, 3 (2013) 93-103.
- [140] A.V. Dudchenko, J. Rolf, K. Russell, W. Duan, D. Jassby, Organic fouling inhibition on electrically conducting carbon nanotube–polyvinyl alcohol composite ultrafiltration membranes, *Journal of Membrane Science*, 468 (2014) 1-10.
- [141] Q. Zhang, C.D. Vecitis, Conductive CNT-PVDF membrane for capacitive organic fouling reduction, *Journal of Membrane Science*, 459 (2014) 143-156.
- [142] J. Benson, I. Kovalenko, S. Boukhalfa, D. Lashmore, M. Sanghadasa, G. Yushin, Multifunctional CNT-polymer composites for ultra-tough structural supercapacitors and desalination devices, *Advanced Materials*, 25 (2013) 6625-6632.
- [143] Y. Liu, W. Ma, Z. Cheng, J. Xu, R. Wang, X. Gang, Preparing CNTs/Ca-Selective zeolite composite electrode to remove calcium ions by capacitive deionization, *Desalination*, 326 (2013) 109-114.
- [144] F.E. Ahmed, B.S. Lalia, N. Hilal, R. Hashaikeh, Electrically conducting nanofiltration membranes based on networked cellulose and carbon nanostructures, *Desalination*, 406 (2017) 60-66.
- [145] S.M. Hosseini, S. Rafiei, A.R. Hamidi, A.R. Moghadassi, S.S. Madaeni, Preparation and electrochemical characterization of mixed matrix heterogeneous cation exchange membranes filled with zeolite nanoparticles: Ionic transport property in desalination, *Desalination*, 351 (2014) 138-144.
- [146] G.L. Soloveichik, Flow Batteries: Current Status and Trends, *Chemical Reviews*, 115 (2015) 11533-11558.
- [147] T. Kim, C.A. Gorski, B.E. Logan, Low energy desalination using battery electrode deionization, *Environmental Science & Technology Letters*, 4 (2017) 444-449.
- [148] J. Lee, S. Kim, C. Kim, J. Yoon, Hybrid capacitive deionization to enhance the desalination performance of capacitive techniques, *Energy & Environmental Science*, 7 (2014) 3683-3689.
- [149] D. Desai, E. S Beh, S. K Sahu, V. Vedharathinam, Q. van Overmeere, C.-F. de Lannoy, A. P Jose, A. R Volkel, J. Rivest, Electrochemical Desalination of Seawater and Hypersaline Brines with Coupled Electricity Storage, 2017.
- [150] Y. Zhang, S.T. Senthilkumar, J. Park, J. Park, Y. Kim, A New Rechargeable Seawater Desalination Battery System, *Batteries & Supercaps*, 1 (2018) 6-10.
- [151] K. Silambarasan, J. Joseph, Redox-Polysilsesquioxane Film as a New Chloride Storage Electrode for Desalination Batteries, *Energy Technology*, (2019) 1800601.
- [152] B. Tong, M.M. Hossain, Z. Yang, C. Cheng, Y. Wang, C. Jiang, T. Xu, Development of heterogeneous cation exchange membranes using functional polymer powders for desalination applications, *Journal of the Taiwan Institute of Chemical Engineers*, 67 (2016) 435-442.

- [153] M.I. Khan, A.N. Mondal, B. Tong, C. Jiang, K. Emmanuel, Z. Yang, L. Wu, T. Xu, Development of BPPO-based anion exchange membranes for electrodialysis desalination applications, *Desalination*, 391 (2016) 61-68.
- [154] X. Xu, L. Lin, G. Ma, H. Wang, W. Jiang, Q. He, N. Nirmalakhandan, P. Xu, Study of polyethyleneimine coating on membrane permselectivity and desalination performance during pilot-scale electrodialysis of reverse osmosis concentrate, *Separation and Purification Technology*, 207 (2018) 396-405.
- [155] T. Chakrabarty, A.M. Rajesh, A. Jasti, A.K. Thakur, A.K. Singh, S. Prakash, V. Kulshrestha, V.K. Shahi, Stable ion-exchange membranes for water desalination by electrodialysis, *Desalination*, 282 (2011) 2-8.
- [156] S.M. Hosseini, P. Koranian, A. Gholami, S.S. Madaeni, A.R. Moghadassi, P. Sakinejad, A.R. Khodabakhshi, Fabrication of mixed matrix heterogeneous ion exchange membrane by multiwalled carbon nanotubes: Electrochemical characterization and transport properties of mono and bivalent cations, *Desalination*, 329 (2013) 62-67.
- [157] C. Fernandez-Gonzalez, B. Zhang, A. Dominguez-Ramos, R. Ibañez, A. Irabien, Y. Chen, Enhancing fouling resistance of polyethylene anion exchange membranes using carbon nanotubes and iron oxide nanoparticles, *Desalination*, 411 (2017) 19-27.
- [158] A. Campione, L. Gurreri, M. Ciofalo, G. Micale, A. Tamburini, A. Cipollina, Electrodialysis for water desalination: A critical assessment of recent developments on process fundamentals, models and applications, *Desalination*, 434 (2018) 121-160.
- [159] Y. Mei, C.Y. Tang, Recent developments and future perspectives of reverse electrodialysis technology: A review, *Desalination*, 425 (2018) 156-174.
- [160] T. Luo, S. Abdu, M. Wessling, Selectivity of ion exchange membranes: A review, *Journal of Membrane Science*, 555 (2018) 429-454.
- [161] H. Chen, L. Shao, T. Ming, Z. Sun, C. Zhao, B. Yang, J. Wang, Understanding the photothermal conversion efficiency of gold nanocrystals, *Small*, 6 (2010) 2272-2280.
- [162] S.-C. Lin, C.-S. Hsu, S.-Y. Chiu, T.-Y. Liao, H.M. Chen, Edgeless Ag-Pt Bimetallic Nanocages: In Situ Monitor Plasmon-Induced Suppression of Hydrogen Peroxide Formation, *Journal of the American Chemical Society*, 139 (2017) 2224-2233.
- [163] Z. Hua, B. Li, L. Li, X. Yin, K. Chen, W. Wang, Designing a novel photothermal material of hierarchical microstructured copper phosphate for solar evaporation enhancement, *The Journal of Physical Chemistry C*, 121 (2016) 60-69.
- [164] Y. Fu, G. Wang, T. Mei, J. Li, J. Wang, X. Wang, Accessible graphene aerogel for efficiently harvesting solar energy, *ACS Sustainable Chemistry & Engineering*, 5 (2017) 4665-4671.
- [165] T. Liu, Y. Li, Photocatalysis: Plasmonic solar desalination, *Nature Photonics*, 10 (2016) 361.
- [166] Y. Zeng, J. Yao, B.A. Horri, K. Wang, Y. Wu, D. Li, H. Wang, Solar evaporation enhancement using floating light-absorbing magnetic particles, *Energy & Environmental Science*, 4 (2011) 4074-4078.
- [167] C. Song, T. Li, W. Guo, Y. Gao, C. Yang, Q. Zhang, D. An, W. Huang, M. Yan, C. Guo, Hydrophobic Cu₁₂Sb₄S₁₃-deposited photothermal film for interfacial water evaporation and thermal antibacterial activity, *New Journal of Chemistry*, 42 (2018) 3175-3179.
- [168] Z. Liu, Z. Yang, X. Huang, C. Xuan, J. Xie, H. Fu, Q. Wu, J. Zhang, X. Zhou, Y. Liu, High-absorption recyclable photothermal membranes used in a bionic system for high-efficiency solar desalination: Via enhanced localized heating, *Journal of Materials Chemistry A*, 5 (2017) 20044-20052.
- [169] J. Zhao, Y. Yang, C. Yang, Y. Tian, Y. Han, J. Liu, X. Yin, W. Que, A hydrophobic surface enabled salt-blocking 2D Ti₃C₂ MXene membrane for efficient and stable solar desalination, *Journal of Materials Chemistry A*, 6 (2018) 16196-16204.
- [170] J. Yao, G. Yang, An efficient solar-enabled 2D layered alloy material evaporator for seawater desalination, *Journal of Materials Chemistry A*, 6 (2018) 3869-3876.
- [171] G. Zhu, J. Xu, W. Zhao, F. Huang, Constructing black titania with unique nanocage structure for solar desalination, *ACS Applied Materials and Interfaces*, 8 (2016) 31716-31721.
- [172] H.-C. Chen, Y.-R. Chen, K.-H. Yang, C.-P. Yang, K.-L. Tung, M.-J. Lee, J.-H. Shih, Y.-C. Liu, Effective reduction of water molecules' interaction for efficient water evaporation in desalination, *Desalination*, 436 (2018) 91-97.
- [173] R. Chen, Z. Wu, T. Zhang, T. Yu, M. Ye, Magnetically recyclable self-assembled thin films for highly efficient water evaporation by interfacial solar heating, *RSC Advances*, 7 (2017) 19849-19855.
- [174] L. Huang, J. Pei, H. Jiang, X. Hu, Water desalination under one sun using graphene-based material modified PTFE membrane, *Desalination*, 442 (2018) 1-7.

- [175] Y. Shao, Z. Jiang, Y. Zhang, T. Wang, P. Zhao, Z. Zhang, J. Yuan, H. Wang, All-Poly(ionic liquid) Membrane-Derived Porous Carbon Membranes: Scalable Synthesis and Application for Photothermal Conversion in Seawater Desalination, *ACS Nano*, 12 (2018) 11704-11710.
- [176] X. Li, W. Xu, M. Tang, L. Zhou, B. Zhu, S. Zhu, J. Zhu, Graphene oxide-based efficient and scalable solar desalination under one sun with a confined 2D water path, *Proceedings of the National Academy of Sciences*, 113 (2016) 13953-13958.
- [177] K.K. Liu, Q. Jiang, S. Tadepalli, R. Raliya, P. Biswas, R.R. Naik, S. Singamaneni, Wood-Graphene Oxide Composite for Highly Efficient Solar Steam Generation and Desalination, *ACS Applied Materials and Interfaces*, 9 (2017) 7675-7681.
- [178] Y. Yang, X. Yang, L. Fu, M. Zou, A. Cao, Y. Du, Q. Yuan, C.-H. Yan, Two-dimensional flexible bilayer Janus membrane for advanced photothermal water desalination, *ACS Energy Letters*, 3 (2018) 1165-1171.
- [179] Q. Gan, T. Zhang, R. Chen, X. Wang, M. Ye, Simple, Low-Dose, Durable, and Carbon-Nanotube-Based Floating Solar Still for Efficient Desalination and Purification, *ACS Sustainable Chemistry and Engineering*, 7 (2019) 3925-3932.
- [180] L. Zhu, M. Gao, C.K.N. Peh, X. Wang, G.W. Ho, Self-Contained Monolithic Carbon Sponges for Solar-Driven Interfacial Water Evaporation Distillation and Electricity Generation, *Advanced Energy Materials*, 8 (2018) 1702149.
- [181] H.M. Wilson, S.R. AR, A.E. Parab, N. Jha, Ultra-low cost cotton based solar evaporation device for seawater desalination and waste water purification to produce drinkable water, *Desalination*, 456 (2019) 85-96.
- [182] H. Raether, *Surface plasmons on smooth and rough surfaces and on gratings*, Springer-Verlag Berlin An, 2013.
- [183] M. Gao, L. Zhu, C.K. Peh, G.W. Ho, Solar absorber material and system designs for photothermal water vaporization towards clean water and energy production, *Energy & Environmental Science*, 12 (2019) 841-864.
- [184] L. Zhou, Y. Tan, J. Wang, W. Xu, Y. Yuan, W. Cai, S. Zhu, J. Zhu, 3D self-assembly of aluminium nanoparticles for plasmon-enhanced solar desalination, *Nature Photonics*, 10 (2016) 393.
- [185] M. Zhu, Y. Li, F. Chen, X. Zhu, J. Dai, Y. Li, Z. Yang, X. Yan, J. Song, Y. Wang, Plasmonic Wood for High-Efficiency Solar Steam Generation, *Advanced Energy Materials*, 8 (2018) 1701028.
- [186] M.S. Zielinski, J.-W. Choi, T. La Grange, M. Modestino, S.M.H. Hashemi, Y. Pu, S. Birkhold, J.A. Hubbell, D. Psaltis, Hollow mesoporous plasmonic nanoshells for enhanced solar vapor generation, *Nano Letters*, 16 (2016) 2159-2167.
- [187] H.D. Kiriarachchi, F.S. Awad, A.A. Hassan, J.A. Bobb, A. Lin, M.S. El-Shall, Plasmonic chemically modified cotton nanocomposite fibers for efficient solar water desalination and wastewater treatment, *Nanoscale*, 10 (2018) 18531-18539.
- [188] L. Yi, S. Ci, S. Luo, P. Shao, Y. Hou, Z. Wen, Scalable and low-cost synthesis of black amorphous Al-Ti-O nanostructure for high-efficient photothermal desalination, *Nano Energy*, 41 (2017) 600-608.
- [189] F. Alnaimat, E. Alhseinat, F. Banat, V. Mittal, Electromagnetic-mechanical desalination: Mathematical modeling, *Desalination*, 380 (2016) 75-84.
- [190] H.B. Han, B. Guo, F. Chai, Influence of magnetic field on aqueous nacl solutions: A foundational research on the desalination method based on the rotating electromagnetic effect, in: *Advanced Materials Research*, 2012, pp. 2607-2611.
- [191] T.Y. Cath, A.E. Childress, M. Elimelech, Forward osmosis: Principles, applications, and recent developments, *Journal of Membrane Science*, 281 (2006) 70-87.
- [192] L. Chekli, S. Phuntsho, H.K. Shon, S. Vigneswaran, J. Kandasamy, A. Chanan, A review of draw solutes in forward osmosis process and their use in modern applications, *Desalination and Water Treatment*, 43 (2012) 167-184.
- [193] Y. Cai, A critical review on draw solutes development for forward osmosis, *Desalination*, 391 (2016) 16-29.
- [194] N. Lubick, Tiny filters fix big water problems, *Environmental Science & Technology*, 41 (2007) 4495-4496.
- [195] Y. Na, S. Yang, S. Lee, Evaluation of citrate-coated magnetic nanoparticles as draw solute for forward osmosis, *Desalination*, 347 (2014) 34-42.
- [196] J. Lu, N. Liu, L. Li, R. Lee, Organic fouling and regeneration of zeolite membrane in wastewater treatment, *Separation and Purification Technology*, 72 (2010) 203-207.
- [197] H. Bai, Z. Liu, D.D. Sun, Highly water soluble and recovered dextran coated Fe₃O₄ magnetic nanoparticles for brackish water desalination, *Separation and Purification Technology*, 81 (2011) 392-399.

- [198] Q. Ge, J. Su, T.-S. Chung, G. Amy, Hydrophilic Superparamagnetic Nanoparticles: Synthesis, Characterization, and Performance in Forward Osmosis Processes, *Industrial & Engineering Chemistry Research*, 50 (2011) 382-388.
- [199] P. Dey, E.L. Izake, Magnetic nanoparticles boosting the osmotic efficiency of a polymeric FO draw agent: Effect of polymer conformation, *Desalination*, 373 (2015) 79-85.
- [200] Q. Zhao, N. Chen, D. Zhao, X. Lu, Thermoresponsive magnetic nanoparticles for seawater desalination, *ACS Applied Materials and Interfaces*, 5 (2013) 11453-11461.
- [201] M.M. Ling, T.-S. Chung, X. Lu, Facile synthesis of thermosensitive magnetic nanoparticles as "smart" draw solutes in forward osmosis, *Chemical Communications*, 47 (2011) 10788-10790.
- [202] Z. Liu, H. Bai, J. Lee, D.D. Sun, A low-energy forward osmosis process to produce drinking water, *Energy & Environmental Science*, 4 (2011) 2582-2585.
- [203] Q. Ge, J. Su, G.L. Amy, T.-S. Chung, Exploration of polyelectrolytes as draw solutes in forward osmosis processes, *Water Research*, 46 (2012) 1318-1326.
- [204] H.G. Schild, Poly (N-isopropylacrylamide): experiment, theory and application, *Progress in polymer science*, 17 (1992) 163-249.
- [205] A. Razmjou, M.R. Barati, G.P. Simon, K. Suzuki, H. Wang, Fast deswelling of nanocomposite polymer hydrogels via magnetic field-induced heating for emerging FO desalination, *Environmental Science and Technology*, 47 (2013) 6297-6305.
- [206] M.M. Ling, K.Y. Wang, T.-S. Chung, Highly Water-Soluble Magnetic Nanoparticles as Novel Draw Solutes in Forward Osmosis for Water Reuse, *Industrial & Engineering Chemistry Research*, 49 (2010) 5869-5876.
- [207] Q. Ge, L. Yang, J. Cai, W. Xu, Q. Chen, M. Liu, Hydroacid magnetic nanoparticles in forward osmosis for seawater desalination and efficient regeneration via integrated magnetic and membrane separations, *Journal of Membrane Science*, 520 (2016) 550-559.
- [208] M.M. Ling, T.-S. Chung, Desalination process using super hydrophilic nanoparticles via forward osmosis integrated with ultrafiltration regeneration, *Desalination*, 278 (2011) 194-202.
- [209] W. Jie, Y. Sa-Sa, L. Wen-Bin, Q. Long-Sheng, W. Gen-Shi, T. Zheng-Yuan, Application of magnetic enhanced coagulation ultrafiltration in seawater pretreatment for RO desalination, *Journal of Tianjin Polytechnic University*, 35 (2016) 61-66.
- [210] J. Wang, S.S. Yang, H. Jia, L.L. Liu, C.M. Mun, G. Yang, S.N. Guo, J.D. Bai, Magnetic flocculation technology in turbidity removal of high turbidity seawater for desalination pretreatment, *Journal of Tianjin Polytechnic University*, 34 (2015) 18-21.
- [211] R. Gehr, Z.A. Zhai, J.A. Finch, S.R. Rao, Reduction of soluble mineral concentrations in CaSO₄ saturated water using a magnetic field, *Water Research*, 29 (1995) 933-940.
- [212] C. Gabrielli, R. Jaouhari, G. Maurin, M. Keddam, Magnetic water treatment for scale prevention, *Water Research*, 35 (2001) 3249-3259.
- [213] A. Kney, S. Parsons, A spectrophotometer-based study of magnetic water treatment: Assessment of ionic vs. surface mechanisms, *Water research*, 40 (2006) 517-524.
- [214] I.B.S. Sayadi, P. Sstat, M.M. Tlili, Assess of physical antiscalant-treatments on conventional electro dialysis pilot unit during brackish water desalination, *Chemical Engineering and Processing: Process Intensification*, 88 (2015) 47-57.
- [215] M.A. Salman, G. Al-Nuwaibit, M. Safar, A. Al-Mesri, Performance of physical treatment method and different commercial antiscalants to control scaling deposition in desalination plant, *Desalination*, 369 (2015) 18-25.
- [216] S. Kobe, G. Dražić, A.C. Cefalas, E. Sarantopoulou, J. Stražičar, Nucleation and crystallization of CaCO₃ in applied magnetic fields, *Crystal Engineering*, 5 (2002) 243-253.
- [217] I.B. Silva, J.C.Q. Neto, D.F. Petri, The effect of magnetic field on ion hydration and sulfate scale formation, *Colloids and Surfaces A: Physicochemical and Engineering Aspects*, 465 (2015) 175-183.
- [218] K.W. Smothers, C.D. Curtiss, B.T. Gard, R.H. Strauss, V.F. Hock, Demonstration and Evaluation of Magnetic Descalers, in, *ENGINEER RESEARCH AND DEVELOPMENT CENTER CHAMPAIGN IL CONSTRUCTION ...*, 2001.
- [219] H. Al-Qahtani, Effect of magnetic treatment on Gulf seawater, *Desalination*, 107 (1996) 75-81.
- [220] D. Hasson, D. Bramson, Effectiveness of Magnetic Water Treatment in Suppressing CaCO₃ Scale Deposition, *Industrial and Engineering Chemistry Process Design and Development*, 24 (1985) 588-592.
- [221] X. Wang, G. Ou, N. Wang, H. Wu, Graphene-based Recyclable Photo-Absorbers for High-Efficiency Seawater Desalination, *ACS Applied Materials & Interfaces*, 8 (2016) 9194-9199.

- [222] H. Sodaye, S. Nisan, C. Poletiko, S. Prabhakar, P.K. Tewari, Extraction of uranium from the concentrated brine rejected by integrated nuclear desalination plants, *Desalination*, 235 (2009) 9-32.
- [223] R.M. Donlan, Biofilms: microbial life on surfaces, *Emerging infectious diseases*, 8 (2002) 881.
- [224] J. Baker, L. Dudley, Biofouling in membrane systems—a review, *Desalination*, 118 (1998) 81-89.
- [225] A. Matin, Z. Khan, S.M.J. Zaidi, M.C. Boyce, Biofouling in reverse osmosis membranes for seawater desalination: Phenomena and prevention, *Desalination*, 281 (2011) 1-16.
- [226] M.J. Hajipour, K.M. Fromm, A. Akbar Ashkarran, D. Jimenez de Aberasturi, I.R.d. Larramendi, T. Rojo, V. Serpooshan, W.J. Parak, M. Mahmoudi, Antibacterial properties of nanoparticles, *Trends in Biotechnology*, 30 (2012) 499-511.
- [227] S.J. Soenen, P. Rivera-Gil, J.-M. Montenegro, W.J. Parak, S.C. De Smedt, K. Braeckmans, Cellular toxicity of inorganic nanoparticles: Common aspects and guidelines for improved nanotoxicity evaluation, *Nano Today*, 6 (2011) 446-465.
- [228] M. Ulbricht, G. Belfort, Surface modification of ultrafiltration membranes by low temperature plasma II. Graft polymerization onto polyacrylonitrile and polysulfone, *Journal of Membrane Science*, 111 (1996) 193-215.
- [229] Q. Li, X. Pan, Z. Qu, X. Zhao, Y. Jin, H. Dai, B. Yang, X. Wang, Understanding the dependence of contact angles of commercially RO membranes on external conditions and surface features, *Desalination*, 309 (2013) 38-45.
- [230] S. Belfer, R. Fainchtain, Y. Purinson, O. Kedem, Surface characterization by FTIR-ATR spectroscopy of polyethersulfone membranes—unmodified, modified and protein fouled, *Journal of Membrane Science*, 172 (2000) 113-124.
- [231] M.N. Abu Seman, M. Khayet, N. Hilal, Development of antifouling properties and performance of nanofiltration membranes modified by interfacial polymerisation, *Desalination*, 273 (2011) 36-47.
- [232] N. Misdan, A.F. Ismail, N. Hilal, Recent advances in the development of (bio)fouling resistant thin film composite membranes for desalination, *Desalination*, 380 (2016) 105-111.
- [233] F. Perreault, A.F. de Faria, S. Nejati, M. Elimelech, Antimicrobial Properties of Graphene Oxide Nanosheets: Why Size Matters, *ACS Nano*, 9 (2015) 7226-7236.
- [234] J.R. Morones, J.L. Elechiguerra, A. Camacho, K. Holt, J.B. Kouri, J.T. Ramirez, M.J. Yacaman, The bactericidal effect of silver nanoparticles, *Nanotechnology*, 16 (2005) 2346.
- [235] S. Kang, M. Pinault, L.D. Pfefferle, M. Elimelech, Single-Walled Carbon Nanotubes Exhibit Strong Antimicrobial Activity, *Langmuir*, 23 (2007) 8670-8673.
- [236] M. Cho, H. Chung, W. Choi, J. Yoon, Different inactivation behaviors of MS-2 phage and *Escherichia coli* in TiO₂ photocatalytic disinfection, *Appl. Environ. Microbiol.*, 71 (2005) 270-275.
- [237] K. Balasubramanian, Antibacterial application of polyvinylalcohol-nanogold composite membranes, *Colloids and Surfaces A: Physicochemical and Engineering Aspects*, 455 (2014) 174-178.
- [238] H.-Y. Wang, X.-W. Hua, F.-G. Wu, B. Li, P. Liu, N. Gu, Z. Wang, Z. Chen, Synthesis of ultrastable copper sulfide nanoclusters via trapping the reaction intermediate: potential anticancer and antibacterial applications, *ACS applied materials & interfaces*, 7 (2015) 7082-7092.
- [239] J. Zhu, J. Hou, Y. Zhang, M. Tian, T. He, J. Liu, V. Chen, Polymeric Antimicrobial Membranes Enabled by Nanomaterials for Water Treatment, 2017.
- [240] M. Toroghi, A. Raisi, A. Aroujalian, Preparation and characterization of polyethersulfone/silver nanocomposite ultrafiltration membrane for antibacterial applications, *Polymers for Advanced Technologies*, 25 (2014) 711-722.
- [241] L.-J. Zhu, L.-P. Zhu, Z. Yi, J.-H. Jiang, B.-K. Zhu, Y.-Y. Xu, Hemocompatible and antibacterial porous membranes with heparinized copper hydroxide nanofibers as separation layer, *Colloids and Surfaces B: Biointerfaces*, 110 (2013) 36-44.
- [242] I. Sawada, R. Fachrul, T. Ito, Y. Ohmukai, T. Maruyama, H. Matsuyama, Development of a hydrophilic polymer membrane containing silver nanoparticles with both organic antifouling and antibacterial properties, *Journal of Membrane Science*, 387-388 (2012) 1-6.
- [243] X. Liu, S. Qi, Y. Li, L. Yang, B. Cao, C.Y. Tang, Synthesis and characterization of novel antibacterial silver nanocomposite nanofiltration and forward osmosis membranes based on layer-by-layer assembly, *Water Research*, 47 (2013) 3081-3092.
- [244] M. Mukherjee, S. De, Antibacterial polymeric membranes: a short review, *Environmental Science: Water Research & Technology*, 4 (2018) 1078-1104.

- [245] M. Sile-Yuksel, B. Tas, D.Y. Koseoglu-Imer, I. Koyuncu, Effect of silver nanoparticle (AgNP) location in nanocomposite membrane matrix fabricated with different polymer type on antibacterial mechanism, *Desalination*, 347 (2014) 120-130.
- [246] A.Y. Booshehri, R. Wang, R. Xu, The effect of re-generable silver nanoparticles/multi-walled carbon nanotubes coating on the antibacterial performance of hollow fiber membrane, *Chemical engineering journal*, 230 (2013) 251-259.
- [247] L. Su, Y. Yu, Y. Zhao, F. Liang, X. Zhang, Strong antibacterial polydopamine coatings prepared by a shaking-assisted method, *Scientific reports*, 6 (2016) 24420.
- [248] L. He, L.F. Dumée, C. Feng, L. Velleman, R. Reis, F. She, W. Gao, L. Kong, Promoted water transport across graphene oxide–poly(amide) thin film composite membranes and their antibacterial activity, *Desalination*, 365 (2015) 126-135.
- [249] C. Cheng, A. He, C. Nie, Y. Xia, C. He, L. Ma, C. Zhao, One-pot cross-linked copolymerization for the construction of robust antifouling and antibacterial composite membranes, *Journal of Materials Chemistry B*, 3 (2015) 4170-4180.
- [250] G. Franci, A. Falanga, S. Galdiero, L. Palomba, M. Rai, G. Morelli, M. Galdiero, Silver nanoparticles as potential antibacterial agents, *Molecules*, 20 (2015) 8856-8874.
- [251] Q.L. Feng, J. Wu, G. Chen, F. Cui, T. Kim, J. Kim, A mechanistic study of the antibacterial effect of silver ions on *Escherichia coli* and *Staphylococcus aureus*, *Journal of biomedical materials research*, 52 (2000) 662-668.
- [252] K. Zodrow, L. Brunet, S. Mahendra, D. Li, A. Zhang, Q. Li, P.J.J. Alvarez, Polysulfone ultrafiltration membranes impregnated with silver nanoparticles show improved biofouling resistance and virus removal, *Water Research*, 43 (2009) 715-723.
- [253] J. Yin, Y. Yang, Z. Hu, B. Deng, Attachment of silver nanoparticles (AgNPs) onto thin-film composite (TFC) membranes through covalent bonding to reduce membrane biofouling, *Journal of Membrane Science*, 441 (2013) 73-82.
- [254] M.S. Rahaman, H. Thérien-Aubin, M. Ben-Sasson, C.K. Ober, M. Nielsen, M. Elimelech, Control of biofouling on reverse osmosis polyamide membranes modified with biocidal nanoparticles and antifouling polymer brushes, *Journal of Materials Chemistry B*, 2 (2014) 1724-1732.
- [255] Z. Yang, Y. Wu, J. Wang, B. Cao, C.Y. Tang, In Situ Reduction of Silver by Polydopamine: A Novel Antimicrobial Modification of a Thin-Film Composite Polyamide Membrane, *Environmental Science & Technology*, 50 (2016) 9543-9550.
- [256] H.-L. Yang, J.C.-T. Lin, C. Huang, Application of nanosilver surface modification to RO membrane and spacer for mitigating biofouling in seawater desalination, *Water Research*, 43 (2009) 3777-3786.
- [257] D.Y. Zhang, J. Liu, Y.S. Shi, Y. Wang, H.F. Liu, Q.L. Hu, L. Su, J. Zhu, Antifouling polyimide membrane with surface-bound silver particles, *Journal of Membrane Science*, 516 (2016) 83-93.
- [258] M. Zhang, R.W. Field, K. Zhang, Biogenic silver nanocomposite polyethersulfone UF membranes with antifouling properties, *Journal of Membrane Science*, 471 (2014) 274-284.
- [259] M. Hu, K. Zhong, Y. Liang, S.H. Ehrman, B. Mi, Effects of Particle Morphology on the Antibiofouling Performance of Silver Embedded Polysulfone Membranes and Rate of Silver Leaching, *Industrial & Engineering Chemistry Research*, 56 (2017) 2240-2246.
- [260] A. Mollahosseini, A. Rahimpour, A new concept in polymeric thin-film composite nanofiltration membranes with antibacterial properties, *Biofouling*, 29 (2013) 537-548.
- [261] E. Ozkan, C.C. Crick, A. Taylor, E. Allan, I.P. Parkin, Copper-based water repellent and antibacterial coatings by aerosol assisted chemical vapour deposition, *Chemical Science*, 7 (2016) 5126-5131.
- [262] J.-H. Qiu, Y.-W. Zhang, Y.-T. Zhang, H.-Q. Zhang, J.-D. Liu, Synthesis and antibacterial activity of copper-immobilized membrane comprising grafted poly(4-vinylpyridine) chains, *Journal of Colloid and Interface Science*, 354 (2011) 152-159.
- [263] R. Hausman, T. Gullinkala, I.C. Escobar, Development of copper-charged polypropylene feedspacers for biofouling control, *Journal of Membrane Science*, 358 (2010) 114-121.
- [264] M. Arsalan, Fabrication, characterization, transportation of ions and antibacterial potential of polystyrene based Cu₃(PO₄)₂/Ni₃(PO₄)₂ composite membrane, *Journal of Industrial and Engineering Chemistry*, 20 (2014) 3568-3577.

- [265] W. Ma, A. Soroush, T.V.A. Luong, M.S. Rahaman, Cysteamine- and graphene oxide-mediated copper nanoparticle decoration on reverse osmosis membrane for enhanced anti-microbial performance, *Journal of Colloid and Interface Science*, 501 (2017) 330-340.
- [266] C. Zhao, J. Lv, X. Xu, G. Zhang, Y. Yang, F. Yang, Highly antifouling and antibacterial performance of poly (vinylidene fluoride) ultrafiltration membranes blending with copper oxide and graphene oxide nanofillers for effective wastewater treatment, *Journal of Colloid and Interface Science*, 505 (2017) 341-351.
- [267] J. Zhu, J. Wang, A.A. Uliana, M. Tian, Y. Zhang, Y. Zhang, A. Volodin, K. Simoens, S. Yuan, J. Li, J. Lin, K. Bernaerts, B. Van der Bruggen, Mussel-Inspired Architecture of High-Flux Loose Nanofiltration Membrane Functionalized with Antibacterial Reduced Graphene Oxide–Copper Nanocomposites, *ACS Applied Materials & Interfaces*, 9 (2017) 28990-29001.
- [268] A.K. Chatterjee, R. Chakraborty, T. Basu, Mechanism of antibacterial activity of copper nanoparticles, *Nanotechnology*, 25 (2014) 135101.
- [269] L. Duan, Q. Zhao, J. Liu, Y. Zhang, Antibacterial behavior of halloysite nanotubes decorated with copper nanoparticles in a novel mixed matrix membrane for water purification, *Environmental Science: Water Research & Technology*, 1 (2015) 874-881.
- [270] A. Zhang, Y. Zhang, G. Pan, J. Xu, H. Yan, Y. Liu, In situ formation of copper nanoparticles in carboxylated chitosan layer: Preparation and characterization of surface modified TFC membrane with protein fouling resistance and long-lasting antibacterial properties, *Separation and Purification Technology*, 176 (2017) 164-172.
- [271] J. Xu, X. Feng, P. Chen, C. Gao, Development of an antibacterial copper (II)-chelated polyacrylonitrile ultrafiltration membrane, *Journal of Membrane Science*, 413-414 (2012) 62-69.
- [272] M. Ben-Sasson, K.R. Zodrow, Q. Genggeng, Y. Kang, E.P. Giannelis, M. Elimelech, Surface Functionalization of Thin-Film Composite Membranes with Copper Nanoparticles for Antimicrobial Surface Properties, *Environmental Science & Technology*, 48 (2014) 384-393.
- [273] W. Ma, A. Soroush, T. Van Anh Luong, G. Brennan, M.S. Rahaman, B. Asadishad, N. Tufenkji, Spray- and spin-assisted layer-by-layer assembly of copper nanoparticles on thin-film composite reverse osmosis membrane for biofouling mitigation, *Water Research*, 99 (2016) 188-199.
- [274] K. Rasool, K.A. Mahmoud, D.J. Johnson, M. Helal, G.R. Berdiyrov, Y. Gogotsi, Efficient antibacterial membrane based on two-dimensional Ti₃C₂T_x (MXene) nanosheets, *Scientific reports*, 7 (2017) 1598.
- [275] M. Li, L. Zhu, D. Lin, Toxicity of ZnO Nanoparticles to *Escherichia coli*: Mechanism and the Influence of Medium Components, *Environmental Science & Technology*, 45 (2011) 1977-1983.
- [276] L.-H. Li, J.-C. Deng, H.-R. Deng, Z.-L. Liu, L. Xin, Synthesis and characterization of chitosan/ZnO nanoparticle composite membranes, *Carbohydrate Research*, 345 (2010) 994-998.
- [277] H. Yu, X. Zhang, Y. Zhang, J. Liu, H. Zhang, Development of a hydrophilic PES ultrafiltration membrane containing SiO₂@ N-Halamine nanoparticles with both organic antifouling and antibacterial properties, *Desalination*, 326 (2013) 69-76.
- [278] Y.-F. Zhao, L.-P. Zhu, Z. Yi, B.-K. Zhu, Y.-Y. Xu, Improving the hydrophilicity and fouling-resistance of polysulfone ultrafiltration membranes via surface zwitterionization mediated by polysulfone-based triblock copolymer additive, *Journal of membrane science*, 440 (2013) 40-47.
- [279] G. Ye, J. Lee, F.o. Perreault, M. Elimelech, Controlled architecture of dual-functional block copolymer brushes on thin-film composite membranes for integrated “defending” and “attacking” strategies against biofouling, *ACS applied materials & interfaces*, 7 (2015) 23069-23079.
- [280] F. Perreault, M.E. Tousley, M. Elimelech, Thin-Film Composite Polyamide Membranes Functionalized with Biocidal Graphene Oxide Nanosheets, *Environmental Science & Technology Letters*, 1 (2014) 71-76.
- [281] J. Zhu, J. Wang, J. Hou, Y. Zhang, J. Liu, B. Van der Bruggen, Graphene-based antimicrobial polymeric membranes: a review, *Journal of Materials Chemistry A*, 5 (2017) 6776-6793.
- [282] R. Zhang, Y. Liu, M. He, Y. Su, X. Zhao, M. Elimelech, Z. Jiang, Antifouling membranes for sustainable water purification: strategies and mechanisms, *Chemical Society Reviews*, 45 (2016) 5888-5924.
- [283] I.E. Mejías Carpio, C.M. Santos, X. Wei, D.F. Rodrigues, Toxicity of a polymer–graphene oxide composite against bacterial planktonic cells, biofilms, and mammalian cells, *Nanoscale*, 4 (2012) 4746-4756.
- [284] Y. Tu, M. Lv, P. Xiu, T. Huynh, M. Zhang, M. Castelli, Z. Liu, Q. Huang, C. Fan, H. Fang, R. Zhou, Destructive extraction of phospholipids from *Escherichia coli* membranes by graphene nanosheets, *Nature Nanotechnology*, 8 (2013) 594.

- [285] W. Choi, J. Choi, J. Bang, J.-H. Lee, Layer-by-Layer Assembly of Graphene Oxide Nanosheets on Polyamide Membranes for Durable Reverse-Osmosis Applications, *ACS Applied Materials & Interfaces*, 5 (2013) 12510-12519.
- [286] Z. Zeng, D. Yu, Z. He, J. Liu, F.-X. Xiao, Y. Zhang, R. Wang, D. Bhattacharyya, T.T.Y. Tan, Graphene oxide quantum dots covalently functionalized PVDF membrane with significantly-enhanced bactericidal and antibiofouling performances, *Scientific reports*, 6 (2016) 20142.
- [287] X. Lu, X. Feng, X. Zhang, M.N. Chukwu, C.O. Osuji, M. Elimelech, Fabrication of a Desalination Membrane with Enhanced Microbial Resistance through Vertical Alignment of Graphene Oxide, *Environmental Science & Technology Letters*, 5 (2018) 614-620.
- [288] J.R. Ray, S. Tadepalli, S.Z. Nergiz, K.-K. Liu, L. You, Y. Tang, S. Singamaneni, Y.-S. Jun, Hydrophilic, bactericidal nanoheater-enabled reverse osmosis membranes to improve fouling resistance, *ACS applied materials & interfaces*, 7 (2015) 11117-11126.
- [289] Y. Li, H. Yuan, A. Von Dem Bussche, M. Creighton, R.H. Hurt, A.B. Kane, H. Gao, Graphene microsheets enter cells through spontaneous membrane penetration at edge asperities and corner sites, *Proceedings of the National Academy of Sciences*, 110 (2013) 12295-12300.
- [290] J. Mao, R. Guo, L.-T. Yan, Simulation and analysis of cellular internalization pathways and membrane perturbation for graphene nanosheets, *Biomaterials*, 35 (2014) 6069-6077.
- [291] A. de Leon, On the antibacterial mechanism of graphene oxide (GO) Langmuir–Blodgett films, *Chemical communications*, 51 (2015) 2886-2889.
- [292] L. Hui, J.-G. Piao, J. Auletta, K. Hu, Y. Zhu, T. Meyer, H. Liu, L. Yang, Availability of the basal planes of graphene oxide determines whether it is antibacterial, *ACS applied materials & interfaces*, 6 (2014) 13183-13190.
- [293] S. Liu, M. Hu, T.H. Zeng, R. Wu, R. Jiang, J. Wei, L. Wang, J. Kong, Y. Chen, Lateral dimension-dependent antibacterial activity of graphene oxide sheets, *Langmuir*, 28 (2012) 12364-12372.
- [294] Y.L.F. Musico, C.M. Santos, M.L.P. Dalida, D.F. Rodrigues, Surface modification of membrane filters using graphene and graphene oxide-based nanomaterials for bacterial inactivation and removal, *ACS Sustainable Chemistry & Engineering*, 2 (2014) 1559-1565.
- [295] S. Gurunathan, J.W. Han, A.A. Dayem, V. Eppakayala, J.-H. Kim, Oxidative stress-mediated antibacterial activity of graphene oxide and reduced graphene oxide in *Pseudomonas aeruginosa*, *International journal of nanomedicine*, 7 (2012) 5901.
- [296] J. Chen, H. Peng, X. Wang, F. Shao, Z. Yuan, H. Han, Graphene oxide exhibits broad-spectrum antimicrobial activity against bacterial phytopathogens and fungal conidia by intertwining and membrane perturbation, *Nanoscale*, 6 (2014) 1879-1889.
- [297] K.A. Mahmoud, B. Mansoor, A. Mansour, M. Khraisheh, Functional graphene nanosheets: The next generation membranes for water desalination, *Desalination*, 356 (2015) 208-225.
- [298] X. Huang, K.L. Marsh, B.T. McVerry, E.M. Hoek, R.B. Kaner, Low-fouling antibacterial reverse osmosis membranes via surface grafting of graphene oxide, *ACS applied materials & interfaces*, 8 (2016) 14334-14338.
- [299] M.-Y. Lim, Y.-S. Choi, J. Kim, K. Kim, H. Shin, J.-J. Kim, D.M. Shin, J.-C. Lee, Cross-linked graphene oxide membrane having high ion selectivity and antibacterial activity prepared using tannic acid-functionalized graphene oxide and polyethyleneimine, *Journal of Membrane Science*, 521 (2017) 1-9.
- [300] S. Kang, M. Herzberg, D.F. Rodrigues, M. Elimelech, Antibacterial effects of carbon nanotubes: size does matter!, *Langmuir*, 24 (2008) 6409-6413.
- [301] C. Yang, J. Mamouni, Y. Tang, L. Yang, Antimicrobial Activity of Single-Walled Carbon Nanotubes: Length Effect, *Langmuir*, 26 (2010) 16013-16019.
- [302] C.D. Vecitis, K.R. Zodrow, S. Kang, M. Elimelech, Electronic-Structure-Dependent Bacterial Cytotoxicity of Single-Walled Carbon Nanotubes, *ACS Nano*, 4 (2010) 5471-5479.
- [303] F. Zhao, F. Qiu, X. Zhang, S. Yu, H.-S. Kim, H.-D. Park, S. Takizawa, P. Wang, Preparation of single-walled carbon nanotubes/polyvinylchloride membrane and its antibacterial property, *Water Science and Technology*, 66 (2012) 2275-2283.
- [304] Y. Yang, C. Nie, Y. Deng, C. Cheng, C. He, L. Ma, C. Zhao, Improved antifouling and antimicrobial efficiency of ultrafiltration membranes with functional carbon nanotubes, *RSC Advances*, 6 (2016) 88265-88276.
- [305] H.J. Kim, Y. Baek, K. Choi, D.-G. Kim, H. Kang, Y.-S. Choi, J. Yoon, J.-C. Lee, The improvement of antibiofouling properties of a reverse osmosis membrane by oxidized CNTs, *RSC Advances*, 4 (2014) 32802-32810.

- [306] P. Gunawan, C. Guan, X. Song, Q. Zhang, S.S.J. Leong, C. Tang, Y. Chen, M.B. Chan-Park, M.W. Chang, K. Wang, R. Xu, Hollow Fiber Membrane Decorated with Ag/MWNTs: Toward Effective Water Disinfection and Biofouling Control, *ACS Nano*, 5 (2011) 10033-10040.
- [307] E. Rusen, A. Mocanu, L.C. Nistor, A. Dinescu, I. Călinescu, G. Mustățea, Ș.I. Voicu, C. Andronescu, A. Diacon, Design of Antimicrobial Membrane Based on Polymer Colloids/Multiwall Carbon Nanotubes Hybrid Material with Silver Nanoparticles, *ACS Applied Materials & Interfaces*, 6 (2014) 17384-17393.
- [308] S. Al Aani, V. Gomez, C.J. Wright, N. Hilal, Fabrication of antibacterial mixed matrix nanocomposite membranes using hybrid nanostructure of silver coated multi-walled carbon nanotubes, *Chemical Engineering Journal*, 326 (2017) 721-736.
- [309] L. Qi, Z. Xu, X. Jiang, C. Hu, X. Zou, Preparation and antibacterial activity of chitosan nanoparticles, *Carbohydrate Research*, 339 (2004) 2693-2700.
- [310] E.I. Cadogan, C.-H. Lee, S.R. Popuri, H.-Y. Lin, Effect of Solvent on Physico-Chemical Properties and Antibacterial Activity of Chitosan Membranes, *International Journal of Polymeric Materials and Polymeric Biomaterials*, 63 (2014) 708-715.
- [311] G. Ye, J. Lee, F. Perreault, M. Elimelech, Controlled Architecture of Dual-Functional Block Copolymer Brushes on Thin-Film Composite Membranes for Integrated "Defending" and "Attacking" Strategies against Biofouling, *ACS Applied Materials & Interfaces*, 7 (2015) 23069-23079.
- [312] C. Liu, A.F. Faria, J. Ma, M. Elimelech, Mitigation of Biofilm Development on Thin-Film Composite Membranes Functionalized with Zwitterionic Polymers and Silver Nanoparticles, *Environmental Science & Technology*, 51 (2017) 182-191.
- [313] L. Zhang, J. Xu, Y. Tang, J. Hou, L. Yu, C. Gao, A novel long-lasting antifouling membrane modified with bifunctional capsaicin-mimic moieties via in situ polymerization for efficient water purification, *Journal of Materials Chemistry A*, 4 (2016) 10352-10362.
- [314] J. Wang, X. Gao, Q. Wang, H. Sun, X. Wang, C. Gao, Enhanced biofouling resistance of polyethersulfone membrane surface modified with capsaicin derivative and itaconic acid, *Applied Surface Science*, 356 (2015) 467-474.
- [315] C. Yao, X. Li, K.G. Neoh, Z. Shi, E.T. Kang, Surface modification and antibacterial activity of electrospun polyurethane fibrous membranes with quaternary ammonium moieties, *Journal of Membrane Science*, 320 (2008) 259-267.
- [316] L. Duan, W. Huang, Y. Zhang, High-flux, antibacterial ultrafiltration membranes by facile blending with N-halamine grafted halloysite nanotubes, *RSC Advances*, 5 (2015) 6666-6674.
- [317] F. Yao, G.-D. Fu, J. Zhao, E.-T. Kang, K.G. Neoh, Antibacterial effect of surface-functionalized polypropylene hollow fiber membrane from surface-initiated atom transfer radical polymerization, *Journal of Membrane Science*, 319 (2008) 149-157.
- [318] F. Liu, B. Qin, L. He, R. Song, Novel starch/chitosan blending membrane: Antibacterial, permeable and mechanical properties, *Carbohydrate Polymers*, 78 (2009) 146-150.
- [319] Y. Sun, Y. Liu, Y. Li, M. Lv, P. Li, H. Xu, L. Wang, Preparation and characterization of novel curdlan/chitosan blending membranes for antibacterial applications, *Carbohydrate Polymers*, 84 (2011) 952-959.
- [320] M. Prama Ekaputra, M.M. Munir, A. Rajak, A. Rahma, A.Y. Nuryantini, Synthesis of antibacterial nanofibrous membrane based on polyacrylonitrile (PAN)/chitosan by electrospinning technique for water purification application, in: *Advanced Materials Research*, Trans Tech Publ, 2015, pp. 76-79.
- [321] A. Cooper, R. Oldinski, H. Ma, J.D. Bryers, M. Zhang, Chitosan-based nanofibrous membranes for antibacterial filter applications, *Carbohydrate Polymers*, 92 (2013) 254-259.
- [322] J. Xu, X. Feng, J. Hou, X. Wang, B. Shan, L. Yu, C. Gao, Preparation and characterization of a novel polysulfone UF membrane using a copolymer with capsaicin-mimic moieties for improved anti-fouling properties, *Journal of Membrane Science*, 446 (2013) 171-180.
- [323] A.B. Rostam, M. Peyravi, M. Ghorbani, M. Jahanshahi, Antibacterial surface modified of novel nanocomposite sulfonated polyethersulfone/polyrhodanine membrane, *Applied Surface Science*, 427 (2018) 17-28.
- [324] S. Kappachery, D. Paul, J.H. Kweon, Effect of N-acetylcysteine against biofouling of reverse osmosis membrane, *Desalination*, 285 (2012) 184-187.
- [325] A. Bera, R.M. Gol, S. Chatterjee, S.K. Jewrajka, PEGylation and incorporation of triazine ring into thin film composite reverse osmosis membranes for enhancement of anti-organic and anti-biofouling properties, *Desalination*, 360 (2015) 108-117.

- [326] Y. Pan, L. Ma, S. Lin, Y. Zhang, B. Cheng, J. Meng, One-step bimodel grafting via a multicomponent reaction toward antifouling and antibacterial TFC RO membranes, *Journal of Materials Chemistry A*, 4 (2016) 15945-15960.
- [327] C. Yao, X. Li, K.G. Neoh, Z. Shi, E.T. Kang, Antibacterial activities of surface modified electrospun poly(vinylidene fluoride-co-hexafluoropropylene) (PVDF-HFP) fibrous membranes, *Applied Surface Science*, 255 (2009) 3854-3858.
- [328] E. Mahmoudi, L.Y. Ng, M.M. Ba-Abbad, A.W. Mohammad, Novel nanohybrid polysulfone membrane embedded with silver nanoparticles on graphene oxide nanoplates, *Chemical Engineering Journal*, 277 (2015) 1-10.
- [329] O. Akhavan, M. Abdollahad, Y. Abdi, S. Mohajezadeh, Silver nanoparticles within vertically aligned multi-wall carbon nanotubes with open tips for antibacterial purposes, *Journal of Materials Chemistry*, 21 (2011) 387-393.
- [330] W. Yuan, G. Jiang, J. Che, X. Qi, R. Xu, M.W. Chang, Y. Chen, S.Y. Lim, J. Dai, M.B. Chan-Park, Deposition of Silver Nanoparticles on Multiwalled Carbon Nanotubes Grafted with Hyperbranched Poly(amidoamine) and Their Antimicrobial Effects, *The Journal of Physical Chemistry C*, 112 (2008) 18754-18759.
- [331] Q. Zhao, J. Hou, J. Shen, J. Liu, Y. Zhang, Long-lasting antibacterial behavior of a novel mixed matrix water purification membrane, *Journal of Materials Chemistry A*, 3 (2015) 18696-18705.
- [332] J.-X. Wang, L.-X. Wen, Z.-H. Wang, J.-F. Chen, Immobilization of silver on hollow silica nanospheres and nanotubes and their antibacterial effects, *Materials Chemistry and Physics*, 96 (2006) 90-97.
- [333] Y. Pan, Z. Yu, H. Shi, Q. Chen, G. Zeng, H. Di, X. Ren, Y. He, A novel antifouling and antibacterial surface-functionalized PVDF ultrafiltration membrane via binding Ag/SiO₂ nanocomposites, *Journal of Chemical Technology & Biotechnology*, 92 (2017) 562-572.
- [334] S.-H. Park, Y.-S. Ko, S.-J. Park, J.S. Lee, J. Cho, K.-Y. Baek, I.T. Kim, K. Woo, J.-H. Lee, Immobilization of silver nanoparticle-decorated silica particles on polyamide thin film composite membranes for antibacterial properties, *Journal of Membrane Science*, 499 (2016) 80-91.
- [335] H. Zhang, G. Chen, Potent Antibacterial Activities of Ag/TiO₂ Nanocomposite Powders Synthesized by a One-Pot Sol-Gel Method, *Environmental Science & Technology*, 43 (2009) 2905-2910.
- [336] D. Guin, S.V. Manorama, J.N.L. Latha, S. Singh, Photoreduction of Silver on Bare and Colloidal TiO₂ Nanoparticles/Nanotubes: Synthesis, Characterization, and Tested for Antibacterial Outcome, *The Journal of Physical Chemistry C*, 111 (2007) 13393-13397.
- [337] H. Shi, F. Liu, L. Xue, H. Lu, Q. Zhou, Enhancing antibacterial performances of PVDF hollow fibers by embedding Ag-loaded zeolites on the membrane outer layer via co-extruding technique, *Composites Science and Technology*, 96 (2014) 1-6.
- [338] C. Liao, P. Yu, J. Zhao, L. Wang, Y. Luo, Preparation and characterization of NaY/PVDF hybrid ultrafiltration membranes containing silver ions as antibacterial materials, *Desalination*, 272 (2011) 59-65.
- [339] B. Kwakye-Awuah, C. Williams, M. Kenward, I. Radecka, Antimicrobial action and efficiency of silver-loaded zeolite X, *Journal of Applied Microbiology*, 104 (2008) 1516-1524.
- [340] D.L. Boschetto, L. Lerin, R. Cansian, S.B.C. Pergher, M. Di Luccio, Preparation and antimicrobial activity of polyethylene composite films with silver exchanged zeolite-Y, *Chemical Engineering Journal*, 204-206 (2012) 210-216.
- [341] H. Shi, F. Liu, L. Xue, Fabrication and characterization of antibacterial PVDF hollow fibre membrane by doping Ag-loaded zeolites, *Journal of Membrane Science*, 437 (2013) 205-215.
- [342] L. Ferreira, A.M. Fonseca, G. Botelho, C.A. Aguiar, I.C. Neves, Antimicrobial activity of faujasite zeolites doped with silver, *Microporous and Mesoporous Materials*, 160 (2012) 126-132.
- [343] S. Demirci, Z. Ustaoglu, G.A. Yilmazer, F. Sahin, N. Baç, Antimicrobial properties of zeolite-X and zeolite-A ion-exchanged with silver, copper, and zinc against a broad range of microorganisms, *Applied biochemistry and biotechnology*, 172 (2014) 1652-1662.
- [344] J. Li, X. Liu, J. Lu, Y. Wang, G. Li, F. Zhao, Anti-bacterial properties of ultrafiltration membrane modified by graphene oxide with nano-silver particles, *Journal of Colloid and Interface Science*, 484 (2016) 107-115.
- [345] G.-E. Chen, Q. Wu, W.-G. Sun, Z.-L. Xu, S.-J. Xu, W.-W. Zhu, X.-P. Zheng, Synergy of graphene oxide-silver nanocomposite and amphiphilic co-polymer F127 on antibacterial properties and permeability of PVDF membrane, *RSC Advances*, 6 (2016) 100334-100343.
- [346] S.W. Chook, C.H. Chia, S. Zakaria, M.K. Ayob, N.M. Huang, H.M. Neoh, M. He, L. Zhang, R. Jamal, A graphene oxide facilitated a highly porous and effective antibacterial regenerated cellulose membrane containing stabilized silver nanoparticles, *Cellulose*, 21 (2014) 4261-4270.

- [347] P.K.S. Mural, M. Sharma, A. Shukla, S. Bhadra, B. Padmanabhan, G. Madras, S. Bose, Porous membranes designed from bi-phasic polymeric blends containing silver decorated reduced graphene oxide synthesized via a facile one-pot approach, *RSC Advances*, 5 (2015) 32441-32451.
- [348] A.F. Faria, C. Liu, M. Xie, F. Perreault, L.D. Nghiem, J. Ma, M. Elimelech, Thin-film composite forward osmosis membranes functionalized with graphene oxide–silver nanocomposites for biofouling control, *Journal of Membrane Science*, 525 (2017) 146-156.
- [349] J. Wang, Y. Wang, Y. Zhang, A. Uliana, J. Zhu, J. Liu, B. Van der Bruggen, Zeolitic Imidazolate Framework/Graphene Oxide Hybrid Nanosheets Functionalized Thin Film Nanocomposite Membrane for Enhanced Antimicrobial Performance, *ACS Applied Materials & Interfaces*, 8 (2016) 25508-25519.
- [350] Y.T. Chung, E. Mahmoudi, A.W. Mohammad, A. Benamor, D. Johnson, N. Hilal, Development of polysulfone-nanohybrid membranes using ZnO-GO composite for enhanced antifouling and antibacterial control, *Desalination*, 402 (2017) 123-132.
- [351] H. Wu, B. Tang, P. Wu, Development of novel SiO₂–GO nanohybrid/polysulfone membrane with enhanced performance, *Journal of Membrane Science*, 451 (2014) 94-102.
- [352] M. Safarpour, V. Vatanpour, A. Khataee, Preparation and characterization of graphene oxide/TiO₂ blended PES nanofiltration membrane with improved antifouling and separation performance, *Desalination*, 393 (2016) 65-78.
- [353] X.-F. Sun, J. Qin, P.-F. Xia, B.-B. Guo, C.-M. Yang, C. Song, S.-G. Wang, Graphene oxide–silver nanoparticle membrane for biofouling control and water purification, *Chemical Engineering Journal*, 281 (2015) 53-59.
- [354] A.F. De Faria, F. Perreault, E. Shauly, L.H. Arias Chavez, M. Elimelech, Antimicrobial electrospun biopolymer nanofiber mats functionalized with graphene oxide–silver nanocomposites, *ACS applied materials & interfaces*, 7 (2015) 12751-12759.
- [355] A. Soroush, W. Ma, Y. Silvino, M. Rahaman, Surface Modification of Thin Film Composite Forward Osmosis Membrane by Silver-Decorated Graphene-Oxide Nanosheets, 2015.
- [356] P.K.S. Mural, A. Banerjee, M.S. Rana, A. Shukla, B. Padmanabhan, S. Bhadra, G. Madras, S. Bose, Polyolefin based antibacterial membranes derived from PE/PEO blends compatibilized with amine terminated graphene oxide and maleated PE, *Journal of Materials Chemistry A*, 2 (2014) 17635-17648.
- [357] M. Mukherjee, S. Panda, S. De, Adhesion resistant chitosan coated iron oxide polyacrylonitrile mixed matrix membrane for disinfection of surface water, 2016.
- [358] H.J. Kim, Y.-S. Choi, M.-Y. Lim, K.H. Jung, D.-G. Kim, J.-J. Kim, H. Kang, J.-C. Lee, Reverse osmosis nanocomposite membranes containing graphene oxides coated by tannic acid with chlorine-tolerant and antimicrobial properties, *Journal of Membrane Science*, 514 (2016) 25-34.
- [359] J. Wang, Y. Wu, Z. Yang, H. Guo, B. Cao, C.Y. Tang, A novel gravity-driven nanofibrous membrane for point-of-use water disinfection: polydopamine-induced in situ silver incorporation, *Scientific reports*, 7 (2017) 2334-2334.
- [360] L.H. Velazquez-Jimenez, E. Vences-Alvarez, J.L. Flores-Arciniega, H. Flores-Zuñiga, J.R. Rangel-Mendez, Water defluoridation with special emphasis on adsorbents-containing metal oxides and/or hydroxides: A review, *Separation and Purification Technology*, 150 (2015) 292-307.
- [361] R. Das, S.B. Abd Hamid, M.E. Ali, A.F. Ismail, M.S.M. Annuar, S. Ramakrishna, Multifunctional carbon nanotubes in water treatment: The present, past and future, *Desalination*, 354 (2014) 160-179.
- [362] G. Lu, Nanoporous materials—an overview, *Nanoporous materials: science and engineering*, 4 (2004).
- [363] A. Aghakhani, S.-F. Mousavi, B. Mostafazadeh-Fard, Desalination of saline water with single and combined adsorbents, *Desalination and Water Treatment*, 51 (2013) 1928-1935.
- [364] M.A. Tofiqy, T. Mohammadi, Salty water desalination using carbon nanotube sheets, *Desalination*, 258 (2010) 182-186.
- [365] F. Perreault, A. Fonseca de Faria, M. Elimelech, Environmental applications of graphene-based nanomaterials, *Chemical Society Reviews*, 44 (2015) 5861-5896.
- [366] O. Lehmann, O. Nir, M. Kuflik, O. Lahav, Recovery of high-purity magnesium solutions from RO brines by adsorption of Mg(OH)₂(s) on Fe₃O₄ micro-particles and magnetic solids separation, *Chemical Engineering Journal*, 235 (2014) 37-45.
- [367] M.H. Sorour, H.A. Hani, H.F. Shaalan, M.M. El Sayed, M.M.H. El-Sayed, Softening of seawater and desalination brines using grafted polysaccharide hydrogels, *Desalination and Water Treatment*, 55 (2015) 2389-2397.

- [368] T.M. Sonqishe, Treatment of brines using commercial zeolites and zeolites synthesized from fly ash derivative, in, University of the Western Cape, 2008.
- [369] T. Wajima, T. Shimizu, T. Yamato, Y. Ikegami, Removal of NaCl from seawater using natural zeolite, *Toxicological & Environmental Chemistry*, 92 (2010) 21-26.
- [370] Z. Xue, Z. Li, J. Ma, X. Bai, Y. Kang, W. Hao, R. Li, Effective removal of Mg²⁺ and Ca²⁺ ions by mesoporous LTA zeolite, *Desalination*, 341 (2014) 10-18.
- [371] M.C. Duke, B. Zhu, C.M. Doherty, M.R. Hill, A.J. Hill, M.A. Carreon, Structural effects on SAPO-34 and ZIF-8 materials exposed to seawater solutions, and their potential as desalination membranes, *Desalination*, 377 (2016) 128-137.
- [372] M. Bhadra, S. Roy, S. Mitra, Enhanced desalination using carboxylated carbon nanotube immobilized membranes, *Separation and Purification Technology*, 120 (2013) 373-377.
- [373] H.Y. Yang, Z.J. Han, S.F. Yu, K.L. Pey, K. Ostrikov, R. Karnik, Carbon nanotube membranes with ultrahigh specific adsorption capacity for water desalination and purification, *Nature communications*, 4 (2013) 2220.
- [374] A.K. Mishra, S. Ramaprabhu, Functionalized graphene sheets for arsenic removal and desalination of sea water, *Desalination*, 282 (2011) 39-45.
- [375] Z. Wang, B. Dou, L. Zheng, G. Zhang, Z. Liu, Z. Hao, Effective desalination by capacitive deionization with functional graphene nanocomposite as novel electrode material, *Desalination*, 299 (2012) 96-102.
- [376] A.G. El-Deen, N.A.M. Barakat, H.Y. Kim, Graphene wrapped MnO₂-nanostructures as effective and stable electrode materials for capacitive deionization desalination technology, *Desalination*, 344 (2014) 289-298.
- [377] A.K. Mishra, S. Ramaprabhu, Magnetite Decorated Multiwalled Carbon Nanotube Based Supercapacitor for Arsenic Removal and Desalination of Seawater, *The Journal of Physical Chemistry C*, 114 (2010) 2583-2590.
- [378] M.L.A. Ouar, M.H. Sellami, S.E. Meddour, R. Touahir, S. Guemari, K. Loudiyi, Experimental yield analysis of groundwater solar desalination system using absorbent materials, *Groundwater for Sustainable Development*, 5 (2017) 261-267.
- [379] E. Wibowo, Sutisna, M. Rokhmat, R. Murniati, Khairurrijal, M. Abdullah, Utilization of Natural Zeolite as Sorbent Material for Seawater Desalination, *Procedia Engineering*, 170 (2017) 8-13.
- [380] M. Safarpour, V. Vatanpour, A. Khataee, H. Zarrabi, P. Gholami, M.E. Yekavalangi, High flux and fouling resistant reverse osmosis membrane modified with plasma treated natural zeolite, *Desalination*, 411 (2017) 89-100.
- [381] P. Swenson, B. Tanchuk, A. Gupta, W. An, S.M. Kuznicki, Pervaporative desalination of water using natural zeolite membranes, *Desalination*, 285 (2012) 68-72.
- [382] H. Dong, L. Zhao, L. Zhang, H. Chen, C. Gao, W.S. Winston Ho, High-flux reverse osmosis membranes incorporated with NaY zeolite nanoparticles for brackish water desalination, *Journal of Membrane Science*, 476 (2015) 373-383.
- [383] A. Garofalo, M.C. Carnevale, L. Donato, E. Drioli, O. Alharbi, S.A. Aljlil, A. Criscuoli, C. Algieri, Scale-up of MFI zeolite membranes for desalination by vacuum membrane distillation, *Desalination*, 397 (2016) 205-212.
- [384] F. Fu, Q. Wang, Removal of heavy metal ions from wastewaters: A review, *Journal of Environmental Management*, 92 (2011) 407-418.
- [385] A. Méndez, G. Gascó, Optimization of water desalination using carbon-based adsorbents, *Desalination*, 183 (2005) 249-255.
- [386] H. Wu, R. Chen, H. Du, J. Zhang, L. Shi, Y. Qin, L. Yue, J. Wang, Synthesis of activated carbon from peanut shell as dye adsorbents for wastewater treatment, *Adsorption Science & Technology*, 37 (2019) 34-48.
- [387] Ihsanullah, A. Abbas, A.M. Al-Amer, T. Laoui, M.J. Al-Marri, M.S. Nasser, M. Khraisheh, M.A. Atieh, Heavy metal removal from aqueous solution by advanced carbon nanotubes: Critical review of adsorption applications, *Separation and Purification Technology*, 157 (2016) 141-161.
- [388] X. Ren, C. Chen, M. Nagatsu, X. Wang, Carbon nanotubes as adsorbents in environmental pollution management: A review, *Chemical Engineering Journal*, 170 (2011) 395-410.
- [389] M.A. Tofighy, T. Mohammadi, Permanent hard water softening using carbon nanotube sheets, *Desalination*, 268 (2011) 208-213.
- [390] C. Santhosh, V. Velmurugan, G. Jacob, S.K. Jeong, A.N. Grace, A. Bhatnagar, Role of nanomaterials in water treatment applications: A review, *Chemical Engineering Journal*, 306 (2016) 1116-1137.
- [391] V.K.K. Upadhyayula, S. Deng, M.C. Mitchell, G.B. Smith, Application of carbon nanotube technology for removal of contaminants in drinking water: A review, *Science of The Total Environment*, 408 (2009) 1-13.

- [392] D. Cohen-Tanugi, J.C. Grossman, Water Desalination across Nanoporous Graphene, *Nano Letters*, 12 (2012) 3602-3608.
- [393] H. Li, T. Lu, L. Pan, Y. Zhang, Z. Sun, Electrosorption behavior of graphene in NaCl solutions, *Journal of Materials Chemistry*, 19 (2009) 6773-6779.
- [394] S.N. Faisal, C.M. Subramaniyam, E. Haque, M.M. Islam, N. Noorbehesht, A.K. Roy, M.S. Islam, H.K. Liu, S.X. Dou, A.T. Harris, A.I. Minett, Nanoarchitected Nitrogen-Doped Graphene/Carbon Nanotube as High Performance Electrodes for Solid State Supercapacitors, Capacitive Deionization, Li-Ion Battery, and Metal-Free Bifunctional Electrocatalysis, *ACS Applied Energy Materials*, 1 (2018) 5211-5223.
- [395] Y. Li, J. Kim, J. Wang, N.-L. Liu, Y. Bando, A.A. Alshehri, Y. Yamauchi, C.-H. Hou, K.C.W. Wu, High performance capacitive deionization using modified ZIF-8-derived, N-doped porous carbon with improved conductivity, *Nanoscale*, 10 (2018) 14852-14859.
- [396] L. Chao, Z. Liu, G. Zhang, X. Song, X. Lei, M. Noyong, U. Simon, Z. Chang, X. Sun, Enhancement of capacitive deionization capacity of hierarchical porous carbon, *Journal of Materials Chemistry A*, 3 (2015) 12730-12737.
- [397] A.F.I. P.S. Goh, and N. Hilal, Desalination Technology and Advancement, *Oxford Research Encyclopedia of Environmental Science*, (2019, DOI: 10.1093/acrefore/9780199389414.013.599).
- [398] A.A. Askalany, A. Freni, G. Santori, Supported ionic liquid water sorbent for high throughput desalination and drying, *Desalination*, 452 (2019) 258-264.
- [399] A.G.N. Wamba, G.P. Kofa, S.N. Koungou, P.S. Thue, E.C. Lima, G.S. Dos Reis, J.G. Kayem, Grafting of Amine functional group on silicate based material as adsorbent for water purification: A short review, *Journal of Environmental Chemical Engineering*, 6 (2018) 3192-3203.
- [400] N. Hilal, G.J. Kim, C. Somerfield, Boron removal from saline water: A comprehensive review, *Desalination*, 273 (2011) 23-35.
- [401] Y. Jiang, D. Liu, M. Cho, S.S. Lee, F. Zhang, P. Biswas, J.D. Fortner, In Situ Photocatalytic Synthesis of Ag Nanoparticles (nAg) by Crumpled Graphene Oxide Composite Membranes for Filtration and Disinfection Applications, *Environmental Science & Technology*, 50 (2016) 2514-2521.
- [402] J. Zhu, A. Uliana, J. Wang, S. Yuan, J. Li, M. Tian, K. Simoens, A. Volodin, J. Lin, K. Bernaerts, Y. Zhang, B. Van der Bruggen, Elevated salt transport of antimicrobial loose nanofiltration membranes enabled by copper nanoparticles via fast bioinspired deposition, *Journal of Materials Chemistry A*, 4 (2016) 13211-13222.
- [403] L. Huang, S. Zhao, Z. Wang, J. Wu, J. Wang, S. Wang, In situ immobilization of silver nanoparticles for improving permeability, antifouling and anti-bacterial properties of ultrafiltration membrane, *Journal of Membrane Science*, 499 (2016) 269-281.
- [404] Z. Wang, J. Sun, Enantioselective [4 + 2] Cycloaddition of o-Quinone Methides and Vinyl Sulfides: Indirect Access to Generally Substituted Chiral Chromanes, *Organic Letters*, 19 (2017) 2334-2337.
- [405] X. Zeng, G. Wang, Y. Liu, X. Zhang, Graphene-based antimicrobial nanomaterials: rational design and applications for water disinfection and microbial control, *Environmental Science: Nano*, 4 (2017) 2248-2266.
- [406] D.Y. Koseoglu-Imer, N. Dizge, I. Koyuncu, Enzymatic activation of cellulose acetate membrane for reducing of protein fouling, *Colloids and Surfaces B: Biointerfaces*, 92 (2012) 334-339.
- [407] J. Hou, G. Dong, B. Luu, R.G. Sengpiel, Y. Ye, M. Wessling, V. Chen, Hybrid membrane with TiO₂ based biocatalytic nanoparticle suspension system for the degradation of bisphenol-A, *Bioresource Technology*, 169 (2014) 475-483.
- [408] Q. Zhao, C. Liu, J. Liu, Y. Zhang, Development of a novel polyethersulfone ultrafiltration membrane with antibacterial activity and high flux containing halloysite nanotubes loaded with lysozyme, *RSC Advances*, 5 (2015) 38646-38653.
- [409] L. Duan, Y. Wang, Y. Zhang, J. Liu, Graphene immobilized enzyme/polyethersulfone mixed matrix membrane: Enhanced antibacterial, permeable and mechanical properties, *Applied Surface Science*, 355 (2015) 436-445.
- [410] J. Ren, H. Luo, Microbial electrochemical cell for simultaneous water desalination, energy production and wastewater treatments, in: *Joint US-China Workshop on Pathways Toward Low Carbon Cities*, 2010, pp. 13-14.
- [411] M. Mehanna, T. Saito, J. Yan, M. Hickner, X. Cao, X. Huang, B.E. Logan, Using microbial desalination cells to reduce water salinity prior to reverse osmosis, *Energy & Environmental Science*, 3 (2010) 1114-1120.
- [412] S. Cheng, B.E. Logan, Evaluation of catalysts and membranes for high yield biohydrogen production via electrohydrogenesis in microbial electrolysis cells (MECs), *Water science and technology*, 58 (2008) 853-857.
- [413] Q. Wen, H. Zhang, Z. Chen, Y. Li, J. Nan, Y. Feng, Using bacterial catalyst in the cathode of microbial desalination cell to improve wastewater treatment and desalination, *Bioresource Technology*, 125 (2012) 108-113.

- [414] F.L. Moruno, J.E. Rubio, P. Atanassov, J.M. Cerrato, C.G. Arges, C. Santoro, Microbial desalination cell with sulfonated sodium poly(ether ether ketone) as cation exchange membranes for enhancing power generation and salt reduction, *Bioelectrochemistry*, 121 (2018) 176-184.
- [415] H.M. Saeed, G.A. Hussein, S. Yousef, J. Saif, S. Al-Asheh, A. Abu Fara, S. Azzam, R. Khawaga, A. Aidan, Microbial desalination cell technology: A review and a case study, *Desalination*, 359 (2015) 1-13.
- [416] H. Han, J.Y. Lee, X. Lu, Thermoresponsive nanoparticles+ plasmonic nanoparticles= photoresponsive heterodimers: Facile synthesis and sunlight-induced reversible clustering, *Chemical Communications*, 49 (2013) 6122-6124.
- [417] C. Liu, J. Heo, Local heating from silver nanoparticles and its effect on the Er³⁺ upconversion in oxyfluoride glasses, *Journal of the American Ceramic Society*, 93 (2010) 3349-3353.
- [418] B. Gupta, P. Shankar, R. Sharma, P. Baredar, Performance Enhancement Using Nano Particles in Modified Passive Solar Still, *Procedia Technology*, 25 (2016) 1209-1216.
- [419] M. Kumar, M. Grzelakowski, J. Zilles, M. Clark, W. Meier, Highly permeable polymeric membranes based on the incorporation of the functional water channel protein Aquaporin Z, *Proceedings of the National Academy of Sciences*, 104 (2007) 20719-20724.
- [420] P.S. Zhong, T.-S. Chung, K. Jeyaseelan, A. Armugam, Aquaporin-embedded biomimetic membranes for nanofiltration, *Journal of Membrane Science*, 407 (2012) 27-33.
- [421] S.P. Sun, K.Y. Wang, N. Peng, T.A. Hatton, T.-S. Chung, Novel polyamide-imide/cellulose acetate dual-layer hollow fiber membranes for nanofiltration, *Journal of Membrane Science*, 363 (2010) 232-242.
- [422] W.R. Bowen, Biomimetic separations – learning from the early development of biological membranes, *Desalination*, 199 (2006) 225-227.
- [423] C.Y. Tang, Y. Zhao, R. Wang, C. Hélix-Nielsen, A.G. Fane, Desalination by biomimetic aquaporin membranes: Review of status and prospects, *Desalination*, 308 (2013) 34-40.
- [424] Q. Li, D. Yang, J. Shi, X. Xu, S. Yan, Q. Liu, Biomimetic modification of large diameter carbon nanotubes and the desalination behavior of its reverse osmosis membrane, *Desalination*, 379 (2016) 164-171.
- [425] D.L. Gin, W. Gu, B.A. Pindzola, W.-J. Zhou, Polymerized lyotropic liquid crystal assemblies for materials applications, *Accounts of chemical research*, 34 (2001) 973-980.
- [426] E.A. Jackson, M.A. Hillmyer, Nanoporous membranes derived from block copolymers: from drug delivery to water filtration, *ACS nano*, 4 (2010) 3548-3553.
- [427] M. Gopinadhan, P. Deshmukh, Y. Choo, P.W. Majewski, O. Bakajin, M. Elimelech, R.M. Kasi, C.O. Osuji, Thermally switchable aligned nanopores by magnetic-field directed self-assembly of block copolymers, *Advanced Materials*, 26 (2014) 5148-5154.
- [428] K.-V. Peinemann, V. Abetz, P.F. Simon, Asymmetric superstructure formed in a block copolymer via phase separation, *Nature materials*, 6 (2007) 992.
- [429] J.I. Clodt, B. Bajer, K. Buhr, J. Hahn, V. Filiz, V. Abetz, Performance study of isoporous membranes with tailored pore sizes, *Journal of Membrane Science*, 495 (2015) 334-340.
- [430] J. Zhu, M. Tian, Y. Zhang, H. Zhang, J. Liu, Fabrication of a novel “loose” nanofiltration membrane by facile blending with Chitosan–Montmorillonite nanosheets for dyes purification, *Chemical Engineering Journal*, 265 (2015) 184-193.
- [431] Q. Fu, E.H.H. Wong, J. Kim, J.M.P. Scofield, P.A. Gurr, S.E. Kentish, G.G. Qiao, The effect of soft nanoparticles morphologies on thin film composite membrane performance, *Journal of Materials Chemistry A*, 2 (2014) 17751-17756.
- [432] S. Loher, O.D. Schneider, T. Maienfisch, S. Bokorny, W.J. Stark, Micro-organism-triggered release of silver nanoparticles from biodegradable oxide carriers allows preparation of self-sterilizing polymer surfaces, *Small*, 4 (2008) 824-832.
- [433] Y. Deng, G. Dang, H. Zhou, X. Rao, C. Chen, Preparation and characterization of polyimide membranes containing Ag nanoparticles in pores distributing on one side, *Materials Letters*, 62 (2008) 1143-1146.
- [434] S.F. Anis, G. Singaravel, R. Hashaikeh, Hierarchical nano zeolite-Y hydrocracking composite fibers with highly efficient hydrocracking capability, *RSC Advances*, 8 (2018) 16703-16715.
- [435] A. Slistan-Grijalva, R. Herrera-Urbina, J.F. Rivas-Silva, M. Ávalos-Borja, F.F. Castellón-Barraza, A. Posada-Amarillas, Synthesis of silver nanoparticles in a polyvinylpyrrolidone (PVP) paste, and their optical properties in a film and in ethylene glycol, *Materials Research Bulletin*, 43 (2008) 90-96.

- [436] N. Song, X. Gao, Z. Ma, X. Wang, Y. Wei, C. Gao, A review of graphene-based separation membrane: Materials, characteristics, preparation and applications, *Desalination*, 437 (2018) 59-72.
- [437] M.E.A. Ali, L. Wang, X. Wang, X. Feng, Thin film composite membranes embedded with graphene oxide for water desalination, *Desalination*, 386 (2016) 67-76.
- [438] J. Lee, S. Jeong, Z. Liu, Progress and challenges of carbon nanotube membrane in water treatment, *Critical reviews in environmental science and technology*, 46 (2016) 999-1046.
- [439] V. Georgakilas, A. Bourlinos, D. Gournis, T. Tsoufis, C. Trapalis, A. Mateo-Alonso, M. Prato, Multipurpose organically modified carbon nanotubes: from functionalization to nanotube composites, *Journal of the American Chemical Society*, 130 (2008) 8733-8740.
- [440] G. Bounos, K.S. Andrikopoulos, H. Moschopoulou, G.C. Lainioti, D. Roilo, R. Checchetto, T. Ioannides, J.K. Kallitsis, G.A. Voyiatzis, Enhancing water vapor permeability in mixed matrix polypropylene membranes through carbon nanotubes dispersion, *Journal of Membrane Science*, 524 (2017) 576-584.
- [441] O.A. Oyetade, A.A. Skelton, V.O. Nyamori, S.B. Jonnalagadda, B.S. Martincigh, Experimental and DFT studies on the selective adsorption of Pb²⁺ and Zn²⁺ from aqueous solution by nitrogen-functionalized multiwalled carbon nanotubes, *Separation and Purification Technology*, 188 (2017) 174-187.
- [442] W. Falath, A. Sabir, K.I. Jacob, Highly improved reverse osmosis performance of novel PVA/DGEBA cross-linked membranes by incorporation of Pluronic F-127 and MWCNTs for water desalination, *Desalination*, 397 (2016) 53-66.
- [443] S.G. Kim, D.H. Hyeon, J.H. Chun, B.-H. Chun, S.H. Kim, Nanocomposite poly(arylene ether sulfone) reverse osmosis membrane containing functional zeolite nanoparticles for seawater desalination, *Journal of Membrane Science*, 443 (2013) 10-18.
- [444] T. Kaminski, S.F. Anis, M.M. Husein, R. Hashaikeh, Hydrocracking of Athabasca VR Using NiO-WO₃ Zeolite-Based Catalysts, *Energy & Fuels*, (2018).
- [445] Y. Zhao, C. Qiu, X. Li, A. Vararattanavech, W. Shen, J. Torres, C. Helix-Nielsen, R. Wang, X. Hu, A.G. Fane, Synthesis of robust and high-performance aquaporin-based biomimetic membranes by interfacial polymerization-membrane preparation and RO performance characterization, *Journal of Membrane Science*, 423 (2012) 422-428.